Molekulare Untersuchungen von Agonisten und Antagonisten der Toll-like Rezeptoren 2 und 4

Molecular investigations of agonists and antagonists of Toll-like receptors 2 and 4

D I S S E R T A T I O N

der Fakultät für Chemie und Pharmazie
der Eberhard-Karls-Universität Tübingen

zur Erlangung des Grades eines Doktors
der Naturwissenschaften

2005

vorgelegt von

Söhnke Voss

Tag der mündlichen Prüfung	20.12.2005
Dekan	Prof. Dr. S. Laufer
1. Berichterstatter	Prof. Dr. G. Jung
2. Berichterstatter	Prof. Dr. K.-H. Wiesmüller

Die vorliegende Arbeit wurde unter Anleitung von

Herrn Prof. Dr. Günther Jung

und unter Betreuung von Herrn PD Dr. Roland Brock und Herrn Prof. Dr. Karl-Heinz Wiesmüller

in der Zeit von Juli 2001 bis November 2005 am Institut für Organische Chemie und am Institut für Zellbiologie der Eberhard-Karls-Universität Tübingen durchgeführt.

Herrn PD Dr. Roland Brock, Herrn Prof. Dr. Karl-Heinz Wiesmüller und Herrn Prof. Dr. Günther Jung danke ich herzlich für die hervorragende Betreuung, das fortwährende Interesse an meiner Arbeit, die exzellenten Arbeitsbedingungen und das mir entgegengebrachte Vertrauen.

DANKSAGUNG

Für die sehr angenehme und konstruktive Arbeitsatmosphäre möchte ich mich bei Dr. Oliver Mader, Dr. Rainer Fischer, Dr. Mariola Fotin-Mleczek, Dr. Martin Elbs, Falk Duchardt, Oda Stoevesandt, Hansjörg Hufnagel, Thomas André, Yi-da Chung, Karsten Köhler, Antje Hoff, Ivo Ruttekolk, Alexander Ganser, Susann Wolf, Günter Roth, Dr. Steffen Weik, Dr. Michael Barth, Dr. Jörg Bauer, Dr. Tobias Seyberth, Dr. Jörn Dengjel, Lynne Yakes und allen nicht erwähnten Kollegen der Arbeitsgruppen Dr. Roland Brock und Prof. Dr. Günther Jung bedanken.

Sehr herzlich danke ich meinen Projektpartnern Prof. Dr. Karl-Heinz Wiesmüller, Prof Dr. Artur J. Ulmer, Dr. Ute Buwitt-Beckmann, PD Dr. Holger Heine, Dr. Renate Spohn und Dr. Claudia Wittland für die interessante und freundliche Zusammenarbeit.

Ganz besonders bedanken möchte ich mich bei Dr. Rainer Fischer für die freundschaftliche Zusammenarbeit, für sein großes Interesse an meiner Arbeit, die vielen konstruktiven Diskussionen, für das Sensor Projekt und seine vielen Visionen.

Dr. Mariola Fotin-Mleczek danke ich ganz herzlich für die exzellente Zusammenarbeit, durch die ich sehr viel gelernt habe, für ihren großen Einsatz im CD14 Projekt, die vielen konstruktiven Diskussionen und das fortwährende Interesse an meiner Arbeit.

Außerdem möchte ich Dr. Tobias Seyberth für die sehr gute Zusammenarbeit im Lipolanthionin Projekt danken.

Mein Dank gilt Prof. Dr. Robert Weissert für die Durchführung der *in vivo* Experimente.

Sehr herzlich danke ich Frau Ursula Becker und Frau Heiderose Neu, die sich stets mit großem Engagement um alle organisatorischen Belange gekümmert haben.

Bei Stefan Welte möchte ich mich für die Zusammenarbeit im CD14 Projekt und die vielen konstruktiven Diskussionen bedanken.

Dr. Mariola Fotin-Mleczek, Dr. Oliver Mader, Günter Roth, Oda Stoevesandt und Antje Hoff danke ich für die Unterstützung bei der Durchführung der Fluoreszenzmessungen.

Mein Dank gilt außerdem Aleksandra Velkova für die Zusammenarbeit im CD14 Projekt und PD Dr. Afroditi Kapurniotu und Prof. Dr. Voelter für die Möglichkeit die CD-Messungen durchführen zu können, sowie für die wertvolle Hilfestellung bei den Messungen.

Meinen fleißigen „Hilfswissenschaftlern“ Hansjörg Hufnagel und Tatjana Tausch danke ich für ihr großes Engagement.

Für die exzellenten Peptide und Lipopeptide danke ich herzlich Nicole Sessler, Luise Schindler und Prof. Dr. Karl-Heinz Wiesmüller.

Ohne die Hilfe von Thomas André bei vielen Computerproblemen wäre ich oft aufgeschmissen gewesen. Dafür vielen Dank.

Prof. Dr. Stefan Stevanović möchte ich für die Möglichkeit danken, in seinem Labor die notwendigen Routine MALDI TOF-Messungen durchführen zu können.

Franziska Löwenstein danke ich für die zuverlässige Erledigung der Spüldienste.

Für die außerordentlich hilfreiche Unterstützung in der Zeit nach dem 30. April 2002 danke ich besonders PD Dr. Roland Brock, Dr. Oliver Mader und Dr. Rainer Fischer.

Zuguterletzt gilt meinen Eltern besonderer Dank für die fortwährende Unterstützung während meines Studiums und der Doktorarbeit.

Für Esther

Table of contents

Abbreviations

For amino-acids the suggestions of the IUPAC-IUB-commission for biological nomenclature [*Eur. J. Biochem.* **1984**, *138*, 9-37] were applied.

Ac	acetyl
ACN	acetonitrile
AcOH	acetic acid
Ac_2O	acetic acid anhydride
Ado	8-amino-3,6-dioxaoctanoic acid
Boc	*tert*.-butyloxycarbonyl
BPI	bactericidal permeability-increasing protein
BSA	bovine serum albumin
CD	cluster of differentiation
DCM	dichloromethane
Dde	1-(4,4-dimethyl-2,6-dioxocyclohexylidene)ethyl
DHAP	2,5 dihydroxyacetophenone
Dhc	S-[2,3-dihydroxypropyl]-cysteine
DIC	N,N'-diisopropyl carbodiimide
DIPEA	N,N'-diisopropylethylamine
DMF	N,N'-dimethylformamide
DMSO	dimethylsulfoxide
DMEM	Dulbecco´s Modified Eagle´s medium
EDT	ethanedithiole
EDTA	ethylenediaminetetraacetic acid
ELISA	enzyme linked immunosorbent assay
equiv.	equivalents
ES-MS	electrospray-MS
EtOH	ethanol
FBS	foetal bovine serum
FCS	fluorescence correlation spectroscopy
FITC	fluorescein isothiocyanate
Fluo	5(6)-carboxyfluorescein

Fmoc	N-(9-fluorenyl)methoxycarbonyl
FRET	fluorescence resonance energy transfer
h	hour
HEPES	N-(2-hydroxyethyl) piperazine-N´-(2-ethanesulfonic acid)
HFIP	hexafluoro-2-isopropanol
HIV	human immunodeficiency virus
HOBt	1-hydroxybenzotriazol
HPLC	high-performance liquid chromatography
IRAK-4	Interleukin-1 receptor-associated kinase
LAL	*Limulus* amebocyte lysate
LALF	*Limulus* anti-LPS factor
Lan	lanthionine
LBP	LPS-binding protein
LP	lipopeptide
LPS	lipopolysaccharide
λ	wavelength
M	molarity
MALDI	matrix-assisted laser desorption ionisation
MALP-2	macrophage-activating lipopeptide-2
MAPK	mitogen-activated protein kinase
MeOH	methanol
MHC	major histocompatibility complex
min	minute
MS	mass spectrometry
Mtt	4-methyltrityl
MTT	3-(4,5-dimethylthiazol-2-yl)-2,5-diphenyl tetrazolium bromide
MyD88	Myeloid differentiation factor 88
m/z	mass/charge ration
NMR	nuclear magnetic resonance
NF-κB	nuclear factor-κ B
Pam_3Cys	*S*-[2,3-bis(palmitoyloxy)-(2*RS*)-propyl]-*N*-palmitoyl-(*R*)-cysteinyl
PAMP	Pathogen-associated molecular pattern
PBS	phosphate-buffered saline

pH	potentia hydrogenii
PMA	phorbol 12-myristate 13-acetate
POPC	1-palmitoyl-2-2-oleoyl-phosphocholine
POPG	1-palmitoyl-2-2-oleoyl-phosphoglycerol
PRR	Pattern recognition receptor
Rh	5(6)-carboxytetramethylrhodamine
RP	reversed phase
RT	room temperature
S0387	2-(4-acetoanilino-1,3-butadienyl)-3,3-dimethyl-1-(4-sulfobutyl)-indolinium inner salt
t	time
Tamra/TAMRA	5(6)-carboxytetramethylrhodamine
t_R	retention time
tBu	*tert*.-butyl
TBTU	2-(1*H*-benzotriazol-1-yl)-1,1,3,3-tetramethyluronium tetrafluoroborate
tert.-BuOH	*tert*.-butyl alcohol
TIS	triisopropylsilane
TFA	trifluoroacetic acid
TFE	trifluoroethanol
TOF	time-of-flight
TLR	Toll-like receptor
TRAF-6	Tumor necrosis factor receptor-associated factor-6
Tris	(hydoxymethyl) aminomethane
Trt	trityl
UV	ultraviolett
V	volume

1 Introduction

1.1 The immune system

The defence of multicellular organisms against invading pathogens is based on their ability to evoke immune responses. In vertebrates, the immune system has been divided into innate and adaptive components. The system of innate immunity is present in almost all multicellular organisms and provides the first line of defence. This non-specific response eliminates the majority of pathogens within minutes or hours. When these innate defences are breached the adaptive immune responses come into play. The adaptive immune system, which is only present in vertebrates, provides a more specific and long lasting protection. It recognizes complexes of peptide antigens and MHC-molecules on antigen presenting cells using antigen receptors expressed on the surface of T and B cells. The high viability of the antigen receptors is achieved by the random rearrangement of the immunoglobulin and T cell receptor genes. Antigen recognition initiates the production of antigen-specific antibodies or activation and proliferation of T cells. At least four to seven days are required to establish these responses.

In contrast to the adaptive immune system, the phylogenetically older innate immune system detects invading microorganisms by recognizing a broad spectrum of universal microbial molecular patterns (Pathogen-associated molecular patterns (PAMPs)) via a limited repertoire of recognition molecules (Pattern recognition receptors (PRR)). These include several classes of receptors, such as the complement receptor, f-Met-Leu-Phe receptor, macrophage mannose receptor, scavenger receptors, CD14 and Toll-like receptors (TLRs). Particularly the discovery of the TLRs and of their involvement in the recognition of microbial components represented a milestone in the elucidation of the mode of action of innate immune responses.

1.2 Toll-like receptors

Toll receptors were originally identified in *Drosophila* by Nüsslein-Volhards group. These proteins are involved in the establishment of dorso-ventral polarity of the developing embryo [1] and anti-fungal immune response of the adult fly [2].

Interestingly, the signaling pathways of *Drosophila* Toll and the mammalian IL-1 receptor are remarkably similar and the cytoplasmic domains of both receptors highly conserved. These congruities lead to the identification of a family of mammalian homologues of the Toll protein, collectively denoted as Toll-like receptors (TLRs) [3]. Up to now, the TLR family consists of 11 members in mammals [4-9] and specificity for different ligands either resides within one receptor itself or is attained through heterodimerization (Figure 1.1).

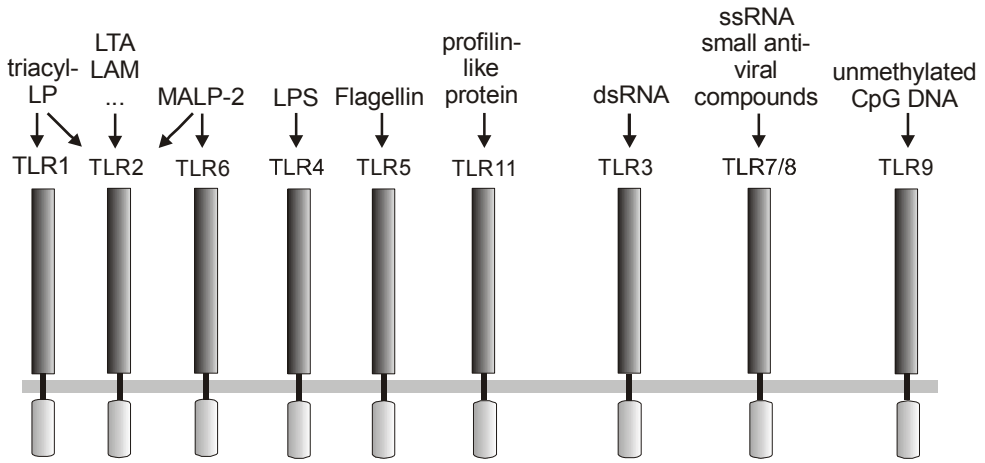

Figure 1.1 Toll-like receptors and their most prominent ligands

Both, the IL-1 receptor (IL-1R) and TLRs contain an intracellular highly conserved region of about 200 amino acids denoted as TIR (Toll/IL-1R) domain [10]. The extracellular domains of both receptors, on the other hand are markedly different. Whereas the IL-1R possesses three immunoglobulin-like structures, the extracellular domains of TLRs form a horseshoe like structure. It is thought that the recognition of PAMPs is accomplished by the concave face of the horseshoe. This domain is derived of 19-25 tandem copies of leucine rich repeats (LRR) of 24 to 29 amino acids each [11] containing the leucine-rich sequence XLXXLXLXX (where X can be any amino acid) (Figure 1.2).

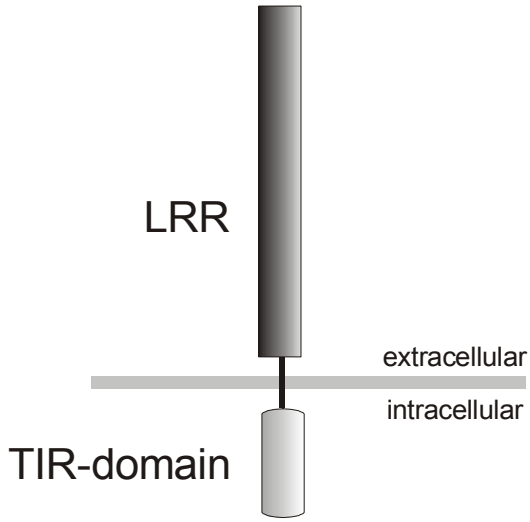

Figure 1.2 Structure of TLR

1.2.1 TLR4

TLR4 is the receptor for lipopolysaccharide (LPS), the main constituent of the outer cell membrane of Gram-negative bacteria. Prior to the identification of the receptor two mouse strains, C3H/HeJ and C57BL10/ScCr, had been known to be hypo-responsive against LPS. Later, it was shown, that both strains contain mutations in the Tlr4 gene leading to a non-functional receptor [12;13]. In addition to TLR4, several other molecules are involved in the LPS-dependent activation of cells. In serum, the highly amphiphatic LPS forms micelles which are recognized by LPS-binding protein (LBP). The acute phase protein accomplishes the transfer of monomeric LPS to CD14. CD14 is a 55 kDa glycoprotein of 356 amino acids that is expressed in a GPI-anchored and in a soluble form. The GPI-anchored form is expressed on cells of the myeloid lineage, i. e. monocytes, macrophages and polymorphonuclear granulocytes [14;15]. The soluble form (sCD14) plays a role in the LPS response of endothelial and epithelial cells [16-18]. The CD14 / LPS complex associates with TLR4 [19;20] leading to the activation of the receptor. Furthermore, MD-2, a molecule that is associated with the extracellular domain of TLR4 was found to directly bind to LPS and to amplify LPS responsiveness of cells [21;22].

Several other PAMPs activate TLR4 in addition to LPS. These compounds include the anti tumor agent taxol [23], diverse classes of viruses [24;25], and endogenous ligands like heat shock proteins [26] and hyaluronic acid. It is

proposed that receptor agonists from endogenous origins, which are released from dead or injured cells, indicate an inflammatory process and therefore function as danger signals [27].

1.2.2 TLR2

TLR2 is characterized by the ability to recognize a wide variety of microbial components including lipoproteins [28-31], lipoteichoic acid [32], lipoarabinomannan [33], glycoinositolphospholipids [34], phenol-soluble modulin [35], zymosan [36], glycolipids [37], *Neisseria* outer membrane porins [38] and atypical LPS from *Leptospira interrogans* and *Porphyromonas gingivalis* [39;40]. For lipopeptide recognition TLR2 forms heterodimers with either TLR1 or 6. Both, the peptide moiety and the acylation pattern of the lipopeptide ligands determine the composition of the receptor dimer. Whereas triacylated lipopeptides are recognized by TLR2/TLR1 heterodimers [41] diacylated lipopeptides activate TLR2 either in a TLR6-dependent [42] or -independent manner [43].

CD14 is also involved in the activation of cells by lipopeptides as found for LPS. On the cell surface CD14 directly interacts with lipopeptides inducing a physical proximity of this complex with TLR2/TLR1 [44]. Since several other molecules were found to activate TLRs in a CD14-dependent manner (Chapter 2) CD14 is considered as a central PRR in innate immunity.

1.2.3 Other TLRs

TLR3, TLR7, TLR8 and TLR9 recognize nucleic acid-like structures and are localized in intracellular compartments. Unmethylated CpG motifs which are abundant in bacteria but absent in vertebrate DNA strongly activate immune cells through TLR9 [45]. Prior receptor activation DNA needs to be internalized into endosomal compartments where signal transduction is initiated [46]. For this reason TLR9-dependent activation of cells is delayed compared to LPS-induced activation [45].

The activation of TLR3, the receptor for viral double stranded (ds) RNA [47] induces a strong antiviral response via TLR3-dependent secretion of type I interferons (IFN-α and –β) by immune cells. Synthetic dsRNA analogues, such as polyinosinic-polycytidylic acid [poly(I:C)] showed comparable agonistic activity and

have found application as adjuvants in vaccinations. TLR7 and 8 recognize single stranded RNA [48;49] and several synthetic antitumor compounds including imidazoquinolines [50;51]. In addition, the activation of immune cells by RNA complexed with protamine is probably accomplished in a TLR7- and 8-dependent manner [52]. TLR5 recognizes flagellin, a complex protein of flagellar extending from the cell wall of Gram-negative bacteria [53] and TLR11 responds to a protozoan profilin-like protein [54]. The ligand of TLR10 has yet not been identified. So far, TLR1 and TLR6 were only identified as co-receptors for TLR2 (Table 1.1).

Table 1.1 Toll-like receptors and their ligands

Receptor	Ligand	Origin
TLR1 (coreceptor)	Triacyl lipopeptides	Bacteria and mycobacteria
TLR2	Lipoproteins/lipopeptides	Various pathogens
	Peptidoglycan	Gram-positive bacteria
	Lipoteichoic acid	Gram-positive bacteria
	Lipoarabinomannan	Mycobacteria
	Phenol-soluble modulin	*Staphylococcus epidermidis*
	Glycoinositolphospholipids	*Trypanosoma cruzi*
	Glycolipids	*Treponema maltophilum*
	Porins	Neisseria species
	Atypical lipopolysaccharide	*Leptospira interrogans*
		Porphyromonas gingivalis
	Zymosan	Fungi
TLR3	Double-stranded RNA	Viruses
TLR4	Lipopolysaccharide	Gram-negative bacteria
	Taxol	Plants
	Heat-shock protein	Host
TLR5	Flagellin	Bacteria
TLR6 (coreceptor)	Diacyl lipopeptides	Mycoplasma
	Lipoteichoic acid	Gram-positiv bacteria
	Zymosan	Fungi
TLR7/8	Single-stranded RNA	Viruses
	Imidazoquinoline	Synthetic compound
TLR9	CpG-containing RNA	Bacteria and Viruses

TLR10	unknown	unknown.
TLR11	protozoan profilin-like protein	Uropathogenic bacteria

1.3 TLR signal transduction

1.3.1 Signal transduction

The interaction of a TLR with its ligand leads to the transcriptional activation of the synthesis of inflammatory cytokines, chemokines, reactive oxygen species, and acute phase proteins primarily mediated by the transcription factor NF-κB. The first event in the TLR-dependent signaling cascade is the recruitment of the adaptor molecule MyD88 to the cytoplasmic domain of the activated receptor [55]. The receptor-bound MyD88 itself recruits the death domain containing serine/threonine-kinase IRAK4 resulting in the activation of the kinase. MyD88 contains a C-terminal TIR and an N-terminal death domain and the interactions are accomplished through homologous TIR/TIR and death/death domain dimerizations, respectively [56]. IRAK4 then binds and activates IRAK1 which itself recruits a further adaptor molecule, TRAF6 [57], to the complex. This association is mediated by the binding of TRAF6 to autophosphorylated residues of IRAK1. Subsequently, the IRAK1/TRAF6 heterodimer dissociates from the receptor complex and associates to a complex of the mitogen-activated protein kinase kinase kinase (MAPKKK), TAK1 and the adaptor molecules TAB1, and TAB2 or TAB3 at the plasma membrane. The binding eventually leads to the translocation of the entire complex to the cytoplasm where TAK activates the inhibitor-κB kinase (IKK) complex. This complex is composed of two catalytic subunits, IKKα and IKKβ, and the scaffold protein, IKKγ/NEMO [58]. The activated kinases phosphorylate inhibitor-κB thereby releasing the inhibitory effect of this protein on NF-κB and initiating the nuclear translocation of the transcription factor. In the nucleus, NF-κB binds to NF-κB-promotor regions and initiates gene transcription [59]. In addition, TAK1 contribute to the activation of MAPKs.

The activation of macrophages by LPS is not strictly dependent on MyD88. Studies with MyD88-deficient macrophages revealed the existence of a MyD88-independent pathway which also results in NF-κB activation [60], however

retarded in comparison to the MyD88-dependent pathway. The MyD88-independent pathway is responsible for the induction of the expression of IFN-inducible genes [61]. In contrast to LPS, lipopeptides activate cells only in a MyD88-dependent manner.

Several other TIR domain-containing adaptor molecules are involved in TLR-dependent signaling in addition to MyD88 and TRAF6. TIRAP (TIR domain-containing adaptor protein/MyD88-adaptor-like (Mal)) is essential for the MyD88-dependent activation mediated by TLR2 and TLR4 [62] whereas the MyD88-independent pathway is dependent on the adaptor molecules TRAM [63] and TRIF [64]. TRAM interacts with the cytoplasmic domain of TLR4 and recruits TRIF to the complex.

The utilization of several adaptor molecules in the TLR-dependent signal transduction enables ligand-specific responses. The synergistic activation of both the MyD88-dependent and MyD88-independent/TRIF-dependent pathways by TLR4 stimulation is a possible explanation for the outstanding immune-stimulating properties of LPS [65].

1.3.2 Negative Regulation

Several molecules, such as TOLLIP, IRAK-M, MyD88s, SIGGIR and ST2 are involved in the negative regulation of the TLR-dependent signal transduction. In resting cells, TOLLIP suppresses the phosphorylation of IRAK1 by binding to the kinase. After receptor stimulation, TOLLIP dissociates from IRAK1 and eventually interacts with the TIR domain of TLR2 and TLR4. IRAK1 then becomes accessible for activation [66].

IRAK-M is an IRAK-family member that lacks a kinase activity. This molecule inhibits the dissociation of the IRAK1-IRAK4 complex from MyD88 [67]. MyD88s, an alternatively spliced variant of MyD88, is expressed in LPS stimulated lymphocytes. After TLR stimulation MyD88s binds to the cytoplasmic domain of TLRs, but fails to bind to IRAK4 [68]. The TIR domain containing proteins, SIGGIR [69] and ST2 [70], inhibit the TIR-dependent signaling pathways by interacting with TLR4, IRAK1 and TRAF6 or MyD88 and TIRAP, respectively.

1.4 Regulation of adaptive immuniy

It is proposed that without the assistance of the innate immunity an appropriate activation the adaptive immune system is not possible. Dendritic cells (DCs), that express a variety of TLRs [71] play a central role in the activation of adaptive immunity. In the periphery, immature DCs are exposed to a multitude of microbial compounds which they engulf by endocytosis. Digested fragments of these pathogens are returned to the cell surface in complex with class II histocompatibility molecules. The activation of the TLRs on the surface of DCs provides the signal for the expression of cytokines including IL-6 and co-stimulatory molecules, such as B7, necessary for the appropriate activation of T cells. Several other molecules expressed on the surface of or secreted by DCs such as chemokine receptors, the co-stimulatory molecules CD80/CD86 or IL-12 contribute to an efficient activation of the cells of the adaptive immunity [72].

1.5 Bacterial cell wall

Based on the property of the bacterial cell wall to differently retain the dye crystal violet during solvent treatment, bacteria were divided in Gram-positive and –negative species. Whereas Gram-negative bacteria lose the dye during solvent treatment, Gram-positive bacteria remain coloured. Differences in the composition of the cell wall are responsible for these characteristics. The cell wall of Gram-positive bacteria is composed of various layers of peptidoglycan (PGN) in which crystal violet dye primarily accumulates. PGN consists of altering N-acetylglucosamine- and N-acetylmuraminic acid units to which other molecules, such as LTA, LAM, lipopeptides and –proteins are connected. Whereas the cell wall of Gram-positive bacteria consists of about 60% to 90% PGN, the cell wall of Gram-negative bacteria contains only 10 to 20% PGN. In Gram-negative bacteria, a single layer of PGN is enclosed by a periplasmatic space and an outer membrane.

The outer leaflet of the outer membrane is mainly composed of LPS (approximately 3.5 x 10^6 molecules per E. coli cell) which contributes to the stability of the cell wall. The amphiphatic LPS can be divided into four different parts: the lipid A, inner and outer core and the O-antigen (Figure 1.3). Lipid A, the

lipid portion of LPS, is essential for the immune-stimulating activities (Galanos 1985; Raetz, 1990). In Lipid A, six or more fatty acid residues of which four are hydroxylated are bound to a phosphorylated glucosamine disaccharide. The second portion of LPS, the inner core, is covalently linked to the lipid A glucosamine residue and consists of two or more 2-keto-3-deoxyoctonic acid (KDO) residues and two or three heptose sugars. The outer core is more variable than the inner core and usually composed of three sugars to which one or more sugars are linked as side chains. The O-antigen is characterized by a high variability and extents from the bacterial surface. It is composed of 20 to 40 repeating units each of five common sugars. Colonies of bacteria with O-antigen containing LPS exhibit a smooth morphology whereas those of bacteria with an O-antigen lacking LPS have a rough surface texture. For this reason, LPS with O-antigen is denoted as smooth-LPS (S-LPS), the O-antigen lacking as rough–LPS (R-LPS). Based on its composition, R-LPS can be divided into several serotypes. For instance, R-LPS consisting only of lipid A and the inner core is denoted as Rd-LPS, whereas Ra-LPS is composed of lipid A, inner and outer core.

To exert their immune-stimulating properties LPS and other PAMPs have to be released from the bacterial cell wall triggered by bacterial death or growth and endogenous or exogenous factors such as complement or several antibiotics.

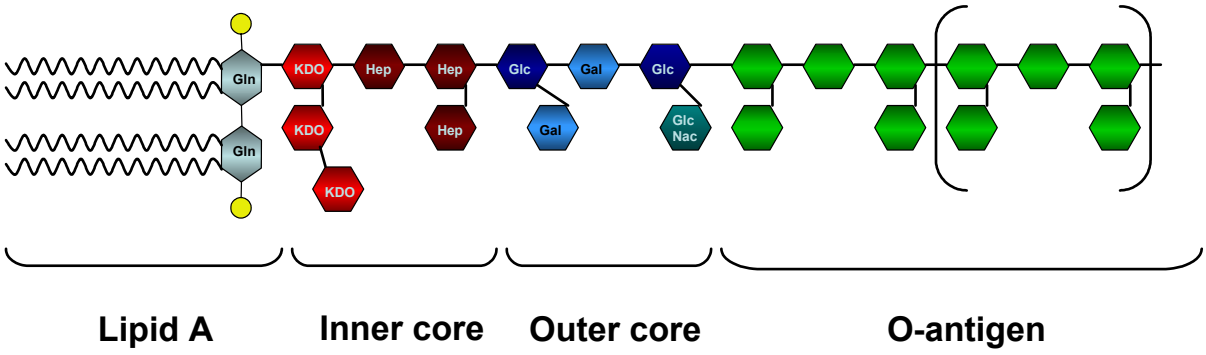

Figure 1.3 Structure of LPS

1.6 Lipoproteins and -peptides

Bacterial lipoproteins are constituents of the outer membrane of Gram-negative bacteria, Gram-positive bacteria and mycoplasma [73-75]. A common feature of lipopeptides from different bacteria is the N-terminal posttranslationally modified amino acid *S*-[2,3-dihydroxypropyl]-cysteine which carries covalently linked long

chain fatty acids at the amino-terminus and on both hydroxy groups of the 1,2-dihydroxypropyl group. In contrast to the lipid part, the protein moieties of different lipoproteins show no conspicuous sequence homology. The most prominent member of this class of molecules is Braun's lipoprotein of 7200 Da which represents the major constituent of the periplasmic space of the cell wall of enterobacteriaceae (Figure 1.4).

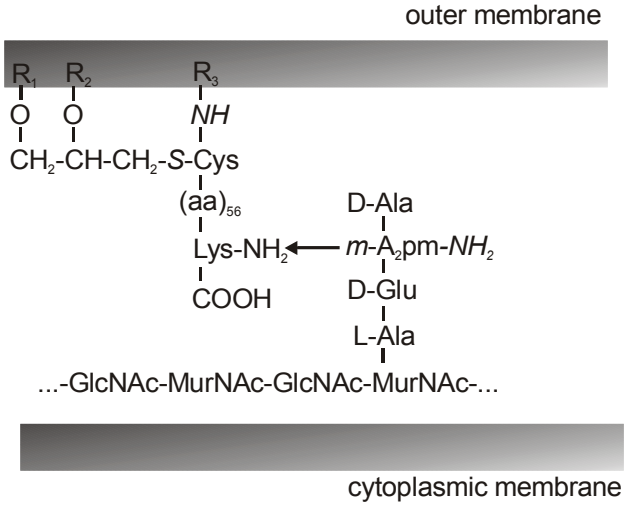

Figure 1.4 Composition and localization of Braun's lipoprotein (m-A2pm-NH2, meso-diaminopimelic acid; GlcNAc, N-acetylglucosamine; MurNAc, N-acetylmuraminic acid)

The hydrophobic N-terminus of this lipoprotein is imbedded into the bilayer of the outer membrane whereas the protein part is covalently or non-covalently associated with the peptidoglycan accomplishing a tight linkage between the murein and the membrane.

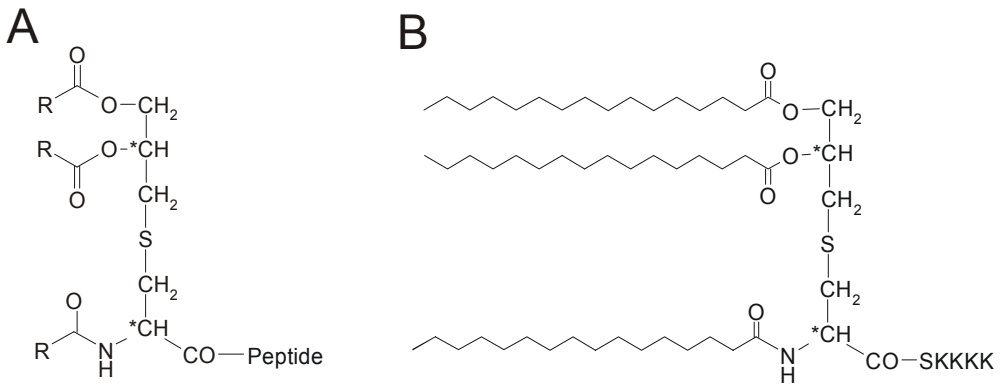

Figure 1.5 Structure of (A) lipopeptides and (B) $Pam_3Cys\text{-}SerLys_4$

Lipoproteins exhibit strong cell stimulating properties *in vivo* and *in vitro* including NF-κB activation, cytokine release, and B cell growth [76-81]. However, these immune stimulatory activities were not restricted to naturally occurring lipoproteins. Also synthetic lipopeptides containing only few amino acids have been shown to be efficient immune activators [79]. Because of their immune-stimulating properties and the absence of toxic side effects [82] lipopeptides attain relevance as adjuvant in vaccinations [83]. For instance, the application of Pam_3Cys-Ser-Ser covalently linked as adjuvant in a peptide-based vaccine against the foot-and-mouth disease virus provided a long-lasting protection [84]. A conjugate of lipopeptide, hapten and haplotype-specific T helper-cell epitope was able to evoke hapten-specific immune responses [85]. Moreover, synthetic lipopeptide conjugates containing MHC class I restricted peptides were able to efficiently prime virus-specific cytotoxic T cells [86]. The water soluble lipopeptide Pam_3Cys-SerLys_4 was shown to induce an immunostimulatory activity that is comparable to that of the complete Freunds Adjuvant (CFA).

Since lipopeptides are accessible by established synthesis protocols [79;80;87-93] and in high purity they are excellent candidates for investigations of the structure-activity relationships of TLR agonists. Spohn et al. [94] investigated whether either variations in the peptide moiety, S-[2,3-dihydroxypropyl]-cysteine scaffold, or length and amount of the fatty acids of lipopeptides influences the activity of these molecule. For the peptide moiety a length of at least two amino acids is essential for activity whereas the sequence of the peptide has almost no influence on the agonistic properties. For triacylated lipopeptides the biological activity was dependent on the length of the fatty acids and a reduction to ten and less carbon-atoms for each fatty acid resulted in a less active analogue. However, lipopeptides that contain only one fatty acid completely lost their immune-stimulating properties. Furthermore, agonistic activity was dependent on the presence of the sulfur atom in the S-[2,3-dihydroxypropyl]-cysteine scaffold and on the configuration of the two stereocenters of the lipoamino acid Pam_3Cys. RR-stereoisomers corresponding to the configuration of the natural N-terminal lipo-amino acid *S*-[2,3-bis(palmitoyloxy)-(2*R*)-propyl]-*N*-palmitoyl-(*R*)-cysteine of the bacterial lipoprotein of di- and triacylated lipopeptides are more active as agonists or adjuvants than the mixture of stereoisomers containing *S*-[2,3-bis(palmitoyloxy)-

(2*RS*)-propyl]-*N*-palmitoyl-(*R*)-cysteine or only the *S*-[2,3-bis(palmitoyloxy)-(2*S*)-propyl]-*N*-palmitoyl-(*R*)-cysteine stereoisomer [83;84;95].

1.7 Sepsis and septic shock

Sepsis is defined as a “systemic inflammatory response syndrome that occurs during infection” [96]. It represents an uncontrolled inflammatory response of the host against invading microorganisms and can lead to a life-threatening condition called septic shock. Paradoxically, due to the improved medical support, represented by invasive equipment, chemotherapy and immune suppression in patients, the cases of sepsis and septic shock have dramatically increased over the last decades. For instance, in the United States there are an estimated 750,000 new cases annually leading to about 200.000 cases of death [97]. Depending on the study Gram-negative bacteria were responsible for about 30 and 80%, Gram-positive bacteria for 6 and 24% of all cases of sepsis [98].

Due to pronounced complexity of the biochemical processes that precede sepsis and septic shock treatment is difficult to carry out. Bacterial compounds trigger the release a multitude of inflammatory mediators from cells of the innate immune system. These mediators are responsible for a number of systemic changes, such as vasodilatation, extravasations of neutrophils and monocytes, activation of leukocytes, lymphocytes and endothelial cells, myocardial suppression, microvascular coagulation, hypoperfusion, hypoxia and apoptosis. These conditions can result in the failure of organ function and finally in the death of the patients.

For the treatment of sepsis scientists have focussed on the identification of agents that interfere with components contributing to the initiation and progress of the disease. These components include bacterial products, early host inflammatory cytokines, bioactive lipid mediators, NO, endogenous immunostimulatory molecules, coagulation components, receptors and molecules involved in the TLR-dependent signal transduction [99]. Several agents have already been conducted in clinical trials such as corticosteroids [100], anti-endotoxin antibodies [101], TNF-α antagonists [102;103], IL-1 receptor antagonists [104] and recombinant activated protein C [105]. However, up to now only activated protein C has found application in the clinic [99] (Table 1.2).

Table 1.2 Selection of potential sepsis and septic shock therapies

Target	Drug	Comment
Endotoxin	Monoclonal α-lipid A antibody HA-1A	HA-1A: Reduced mortality in patients with Gram-negative sepsis but increased mortality in septic patients without Gram-negative bacteraemia [101]. *In vitro* studies revealed that HA-1A insufficiently neutralize endotoxin
	BPI 21-kDa peptide (rBPI21)	Modest reduction of mortality in human sepsis (Phase III) [106]
	cationic antimicrobial protein 18 kDa (CAP18)	Biological activity in preclinical studies [107]
	Polymyxin-B-dextran conjugate	No benefit (Phase II, not published)
	E5531	Synthetic endotoxin antagonist [108]
	Polyvalent immunoglobulin (intravenous immunoglobuline (IVIG))	Concentrated immunoglobulin from multiple donors enabled a significant mortality benefit
	Soluble TLR4	Inhibited LPS-mediated TNF-α secretion in mice [109]
Toll-like receptors	α-TLR2 antibody (T2.5)	Antagonistic antibody against the extracellular domain of TLR2. Inhibition of lipopeptide-induced TNF-α release in mice [110]
	Hydrocinnamoyl-*L*-valyl pyrrolidine	Blocks the Intracellular TIR-TIR domain interaction, thereby inhibiting IL-1-induced fever response [111]
Inflammatory cytokines	TNFR-Fc-fusion proteins of p55 and p75	p55 had no benefit in human sepsis and p75 was harmful [102;112]
	α-TNF antibodies	Effective in primates and mice but ineffective in humans [113]
	Recombinant IL-1 receptor antagonist (IL-1ra)	Small mortality benefit in human sepsis [104]
Lipid mediators Phosphlipase A_2,	sPLA2 small molecule inhibitor	No benefit

Platelet-activating factor	(Ly315920) and synthetic PAF receptor antagonist	
Prostaglandins	Ibuprofen	No benefit
Inducible nitric oxid synthase (iNOS)	*L*-*N*-monomethyl arginine (*L*-NMMA) *N*-omega-nitro-*L*-arginine methyl ester (*L*-NAME)	*L*-NMMA was harmful due to increase in blood pressure
Coagulation	Recombinant activated protein C (rAPC)	Significant reduction of mortality [105], due to decreases of inflammation by inhibition of platelet activation, neutrophil recruitment, and mast-cell degranulation, cytokine release in monocytes and adhesive interactions between neutrophils and endothelial cells. Despite of the induction of serious bleeding rAPC is the first drug for treatment of patients with severe sepsis in the clinic
	Antithrombin III	No benefit
Blood glucose	Insulin	Lowers mortality rate by an unknown mechanism
Immune response	IFN-γ	Immune enhancing therapy is beneficial in the hypo-immune phase of sepsis which occurs often prior death of the patients [114]
	Corticosteroids	physiological doses could improve survival (Phase III) [115] but large doses enhanced mortality in human sepsis

The failure to efficiently reduce the mortality rate of septic shock might be due to the outstanding relevance of the innate immune system. A total blockage of its components has found to be contraindicative. For instance, when soluble TNF-receptors were administered at high doses in patients with sepsis an increased mortality rate was observed [102]. This is in accordance with results from experiments with C3H/HeJ mice. The complete loss of TLR4 of these mice also led to an increased mortality rate after *S. typhimurium* challenge [116].

One important strategy for the treatment of sepsis constitutes the neutralization of PAMPs responsible for the initiation and progress of the disease. One factor that results in the increased release of PAMPs from the bacterial cell wall is the application of antibiotics for treatment of patients with bacteraemia. Especially

antibiotics of the β-lactam type [117] exhibit lytic properties against bacterial cells leading to enhanced endotoxin concentrations in serum [118]. For this reason, various investigations have focused on the identification of agents capable of neutralizing endotoxin. Several agents, including anti-LPS antibodies, LPS-binding proteins, peptides and lipopeptides have shown to neutralize endotoxin *in vivo* and *in vitro*. For instance, bactericidal permeability-increasing protein (BPI) a 55 kDa protein secreted from neutrophils and the lipopeptide antibiotic polymyxin B [119] exhibit strong LPS-neutralizing capacity [120]. Peptides with antimicrobial activity and especially those of the group of cationic α-helical peptides often possess LPS-neutralizing activity in addition to their lytic properties.

1.8 Antimicrobial peptides

Antimicrobial peptides are produced by vertebrates, invertebrate and plants and constitute an important component of the innate immune system. Among them peptides with cationic, amphipathic structures are particularly abundant and up to now, more than 500 natural occurring peptides of this class have been identified. Based on their structure cationic antimicrobial peptides can be divided into four different groups: α-helical, β-sheet, loop, and extended peptides [121] (Table 1.3)

Table 1.3 Several types of cationic antimicrobial peptides.

Peptide	Class	Host	Sequence
LL-37 (CAP18)	α-helical	Human	LLGDFFRKSKEKIGKEFKRIVYRIKDFLRNLVPRTES
Tachyplesin-1	β-sheet	Horseshoe crab	KWCFRVCYRGICYRRCR
Thanatin	loop	Spinded soldier bug	GSKKPVPIIYCNRRTGKCQRM
Indolicidin	extended	Bovine	ILPWKWPWWPWRR

The antimicrobial activity of those peptides is based on the property to interact with bacterial membranes [121]. This binding is mediated by electrostatic interactions between cationic charges of the peptide and the negatively charged

LPS in the outer leaflet of the outer membrane of the bacterial cell wall. Thereby the peptides displace divalent cations from LPS resulting in the destabilization of the membrane structure and translocation into the bacterium. This process is called self-promoted uptake. Subsequently peptides breach the cytoplasmic membrane in a disruptive or non-disruptive manner. Most cationic α-helical antimicrobial peptides exhibit membrane disruptive properties and three models have been described: the barrel stave, the micellar aggregate and the carpet model. In the barrel-stave model [122;123], the amphipathic peptides form transmembrane pores which destroy the membrane potential and enable leakage of cytoplasmic components. Within the pores the hydrophobic side chains of the peptides face into the lipid environment whereas the polar side chains point inwards into the pores [124]. In the micellar aggregate model the peptides form micelles or aggregates inside the membrane [125]. The translocation of the peptides into the cytoplasm is accomplished by collapse of these structures. In the carpet model, peptides arrange parallel to the bilayer without intruding into the membrane [126]. This arrangement results in a local disturbance of membrane stability leading to the disruption of the membrane potential, the disintegration of the membrane and followed by leakage of cytoplasmic components.

1.8.1 α-Helical peptides

A considerable number of α-helical antimicrobial peptides and their synthetic derivatives possess LPS-binding and –neutralizing activity [127-129]. The α-helix structure is often interrupted by a bend in the centre of the molecule. Magainins are α-helical peptides from *Xenopus laevis* [130] which possesses antimicrobial activities at concentrations 50 μg/ml against *E. coli*. It was shown that the 23-peptide magainin 2 uses the the micellar-aggregate model for bacterial killing [125]. As determined by investigations of the structure-activity relationships of magainins, this activity was dependent on both, the length and the positive net charge of the peptide. Truncation to fewer than 20 residues led to a loss in activity due to the disability of the shorter analogue to span the lipid bilayer [131] whereas the enhancement of total net charge led to an increase in antimicrobial activity [132].

Alamethicin, isolated from the fungus *Trichoderma viride* [122;133], is a well characterized α-helical peptide with antimicrobial activity. In membranes, synthetic analogues of alamethicin form circular oligomeric bundles [134] following the barrel stave mechanism. This leads to the formation of a large number of small potential dependent channels of varying size allowing the leakage of ions at nM concentrations and lysis of cells at μM concentrations.

1.8.2 β-Sheet peptides

β-Sheet peptides possess an antiparallel β-sheet structure stabilized by disulfide bonds. Tachyplesins are peptides with 17-18 residues of this class isolated from the haemocytes of the Japanese horseshoe crab, *Tachypleus tridentatus* [135]. Because linearization of the peptides results in a loss of function, the β-sheet structure is a prerequisite for activity. The mode of action, however, is poorly understood and, despite of their high affinity for LPS [136], it is thought that Tachyplesins also address intracelluar targets [137].

1.8.3 Extended peptides

Because of their high proline and/or glycine content extended peptides do not exhibit classical secondary structure. These peptides interact with membrane lipids via hydrogen bond and van der Waals interactions. Indolicidin, isolated from granules of bovine neutrophils has the highest known content of tryptophan of all naturally occurring peptides [138;139]. To exhibit antimicrobial activity (10 μg/ml) the 13-peptide forms feature less aggregate channels which lead to a translocation of the peptide into the cytoplasm. In contrast, it does not have a high affinity for LPS compared to tachyplesins [140].

1.8.4 Loop peptides

Loop peptides such as the 21-residue peptide Thanatin, isolated from spined soldier bug *Podisus maculiventris* [141] are characterized by a loop structure, stabilized by disulfide, amide or isopeptide bonds. Thanatin possesses an antimicrobial activity against Gram-negative and –positive bacteria as well as

activity against fungi. For granmycin S, another member of this family, also LPS-neutralizing capacity was observed [142].

2 A CD14 domain with LPS-binding and –neutralizing activity

This chapter was adapted from a manuscript accepted for publication in *ChemBioChem*. The author of this thesis performed all experiments except site directed mutagenesis.

2.1 Summary

The 55 kDa protein CD14 binds to lipopolysaccharide (LPS) and several other bacterial cell wall components. CD14 plays a central role in TLR2- and TLR4-mediated signaling in the innate immune response. To identify the structural determinants involved in ligand recognition synthetic peptides of 20 amino acids covering the complete CD14 sequence with ten amino acids overlap were tested for their potential to neutralize the LPS-dependent induction of IL-8 secretion in human myelomonocytic THP-1 cells. The peptide CD14 (81-100) exhibited a strong neutralizing activity, which was demonstrated to be based on its ability to bind to LPS. A detailed analysis of the structure-activity relationships revealed a set of aliphatic residues involved in binding that are highly conserved among CD14 proteins from different species. Mutant proteins, in which the relevant residues were exchanged, failed to bind LPS in cellular experiments. Circular dichroism spectroscopy showed that the peptide assumed an α-helical secondary structure under mild helix-inducing conditions. Peptides corresponding to the structural determinants of LPS-binding proteins are potential agents for interfering with the initiation of LPS-mediated immunological disorders, such as septic shock. Therefore analogues of the CD14-derived LPS-binding peptide were synthesized with improved solubility and inhibitory activity in cellular assays and in the *Limulus* amebocyte lysate assay. In summary, our results confirm that this domain and especially leucine residues 87, 91 and 94 contribute to the LPS-binding site of human CD14. The corresponding peptides constitute a basis for the generation of LPS-neutralizing agents.

2.2 Introduction

Lipopolysaccharide (LPS) is a highly potent immune stimulatory component of the cell wall of Gram-negative bacteria. Low concentrations in blood lead to moderate immune responses in healthy humans, whereas higher concentrations may induce massive release of cytokines, resulting in life threatening disorders such as septic shock [143]. Once released from the bacterial cell wall, LPS is sequestered by the serum protein lipopolysaccharide-binding protein (LBP), which transfers LPS to CD14 [144;145]. CD14 is a 55 kDa glycoprotein of 356 amino acids (Figure 2.1) that is expressed in a GPI-anchored and in a soluble form.

```
       -10         01          11          21          31          41
         |          |           |           |           |           |
MERASCLLLL LLPLVHVSAT TPEPCELDDE DFRCVCNFSE PQPDWSEAFQ CVSAVEVEIH

        51          61          71          81          91         101
         |          |           |           |           |           |
AGGLNLEPFL KRVDADADPR QYADTVKALR VRRLTVGAAQ VPAQLLVGAL RVLAYSRLKE

       111         121         131         141         151         161
         |          |           |           |           |           |
LTLEDLKITG TMPPLPLEAT GLALSSLRLR NVSWATGRSW LAELQQWLKP GLKVLSIAQA

       171         181         191         201         211         221
         |          |           |           |           |           |
HSPAFSCEQV RAFPALTSLD LSDNPGLGER GLMAALCPHK FPAIQNLALR NTGMETPTGV

       231         241         251         261         271         281
         |          |           |           |           |           |
CAALAAAGVQ PHSLDLSHNS LRATVNPSAP RCMWSSALNS LNLSFAGLEQ VPKGLPAKLR

       291         301         311         321         331         341
         |          |           |           |           |           |
VLDLSCNRLN RAPQPDELPE VDNLTLDGNP FLVPGTALPH EGSMNSGVVP ACARSTLSVG

       351
         |
VSGTLVLLQG ARGFA
```

Figure 2.1 Amino acid sequence of human CD14. The mature glycoprotein has a molecular weight of 55 kDa and consists of 356 amino acids. The signal peptide comprises 19 amino acids (grey). The protein is characterized by a high leucine content (17.7%) and eleven leucine-rich repeats of 21 to 36 residues which are located within the C-terminal part (residue 73 to 349). LRR 1 contains 29 amino acids and is underlined in the sequence.

The GPI-anchored form is preferentially expressed on cells of the myeloid lineage, i. e. monocytes, macrophages and polymorphonuclear granulocytes [14;15]. The soluble form (sCD14) plays a role in the LPS response of endothelial and epithelial cells [16-18]. The endotoxin-CD14 complex engages Toll-like receptor 4 (TLR4) [12], initiating an intracellular signaling cascade and the expression of genes involved in the regulation of the immune response.

In addition to LPS, CD14 binds a panel of components of Gram-negative and -positive bacteria which are implicated in the initiation of TLR2-dependent signal transduction. These components include lipoarabinomannan of *Mycobacterium tuberculosis* [146;147], peptidoglycan [148], lipoteichoic acid [149], and spirochetal outer membrane lipoproteins and lipopeptides [150]. For this reason, CD14 was defined as a pattern recognition receptor in innate immunity [147].

Because of this central role, several studies have focused on the identification of structural elements in CD14 involved in ligand recognition and binding. It was shown, that the N-terminal part comprising amino acids 1-152 is sufficient for binding and for enabling cellular responses to LPS, both for the soluble and the membrane-bound form [151;152]. Hydrophilic regions and amino acids within the N-terminal portion were identified for serum-dependent binding of LPS to CD14 by constructing a series of single and combined deletion mutants of membrane-anchored CD14 [153]. However, only one of these mutations affected the LPS-binding of sCD14 in a further study [154]. Due to these discrepancies, the authors proposed that different structural determinants may contribute to LPS receptor function for the soluble and the membrane-anchored forms of CD14. The involvement of individual hydrophilic amino acids within the N-terminal 66 amino acids in binding soluble CD14 to LPS was further investigated by serine replacement and charge reversal [155;156]. However, only charge reversal of amino acid side chains abolished the function of the protein. Amino acids 57 to 64 were protected by LPS from the action of Asp-N protease and chymotrypsin and deletion of this particular region resulted in a non-functional mutant which neither bound LPS nor triggered cellular responses to LPS [157;158]. Evidence for a contribution of amino acids 39 to 44 to LPS-binding was obtained from a mutant in which all amino acids were exchanged by a stretch of alanine residues [159]. Alternatively, a further study suggested that the LPS-binding site might be a conformational epitope comprising several other regions of the protein [160].

Furthermore, one report showed that amino acids 9 to 13 and 91 to 101 participate in sCD14-mediated signaling, however, not for all of the tested immunologically relevant cell types [161]. In summary, in spite of these investigations, many questions on the function of CD14 still remain.

Synthetic peptides covering parts of a protein represent an alternative strategy for the identification of ligand-binding domains. Peptides derived from *Tachypleus* anti-LPS factor [162], *Limulus* anti-LPS factor (LALF) [163;164], bactericidal/permeability increasing protein (BPI) [165], human cationic antibacterial protein of 18 kDa (hCAP18) [107;128], lactoferrin [166], LBP [167], and the lipopeptide antibiotic polymyxin B [168] have been identified as endotoxin-binding and -neutralizing agents. A structural comparison of these LPS-binding peptides and further analyses of structure-activity relationships showed that an amphiphilic structure with a net positive charge as well as a considerable hydrophobicity are a general characteristic of these molecules. The spatial organization of the positive and hydrophobic moieties largely determines the LPS-binding and -neutralizing activity [169-171]. It can be assumed that the positively charged amino acid residues interact with the negatively charged moieties of the LPS such as the phosphate groups whereas hydrophobic amino acids may bind to the fatty acid chains of LPS [172].

LPS-binding peptides might possess potential as drugs for the treatment of sepsis and septic shock [127;128;173] and for the generation of affinity reagents for the removal of LPS from the blood stream [174]. Analyses of structure-activity relationships of such peptides that contribute to an understanding of the mode of binding are therefore highly relevant for the generation of optimized LPS-neutralizing agents.

To identify structural determinants of CD14 involved in LPS-binding a systematic peptide-based approach using 20-peptides with 10 amino acids overlap that covered the complete mature protein was performed. 20-Peptides are sufficiently long to form secondary structure elements corresponding to those formed in full length proteins [175]. Initially all peptides were screened for their ability to antagonize the LPS-induced IL-8 secretion in THP-1 cells. The rather hydrophobic peptide corresponding to amino acids 81 to 100 had a strong inhibitory activity. This activity was attributed to a direct interaction of the peptide with LPS. Detailed analyses of structure-activity relationships revealed that leucine residues are

required of this inhibitory activity. The relevance of the respective residues for ligand recognition by the full-length protein was confirmed by functional analysis of mutant CD14 molecules. The analysis of the structure-activity relationships of this peptide led to the rational design of LPS-neutralizing molecules with improved activity.

2.3 Results

2.3.1 Screening of overlapping 20-peptides for inhibition of LPS-induced IL-8 production in THP-1 cells.

To identify functional domains of human CD14 that interfere with LPS-induced signaling the entire mature 356-amino acid protein was covered by 35 synthetic 20-peptides with 10 amino acids overlap (Table 2.1).

All peptides were synthesized as fluorescein-labeled peptide amides by parallel solid-phase peptide synthesis using Fmoc-chemistry. N-terminal coupling of carboxyfluorescein was performed using optimized procedures for the labeling of peptide collections with uniform yields [176]. Labeling with carboxyfluorescein (i) allowed the reliable determination of peptide concentrations based on the absorption of the fluorophore and (ii) enabled the detection of potential interactions with living cells using fluorescence microscopy and flow cytometry.

Except for the peptide corresponding to amino acids 21 to 40 all peptides were obtained in purities exceeding 75% as determined by RP-HPLC. Peptides were used for biological testing without further purification. For some hydrophobic peptides precipitates formed upon dilution of DMSO stock solutions into aqueous buffers. This problem was circumvented by first diluting the DMSO stock solutions 1:10 in *tert.*-butyl alcohol/H_2O (4:1) followed by dilution in aqueous buffers to the working concentrations.

Table 2.1 To cover the entire sequence of mature human CD14 fluorescein-labeled peptide amides of 20 amino acids with 10 amino acids overlap were synthesized. Except for peptide corresponding to amino acids 21-40 all peptides were obtained in purities exceeding 75%. Peptide amides were tested for their capacity to interfere with the LPS-induced IL-8 secretion.

Sequence position	Peptide sequence
1-20	Fluo-TTPEPCELDDEDFRCVCNFS-NH_2
11-30	Fluo-EDFRCVCNFSEPQPDWSEAF-NH_2
21-40	Fluo-EPQPDWSEAFQCVSAVEVEI-NH_2
31-50	Fluo-QCVSAVEVEIHAGGLNLEPF-NH_2
41-60	Fluo-HAGGLNLEPFLKRVDADADP-NH_2
51-70	Fluo-LKRVDADADPRQYADTVKAL-NH_2
61-80	Fluo-RQYADTVKALRVRRLTVGAA-NH_2
71-90	Fluo-RVRRLTVGAAQVPAQLLVGA-NH_2
81-100	Fluo-QVPAQLLVGALRVLAYSRLK-NH_2
91-110	Fluo-LRVLAYSRLKELTLEDLKIT-NH_2
101-120	Fluo-ELTLEDLKITGTMPPLPLEA-NH_2
111-130	Fluo-GTMPPLPLEATGLALSSLRL-NH_2
121-140	Fluo-TGLALSSLRLRNVSWATGRS-HN_2
131-150	Fluo-RNVSWATGRSWLAELQQWLK-NH_2
141-160	Fluo-WLAELQQWLKPGLKVLSIAQ-NH_2
151-170	Fluo-PGLKVLSIAQAHSPAFSCEQ-NH_2
161-180	Fluo-AHSPAFSCEQVRAFPALTSL-NH_2
171-190	Fluo-VRAFPALTSLDLSDNPGLGE-NH_2
181-200	Fluo-DLSDNPGLGERGLMAALCPH-NH_2
191-210	Fluo-RGLMAALCPHKFPAIQNLAL-NH_2
201-220	Fluo-KFPAIQNLALRNTGMETPTG-NH_2
211-230	Fluo-RNTGMETPTGVCAALAAAGV-NH_2
221-240	Fluo-VCAALAAAGVQPHSLDLSHN-NH_2
231-250	Fluo-QPHSLDLSHNSLRATVNPSA-NH_2
241-260	Fluo-SLRATVNPSAPRCMWSSALN-NH_2
251-270	Fluo-PRCMWSSALNSLNLSFAGLE-NH_2
261-280	Fluo-SLNLSFAGLEQVPKGLPAKL-NH_2
271-290	Fluo-QVPKGLPAKLRVLDLSCNRL-NH_2
281-300	Fluo-RVLDLSCNRLNRAPQPDELP-NH_2
291-310	Fluo-NRAPQPDELPEVDNLTLDGN-NH_2
301-320	Fluo-EVDNLTLDGNPFLVPGTALP-NH_2
311-330	Fluo-PFLVPGTALPHEGSMNSGVV-NH_2
321-340	Fluo-HEGSMNSGVVPACARSTLSV-NH_2
331-350	Fluo-PACARSTLSVGVSGTLVLLQ-NH_2
337-356	Fluo-TLSVGVSGTLVLLQGARGFA-NH_2

Peptides were tested for their ability to interfere with LPS-induced IL-8 secretion in human monocyte-derived THP-1 myelomonocytic leukaemia cells. At a concentration of 10 μM one peptide, corresponding to amino acids 81 to 100 of human CD14, reduced the secretion of IL-8 by 80%. All other peptides exhibited

no significant inhibitory capacity (Figure 2.2). The peptide CD14 (21-40) was not obtained in adequate purity.

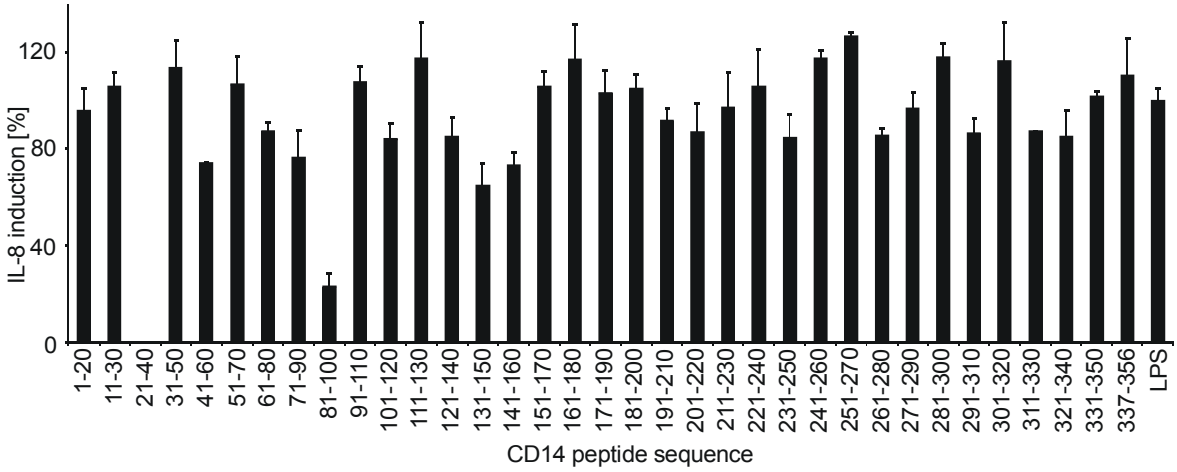

Figure 2.2 Influence of 20-peptide amides derived from human CD14 on the LPS-induced IL-8 secretion in THP-1 cells. After 10 min incubation with fluorescein-labeled peptide amides (10 μM), THP-1 cells were treated with LPS (*E. coli* O111:B4, 20 ng/ml) for 5 h. The secretion of IL-8 was detected in cell free supernatants by ELISA. The LPS-induced IL-8 secretion is shown in relation to a sample that was incubated with buffer containing a concentration of DMSO/*tert.*-butyl alcohol corresponding to the one of the peptide-containing samples and stimulated with LPS. The individual 20-peptide amides are specified by their amino acid positions. In several synthetic approaches peptide CD14 (21-40) was not obtained in adequate purity (>75%). The error bars represent the standard deviation of triplicates within one experiment.

For a fine mapping of the active region of the peptide CD14 (81-100) a further set of nine 20-peptides covering amino acids 73 to 108 with 18 amino acids overlap was synthesized and tested (Table 2.2). This second scan again confirmed CD14 (81-100) with the natural sequence as the most active peptide (Figure 2.3).

Table 2.2 For fine mapping of region 73 to 108 of mature human CD14 fluorescein-labeled peptide amides of 20 amino acids with 18 amino acids overlap were synthesized. Peptides were tested for their capacity to influence the LPS-induced IL-8 secretion.

Peptide	Sequence
73-92	Fluo-RRLTVGAAQVPAQLLVGALR-NH_2
75-94	Fluo-LTVGAAQVPAQLLVGALRVL-NH_2
77-96	Fluo-VGAAQVPAQLLVGALRVLAY-NH_2
79-98	Fluo-AAQVPAQLLVGALRVLAYSR-NH_2
81-100	Fluo-QVPAQLLVGALRVLAYSRLK-NH_2
83-102	Fluo-PAQLLVGALRVLAYSRLKEL-NH_2
85-104	Fluo-QLLVGALRVLAYSRLKELTL-NH_2
87-106	Fluo-LVGALRVLAYSRLKELTLED-NH_2
89-108	Fluo-GALRVLAYSRLKELTLEDLK-NH_2

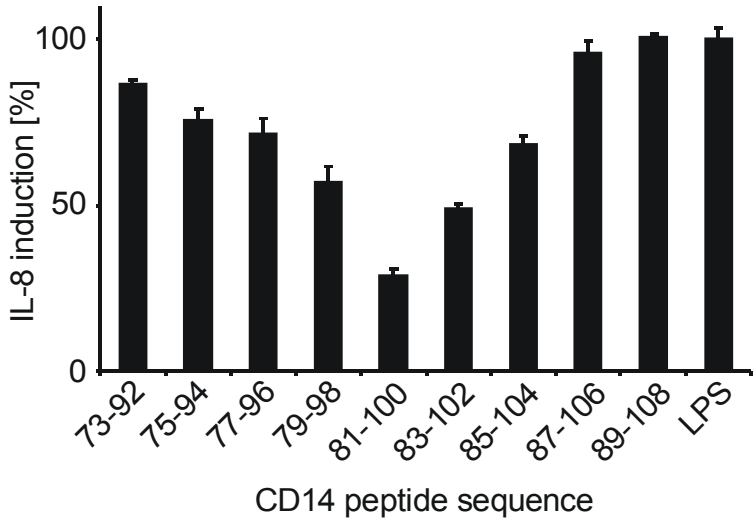

Figure 2.3 Fine mapping of the region covering amino acids 73 to 108 of human CD14. After incubation (10 min) with fluorescein-labeled peptide amides (10 μM) cells were stimulated with LPS (20 ng/ml) for 5 h. Cell free supernatants were collected and analysed for IL-8 secretion by ELISA. The LPS-induced IL-8 secretion is shown in relation to a sample only stimulated with LPS. The individual 20-peptides are specified by their amino acid positions. Error bars represent the standard deviation of triplicates.

The inhibitory effect of CD14 (81-100) was concentration-dependent (Figure 2.4). Viability of cells was fully preserved for all peptides as determined by MTT-assay (data not shown). At concentrations above 15 μM cytotoxicity of peptide CD14 (81-100) was observed.

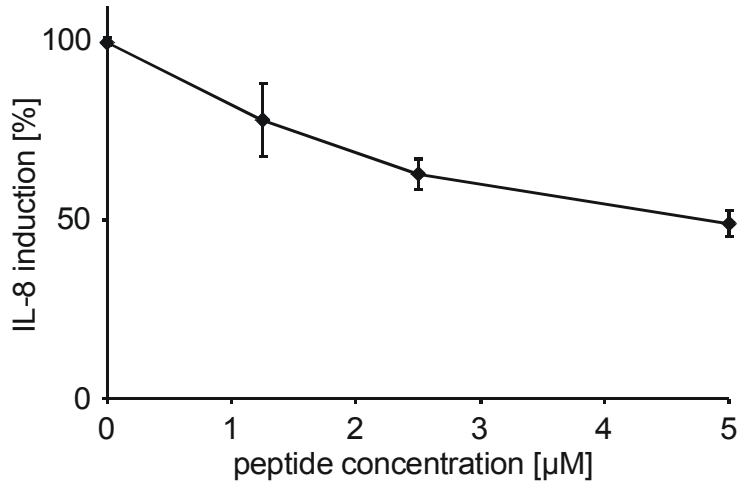

Figure 2.4 Concentration dependence of the LPS-neutralizing activity of CD14 (81-100). After 10 min incubation with the fluorescein-labeled peptide amide at the indicated concentrations, cells were stimulated with LPS (20 ng/ml) for 5 h. The LPS-induced IL-8 secretion is shown in relation to a sample stimulated with LPS in the absence of peptide. Error bars represent the standard deviation of triplicates.

2.3.2 Identification of residues in CD14 (81-100) critical for the inhibition of IL-8 secretion.

Residues important for the inhibitory capacity of CD14 (81-100) were identified by performing an alanine scan through the entire 20-amino acid sequence (Table 2.3).

Table 2.3 Fluorescent peptide amides with alanine substitutions for each amino acid position.

Substituted amino acid	Sequence
Q	Fluo-**A**VPAQLLVGALRVLAYSRLK-NH_2
V	Fluo-Q**A**PAQLLVGALRVLAYSRLK-NH_2
P	Fluo-QV**A**AQLLVGALRVLAYSRLK-NH_2
A	Fluo-QVP**A**QLLVGALRVLAYSRLK-NH_2
Q	Fluo-QVPA**A**LLVGALRVLAYSRLK-NH_2
L	Fluo-QVPAQ**A**LVGALRVLAYSRLK-NH_2
L	Fluo-QVPAQL**A**VGALRVLAYSRLK-NH_2
V	Fluo-QVPAQLL**A**GALRVLAYSRLK-NH_2
G	Fluo-QVPAQLLV**A**ALRVLAYSRLK-NH_2
A	Fluo-QVPAQLLVG**A**LRVLAYSRLK-NH_2
L	Fluo-QVPAQLLVGA**A**RVLAYSRLK-NH_2
R	Fluo-QVPAQLLVGAL**A**VLAYSRLK-NH_2
V	Fluo-QVPAQLLVGALR**A**LAYSRLK-NH_2
L	Fluo-QVPAQLLVGALRV**A**AYSRLK-NH_2
A	Fluo-QVPAQLLVGALRVL**A**YSRLK-NH_2
Y	Fluo-QVPAQLLVGALRVLA**A**SRLK-NH_2
S	Fluo-QVPAQLLVGALRVLAY**A**RLK-NH_2
R	Fluo-QVPAQLLVGALRVLAYS**A**LK-NH_2
L	Fluo-QVPAQLLVGALRVLAYSR**A**K-NH_2
K	Fluo-QVPAQLLVGALRVLAYSRL**A**-NH_2

When leucines at positions 11 and 14, corresponding to positions 91 and 94 of mature CD14, were replaced by alanine the ability of the peptide to inhibit the LPS-induced IL-8 secretion was almost or fully lost. For peptides mutated at amino acids in positions 6, 7, 9, 12, and 16-20 the LPS-induced IL-8 secretion was 50 to

70%. In contrast, exchange of amino acids 1-3, 5, 8 and 13 by alanine did not affect the ability to inhibit the LPS-induced IL-8 secretion on THP-1 cells (Figure 2.5).

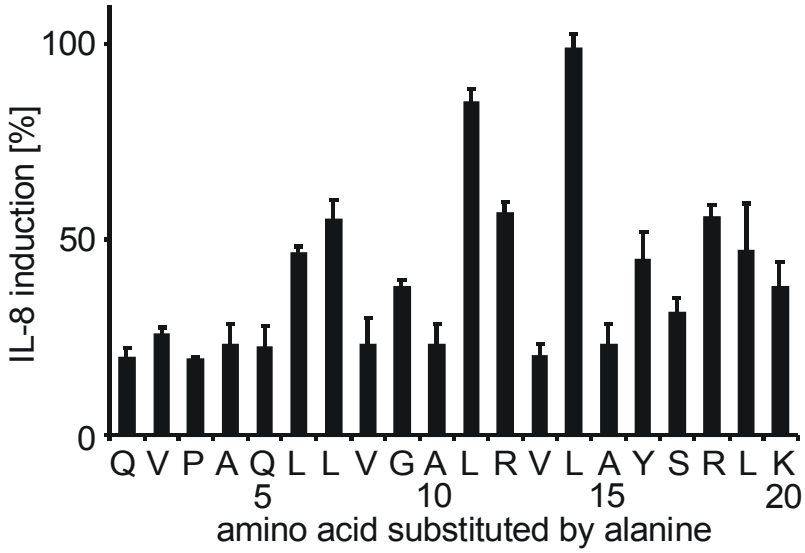

Figure 2.5 Alanine scan for the identification of residues critical for CD14 (81-100) activity. Fluorescent peptide amides with positional alanine substitutions were screened for their ability to suppress the IL-8 production of LPS-stimulated THP-1 cells. Incubation conditions were identical to those described for Figure 2.2. Error bars represent the standard deviation of triplicates.

2.3.3 Inhibitory activity of the murine homolog of CD14 (81-100) and the conservation of the sequence in CD14 proteins of different species.

To address, whether the activity of the human CD14-derived peptide represented a functionally conserved property of the protein and not just an activity of this particular peptide, the corresponding fluorescein labeled peptide amide Fluo-RIPSRILFGALRVLGISGLQ-NH_2 from murine CD14 was synthesized (Table 2.4) and tested for its capacity to inhibit the LPS-induced IL-8 secretion in human THP-1 cells. The inhibitory activity of the murine peptide was comparable to the one of the human counterpart (Figure 2.6). The human and murine peptides have a high sequence similarity with identical amino acid residues in positions 3, 7, 9 to 14, 17 and 19 and conservative exchanges in positions 2, 6 and 15.

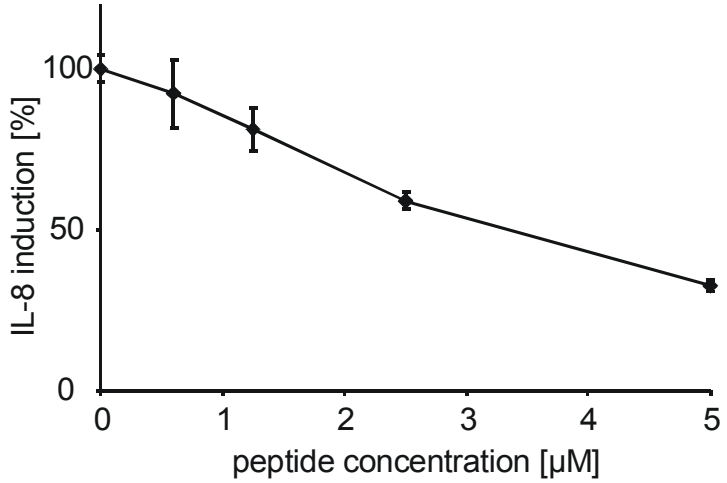

Figure 2.6 Titration of THP-1 cells with mCD14 (96-115). THP-1 cells were incubated with the fluorescein-labeled peptide amide at the indicated concentrations for 10 min. Subsequently cells were stimulated with LPS (20 ng/ml) for 5 h and the LPS-induced IL-8 secretion was determined in cell free supernatants by ELISA. IL-8 secretion is shown in relation to a sample stimulated with LPS in the absence of peptide. Error bars represent the standard deviation of triplicates.

A further sequence comparison of the human CD14 (81-100) peptide with the corresponding sequences of the murine, bovine, rat and rabbit proteins revealed a strict conservation of leucines 11 and 14, both of which were shown to be essential for the inhibitory activity of the human peptide. In addition, leucines in positions 7 and 19 were also fully conserved and in positions 2 and 6 only residues with aliphatic side chains were present (Table 2.4).

Table 2.4 Sequence comparison amino acids 81-100 of human CD14 with the corresponding sequences of CD14 proteins from other species. Leucine residues in position 11 and 14 are bold-face.

Species	Amino acids[1]	Sequence
human	100-119	QVPAQLLVGA**L**RV**L**AYSRLK
bovine	99-118	QVPAQLLVAV**L**RA**L**GYSRLK
rabbit	100-119	QVPAPLLLGV**L**RV**L**GYSRLK
mouse	96-115	RIPSRILFGA**L**RV**L**GISGLQ
rat	101-120	RVPTQILFGT**L**RV**L**GYSGLR

[1] The amino acid positions of the sequences refer to the ones of the immature proteins containing the putative signal peptides.

2.3.4 Binding of CD14 (81-100) to LPS aggregates

Previous studies have shown that the domain comprising the amino acid residues 91-100 in human CD14 was involved in LPS-signaling rather than LPS-binding [160]. Therefore we first assumed that CD14 (81-100) might interact with proteins involved in TLR4-dependent signaling, probably downstream of CD14. To determine whether the peptide interact with cells a fluorescein-labeled analogue of CD14 (81-100) was incubated with signaling competent THP-1 cells and analysed by confocal laser scanning microscopy and flow cytometry. However, up to a peptide concentration of 10 μM no binding of the peptide to the cells could be detected. Next, THP-1 cells were co-incubated with an analogue of CD14 (81-100) that was N-terminally labeled with the Cy5-like dye S0387 [177] and FITC-LPS. Again, the CD14 derived peptide did not bind to the cells but colocalized with aggregates of the TLR4-agonist probably resulting from a direct interaction between the two molecules (Figure 2.7).

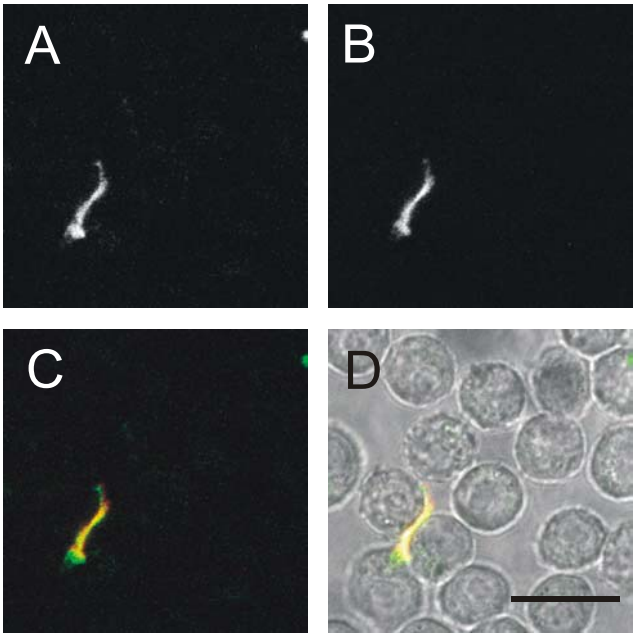

Figure 2.7 Co-incubation of THP-1 cells with a S0387-labeled peptide amide corresponding to the sequence 81-100 of human CD14 (10 μM) and FITC-LPS (1 μg/ml). After 30 min incubation cells were washed twice with medium and samples were imaged by confocal laser scanning microscopy: (A) FITC-LPS, (B) S0387-labeled peptide CD14 (81-100), merged (C), and transmission (D). The scale bar represents 20 μm.

2.3.5 Direct binding of bead-immobilized CD14 (81-100) to FITC-LPS

Due to the fact that the inhibitory fluorescein-labeled peptides did not bind to cells, but directly interact with LPS aggregates, we more precisely investigated whether CD14 (81-100) exerted its inhibitory activity on IL-8 secretion by specifically binding to LPS. With a surplus in positive charge and a significant fraction of hydrophobic residues, CD14 (81-100) shares structural characteristics with other LPS-binding and -neutralizing peptides. Analogues of CD14 (81-100) N-terminally elongated by two 8-amino-3,6-dioxaoctanoic acid spacer moieties and biotin were synthesized (Table 2.5) and bound to streptavidin-conjugated Sepharose beads.

Table 2.5 Biotinylated peptide amides for immobilization on streptavidin-conjugated Sepharose beads to determine binding of FITC-LPS to CD14 (81-100). The peptides contain two 8-amino-3,6-dioxaoctanoic acid spacers (Ado) between the biotin and the peptide moiety.

Position	Sequence
81-100	Biotin-Ado-Ado-QVPAQLLVGALRVLAYSRLK-NH_2
171-190	Biotin-Ado-Ado-VRAFPALTSLDLSDNPGLGE-NH_2

The interaction of LPS with the peptide was investigated by incubation of a fluorescein-labeled LPS with beads loaded with CD14 (81-100) (Figure 2.8). Binding of FITC-LPS to the beads was specific for CD14 (81-100). For beads without peptide or loaded with the inactive peptide CD14 (171-190), bead-associated fluorescence could be completely removed by washing the beads three times with PBS containing Tween (0.2%). The specificity of the binding was further confirmed by incubation of the CD14 (81-100)-loaded beads in the presence of FITC-LPS and either a 50-fold excess of unlabeled LPS or in the presence of a CD14 (81-100) analogue with improved solubility (peptide 31, see below).

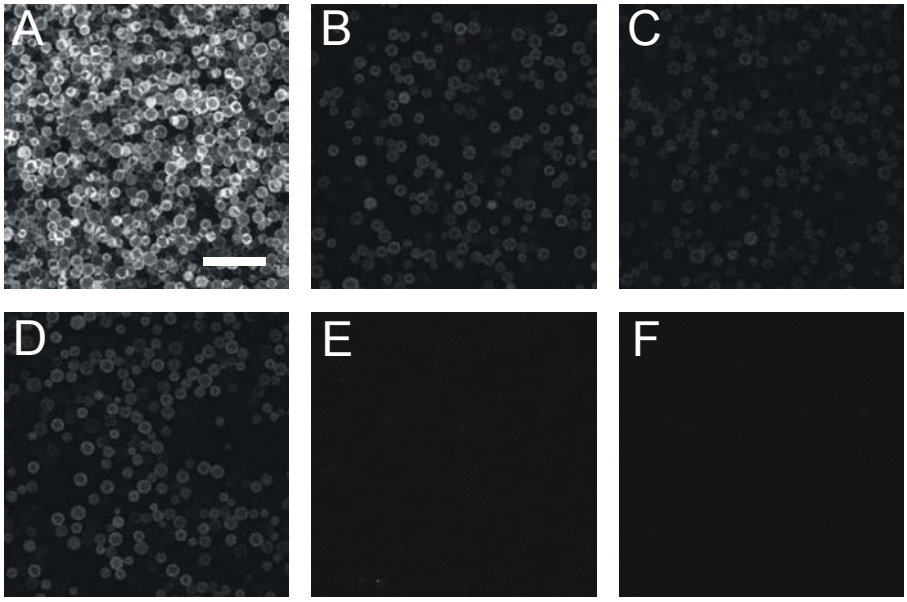

Figure 2.8 LPS-binding by CD14 (81-100). Streptavidin beads loaded with biotinylated CD14 (81-100) were incubated with (A) FITC-LPS (2 μg/ml), (B) co-incubation with FITC-LPS and 150 μg/ml unlabeled LPS, co-incubation with (C) 20 μM or (D) 2 μM unlabeled peptide 31 (Table 2.7). The specificity of the LPS binding was further confirmed by incubation of peptide-free streptavidin beads with FITC-LPS and (E) by incubation of streptavidin beads loaded with biotinylated peptide CD14 (171-190) with FITC-LPS (F). Beads were analysed by fluorescence microscopy. The scale bar corresponds to 200 μm.

2.3.6 Validation of the LPS-binding site in the full length protein

In the recently published crystal structure of human CD14 [178] leucine residues at positions 87, 91 and 94 point inwards into the putative LPS-binding pocket (Figure 2.9). However, the crystal structure was obtained in the absence of ligand and therefore a functional role of these residues in the recognition of ligand still remains to be demonstrated. The alanine scan suggested that at least in the context of the CD14-derived peptide these residues are required for the inhibitory activity.

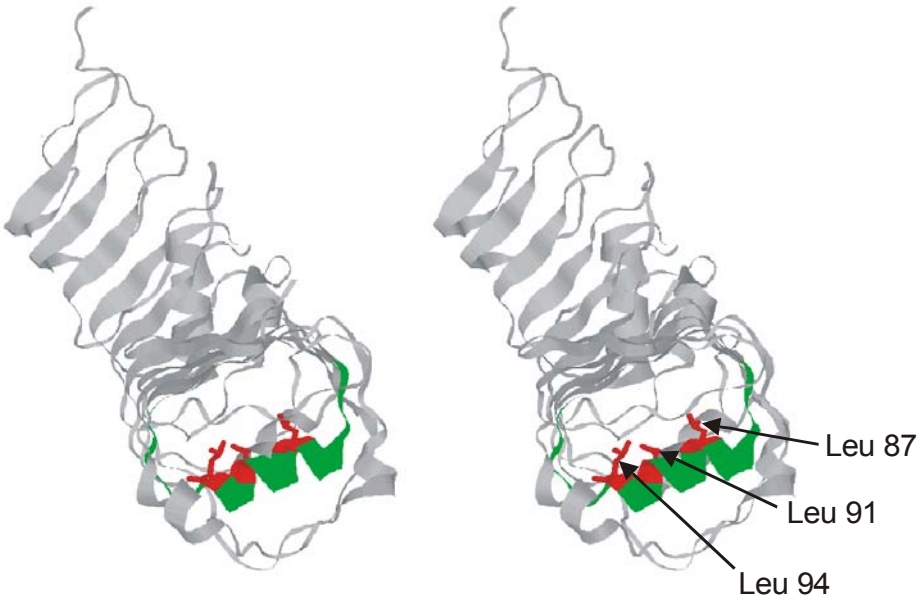

Figure 2.9. The crystal structure of CD14. Residues 81-100, comprising helix 4, are coloured in green and leucine residues 87, 91 and 94 are shown in red. Side chains of the leucine residues point into the N-terminal pocket which corresponds to the putative LPS binding site of the protein.

To validate this result in the context of the entire protein, mutant CD14 proteins, in which the relevant leucine residues were changed to either glutamine or proline residues, were expressed in HEK 293T cells and analysed for FITC-LPS binding by flow cytometry and confocal laser scanning microscopy (Figure 2.10). Cells expressing the wild type CD14 protein bound FITC-LPS efficiently, whereas cells expressing mutant CD14 proteins at comparable levels did not show any LPS-binding capacity. Confocal laser scanning microscopy confirmed that cells expressing high levels of the mutant protein at the plasma membrane did not show any LPS binding.

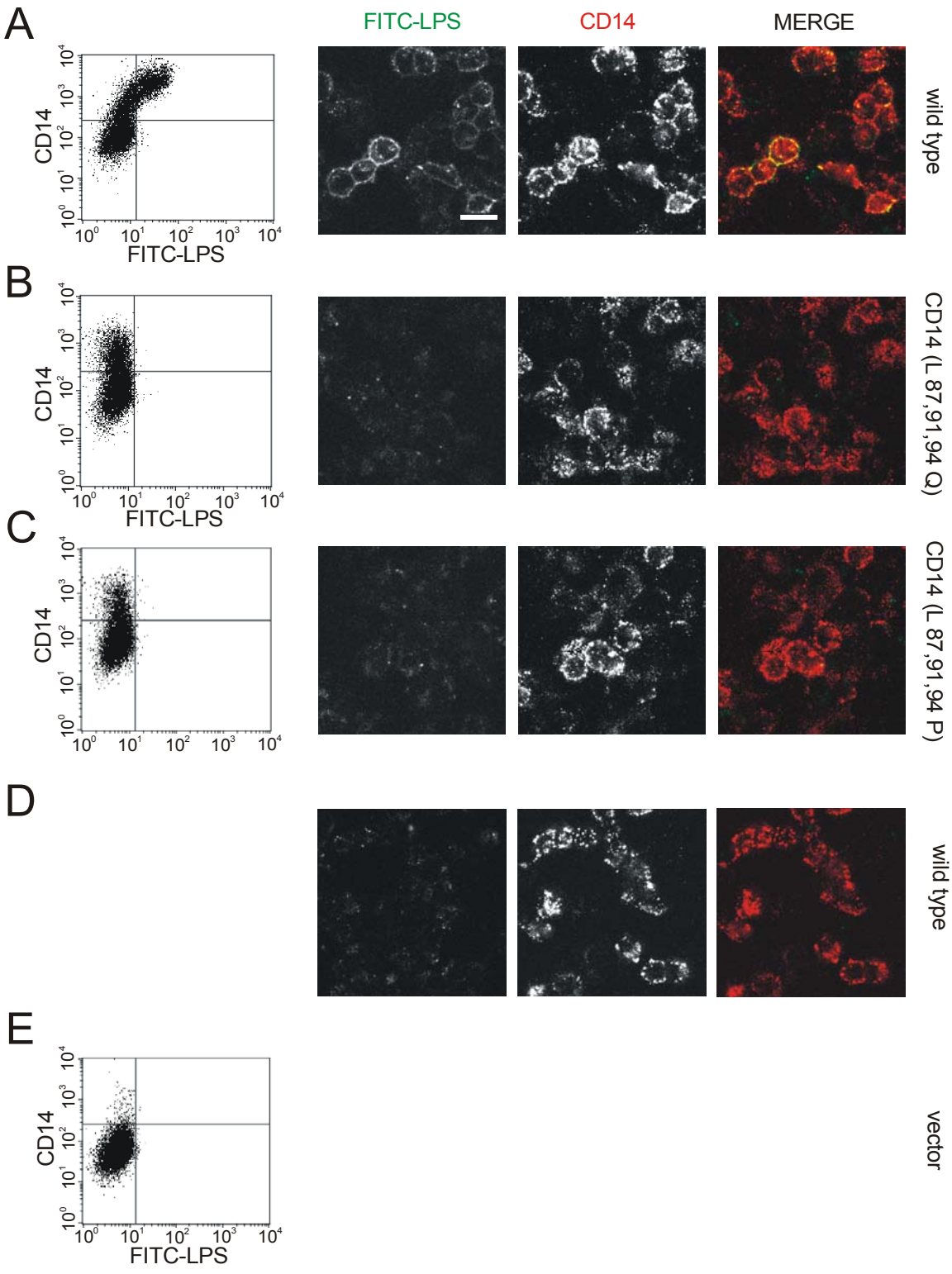

Figure 2.10 Binding of LPS to HEK 293T cells expressing wild-type and mutated CD14. Wild type CD14 (A), CD14 [Leu 87, 91, 94 Gln] (B), and [Leu 87, 91, 94 Pro] (C) were expressed in HEK 293T cells and binding of FITC-LPS was determined by flow cytometry and fluorescence microscopy. Cells expressing wild-type CD14 that were not incubated with FITC-LPS (D) and cells electroporated with the vector alone and incubated with FITC-LPS (E) served as negative controls. Electroporated cells were seeded at a density of 100,000/well in 96-well plates or 40,000 cells/well

in 8-well chambered cover glasses for analysis by flow cytometry or confocal laser scanning microscopy, respectively. Cells were incubated with FITC-LPS (1 μg/ml) for 1 h at 4°C. Then cells were incubated with a polyclonal sheep anti-human CD14 antibody (5 μg/ml) followed by incubation with a phycoerythrin-conjugated donkey anti-sheep antibody (1:100 dilution) for 1 h in each case. Shown are dot plots of phycoerythrin fluorescence versus fluorescein fluorescence of cells analysed by flow cytometry and confocal microscopy images. The scale bar represents 20 μm.

2.3.7 Inhibitory activity of derivatives of CD14 (81-100) with higher solubility.

LPS-binding peptides derived from LPS-binding proteins provide a valuable source of LPS-neutralizing agents with therapeutic potential. However, CD14 (81-100) exhibited only poor solubility. For this reason analogues of CD14 (81-100) with improved solubility were designed using two different strategies: (i) C-terminal elongation of the peptide with a tetra-lysine or a penta-glutamic acid stretch and (ii) replacement of uncharged amino acids within the peptide by either lysine or glutamic acid residues. The results of the alanine scan suggested that amino acids at positions 5, 9, 13, and 17 could be exchanged with minimum loss of biological activity. A total of four internally substituted analogues with either lysine or glutamic acid in all four positions or alternating substitutions of lysine/glutamic acid or glutamic acid/lysine were synthesized (Table 2.6).

Table 2.6 CD14 (81-100) analogues with increased solubility. In the fluorescein-labeled peptide amides 23 and 24 leucine residues at positions 11 and 14 were replaced by alanine in order to confirm the significance of these residues for the LPS-neutralizing activity.

Peptide	Sequence
Peptide 1	Fluo-QVPAQLLVGALRVLAYSRLK-NH_2
Peptide 11	Fluo-QVPAKLLVKALRKLAYKRLK-NH_2
Peptide 12	Fluo-QVPAKLLVEALRKLAYERLK-NH_2
Peptide 13	Fluo-QVPAELLVKALRELAYKRLE-NH_2
Peptide 14	Fluo-QVPAELLVEALRELAYERLE-NH_2
Peptide 21	Fluo-QVPAQLLVGALRVLAYSRLKKKKK-NH_2
Peptide 22	Fluo-QVPAQLLVGALRVLAYSRLKEEEEE-NH_2
Peptide 23	Fluo-QVPAQLLVGAARVLAYSRLKKKKK-NH_2
Peptide 24	Fluo-QVPAQLLVGALRVAAYSRLKKKKK-NH_2

The substitutions markedly increased the solubility of all peptides so that concentrations of up to 50 μM in aqueous buffers could be tested.

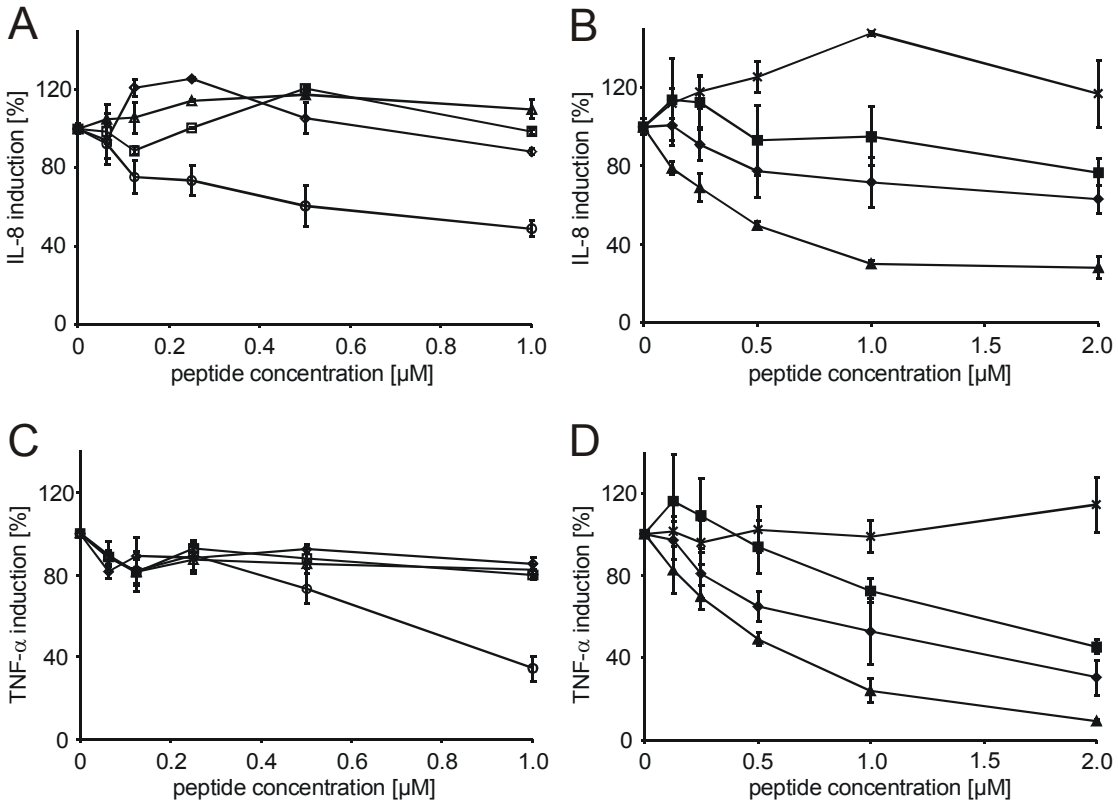

Figure 2.11 LPS-neutralizing activity of CD14 (81-100) analogues with increased solubility. The peptides were tested for their ability to suppress LPS-induced IL-8 secretion in THP-1 cells (A-B) and LPS-induced TNF-α secretion in THP-1 cells differentiated with PMA (C-D). After incubation with varying concentrations of fluorescent peptide amides (10 min) cells were stimulated with LPS (20 ng/ml) for 5 h. The higher toxicity of the analogues with substitutions within the peptide (peptides 11, 12, 13, 14) precluded a testing of concentrations above 1 μM. The symbols correspond to the following fluorescent peptide amides (Table 2.6): peptide 11: ○; peptide 12: ◊; peptide 13: □; peptide 14: Δ; peptide 21: ▲; peptide 22: x; peptide 23: ♦; peptide 24: ■. Error bars represent the standard deviation of triplicates.

However, only for the peptide in which all residues were substituted for lysine (peptide 11) and for the peptide with the C-terminal tetra-lysine (peptide 21) the capacity to inhibit IL-8 secretion was preserved or even improved (Figure 2.11A,B). For the latter an IC_{50} value of about 500 nM and a maximum inhibition of 80% at a concentration of 1 μM were determined. For peptide 11 with the internal lysine substitutions, the IL-8 secretion was inhibited by 50% at a concentration of 1 μM. In agreement with the results of the alanine scan lysine-elongated analogues

containing alanine substitutions of leucines in position 11 and 14 (peptides 23 and 24) exhibited a significant decrease in inhibitory activity in the applied concentration range.

Concerning the significance of TNF-α in the clinical progress of septic shock [179;180], the analogues with higher solubility were tested for their capacity to inhibit the secretion of this cytokine (Figure 2.11C,D). In order to render the THP-1 cells competent for the LPS-dependent secretion of TNF-α the cells were incubated with PMA for 72 h prior to stimulation with LPS. Peptides 11 and 21 inhibited the LPS-induced TNF-α secretion in a dose-dependent manner. In accordance with the results obtained for the inhibition of IL-8 induction, the introduction of negative charges within the peptide or at the C-terminus abolished the inhibitory activity. Substitution of leucines in positions 11 (peptide 23) and 14 (peptide 24) reduced but did not fully abolish the inhibitory activity of the peptides.

Several peptides exhibited cytotoxic effects against THP-1 cells detected as a reduction in the absorbance measured in the MTT test. Peptide CD14 (81-100) was cytotoxic at concentrations above 15 μM. Peptides 11 and 21 displayed cytotoxicity at concentrations higher than 1 μM and 5 μM, respectively. In contrast, peptides 12, 13, 14, 22, 23 and 24 that exhibited no or reduced inhibitory activity also showed no cytotoxic effect against THP-1 cells even at higher concentrations. Cytotoxicity in the lower to mean micromolar range is a general observation for cationic LPS-binding and antimicrobial peptides [181].

2.3.8 Confirmation of the LPS neutralizing activity by the *Limulus* amebocyte lysate assay

To validate the LPS-neutralizing capacity of the CD14-derived peptides by a further well established assay, the chromogenic *Limulus* amebocyte lysate (LAL) assay was performed (Figure 2.12). Initial experiments had shown that peptide concentrations in the lower to mean micromolar range were required to determine the activity in the LAL test. For this reason, this analysis was restricted to the analogues with higher solubility containing lysine substitutions at position 5, 9, 13 and 17. To exclude a disturbance of the read-out of the LAL test by the fluorescein moiety, for this study all peptides were N-terminally acetylated instead of fluorescein-labeled (Table 2.7).

Table 2.7 Acetylated 20-peptide amide analogues of CD14 (81-100) used for the analysis of the structure-activity relationships.

Peptide	Sequence
Peptide 30	Ac-QVPAQLLVGALRVLAYSRLK-NH_2
Peptide 31	Ac-QVPAKLLVKALRKLAYKRLK-NH_2
Peptide 32	Ac-QVPAKLLVKAARKLAYKRLK-NH_2
Peptide 33	Ac-QVPAKLLVKAARKAAYKRLK-NH_2
Peptide 34	Ac-QVPAKLLVKAQRKLAYKRLK-NH_2
Peptide 35	Ac-QVPAKLLVPALRKLAYKRLK-NH_2
Peptide 36	Ac-QVAAKLLVKALRKLAYKRLK-NH_2
Peptide 37	Ac-QVPAQLLVGAARVLAYSRLK-NH_2
Peptide 38	Ac-KVPAKLLVKALRKLAYKRLK-NH_2

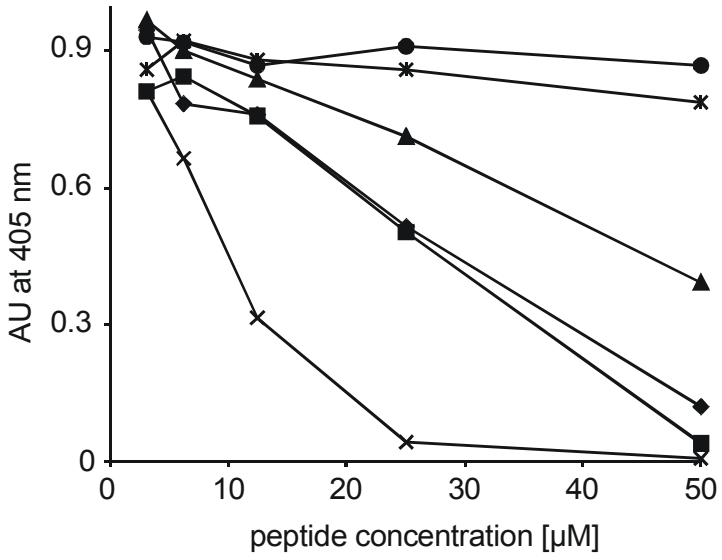

Figure 2.12 Inhibition of the endotoxin-induced LAL reaction by acetylated peptide amide analogues of CD14 (81-100). Increasing concentrations of peptide amides were incubated with LPS (1 endotoxin unit) for 45 min and subsequently the LAL reaction was performed as described under experimental procedures. Absorbance was quantitated at a wavelength of 405 nm. Symbols correspond to the following acetylated peptide amides (Table 2.7): peptide 31: ♦; peptide 32: ■; peptide 33: ▲; peptide 34: ●; peptide 35: ✱; peptide 36: x.

In contrast to the native sequence, for the analogue with the internal lysine substitutions (peptide 31) the substitution of a relevant leucine residue in position 11 by alanine (peptide 32) did not decrease the inhibitory activity. However, when both relevant leucine residues in position 11 and 14 were exchanged (peptide 33), a decrease in activity by 50% was observed. Both, the exchange of the leucine residue at position 11 by a glutamine residue (peptide 34), and the exchange of a lysine residue by proline in position 9 (peptide 35) led to a complete loss of activity in the tested concentration range of up to 50 μM. In contrast, substitution of the naturally occurring proline at position 3 by an alanine residue (peptide 36) increased the activity more than two-fold, yielding an IC_{50} of about 10 μM (Figure 2.12).

The LAL assay was applied to determine the ability of the CD14-derived peptides to neutralize LPS other than *E. coli* serotype O111:B4. These include LPS from *Pseudomonas aeroginosa*, *Klebsiella pneumoniae*, *Salmonella friedenau*, *Salmonella typhimurium* and Rd-LPS from *E. coli* (Figure 2.13).

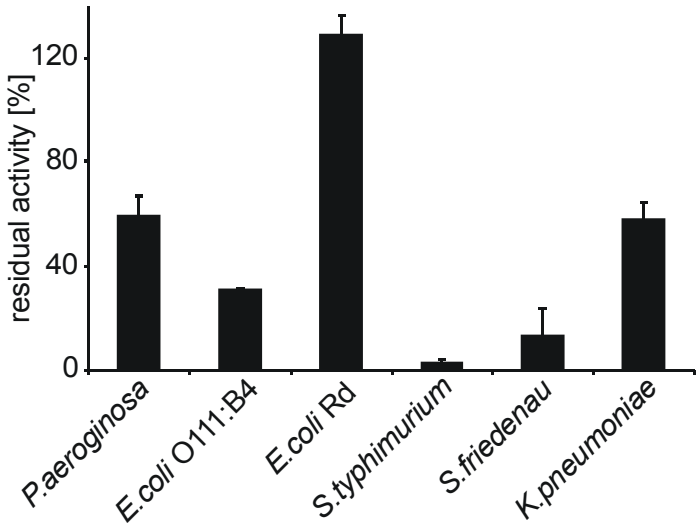

Figure 2.13 Inhibition of the LAL reaction induced by several endotoxins by a CD14-derived peptide amide. Peptide 31 (50 μM) was incubated with LPS (2 endotoxin units) for 45 min prior performing the LAL reaction as described under experimental procedures. Error bars represent mean deviations of triplicates.

The derivative with enhanced solubility (peptide 31) was able to almost completely block both types of LPS from Salmonella at a concentration of 50 μM. The inhibitory activity was even stronger than that against O111:B4 LPS from *E.*

coli. LPS from *Pseudomonas aeroginosa* and *Klebsiella pneumoniae* were inhibited by about 50%. Interestingly, in contrast to the smooth type LPS, peptide 34 was not able to neutralize Rd-LPS from the rough mutant from *E. coli*, which lacks the O-antigen, at the tested concentrations.

Next, it was tested whether the peptide corresponding to the native sequence was able to inhibit the IL-8 induction induced by LPS molecules other than *E. coli* serotype O111:B4. Only LPS from *Pseudomonas aeroginosa* and *Salmonella typhimurium* induced an IL-8 and TNF-α response in THP-1 cells and therefore only these two LPS could be applied for these inhibition experiments. For both LPS molecules a concentration-dependent inhibition of the IL-8 secretion was observed (Figure 2.14). In accordance to the results obtained from the LAL assay the inhibitory activity of CD14 (81-100) against LPS from *S. typhimurium* was stronger than that against *E. coli* and *P. aeroginosa* LPS.

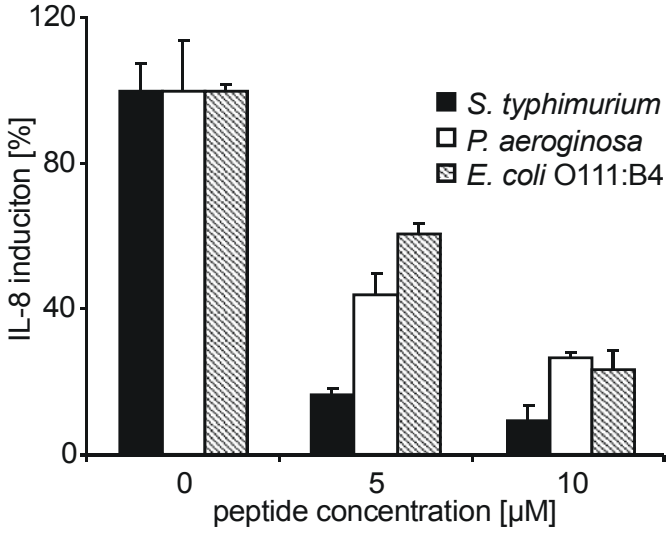

Figure 2.14 Inhibition of the IL-8 secretion induced by several endotoxins by peptide amide CD14 (81-100). Peptide CD14 (81-100) was incubated at the indicated concentrations with THP-1 cells for 10 min and subsequently cells were stimulated with LPS (100 ng/ml) for 5 h. IL-8 secretion was determined in the supernatant of the cells by ELISA. Error bars represent mean deviations of triplicates.

2.3.9 Determination of peptide conformation by CD spectroscopy.

In the crystal structure of CD14, amino acids 81 to 100 comprise an α-helix segment (amino acids 82-94) that is followed by a sharp bend of residues present in an elongated conformation (Figure 2.9). Only in an α-helical conformation the three leucine side chains required for the LPS-neutralizing activity of the peptide are placed on one face of the α-helix. Circular dichroism measurements allowed an estimation of the α-helix content for the peptides (Figure 2.15).

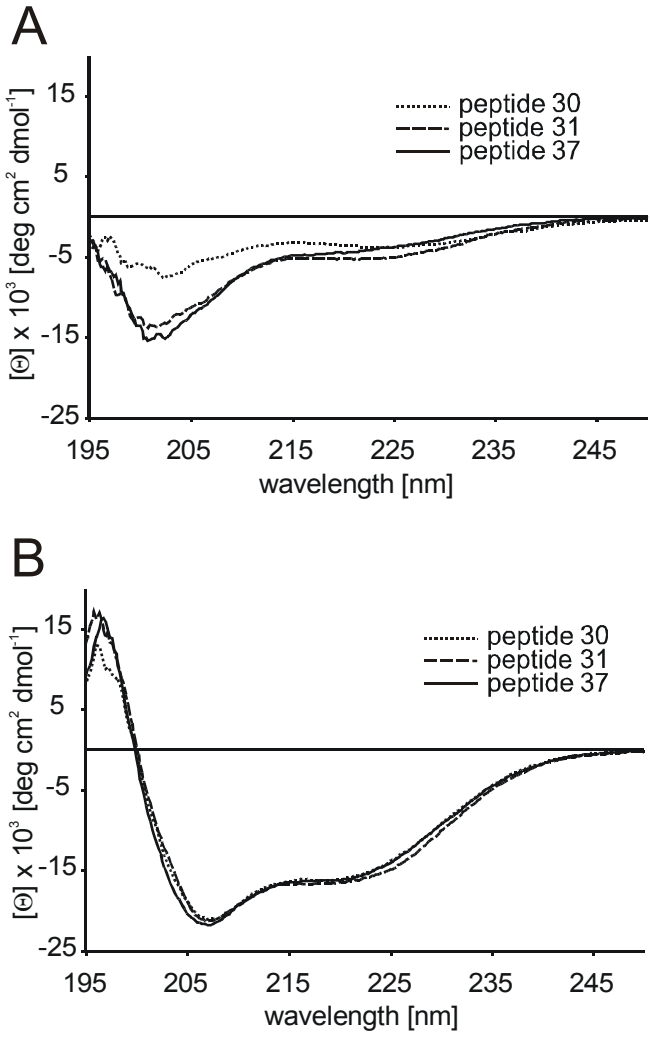

Figure 2.15 Secondary structures of CD14-derived peptides determined by CD-spectroscopy. Far UV-CD spectra for three CD14-derived acetylated peptide amides are shown as mean residue molar ellipticity versus wavelength (nm). The spectra were recorded at a peptide concentration of 10 μM at room temperature (A) in 10 mM sodium phosphate buffer, pH 7.4 without or (B) in 10 mM sodium phosphate buffer to which TFE was added to 20% (v/v).

In phosphate buffer the peptides 30, 31 and 37 (Table 2.7) had little secondary structure, as evidenced by a negative ellipticity at 200 nm (Figure 2.15A). As shown in Figure 2.15B the CD spectra of the individual peptides in the presence of 20% (v/v) TFE, an organic solvent that is often used as a membrane mimetic to lower the polarity, were almost indistinguishable from each other. The α-helix content increased in the presence of TFE from 31 to 52, 33 to 64 and 31 to 62% for peptides 30, 31 and 37, respectively (Figure 2.16). The reduced hydrophobicity and enhanced amphipathicity of peptide 31 slightly enhanced the helix content compared to the native sequence. These results indicate that the lower activity of the peptides with the leucine to alanine exchanges were not due to structural effects but rather to a loss of molecular contacts required for tight binding to LPS.

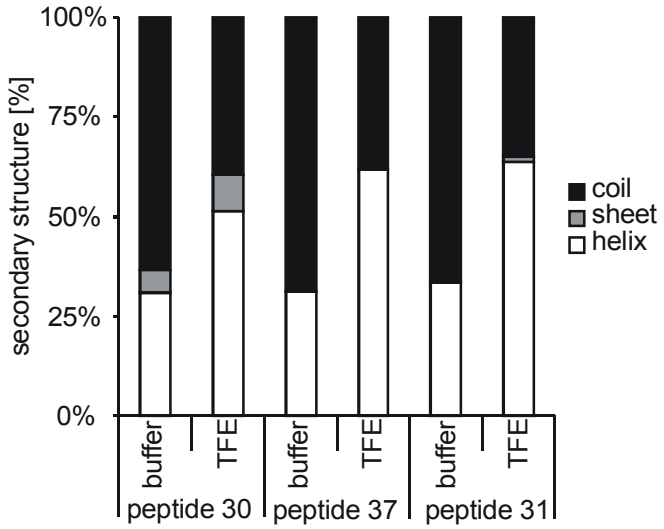

Figure 2.16 Secondary structure content of peptides 30, 37 and 31 determined by CDfit. The spectra were recorded in 10 mM sodium phosphate buffer, pH 7.4 without (A) or in the presence of 20% TFE (B) at a peptide concentration of 10 μM at room temperature.

Based on the results from the CD-measurements the positions of the residues forming an α-helix are illustrated in a helical-wheel projection (Figure 2.17).

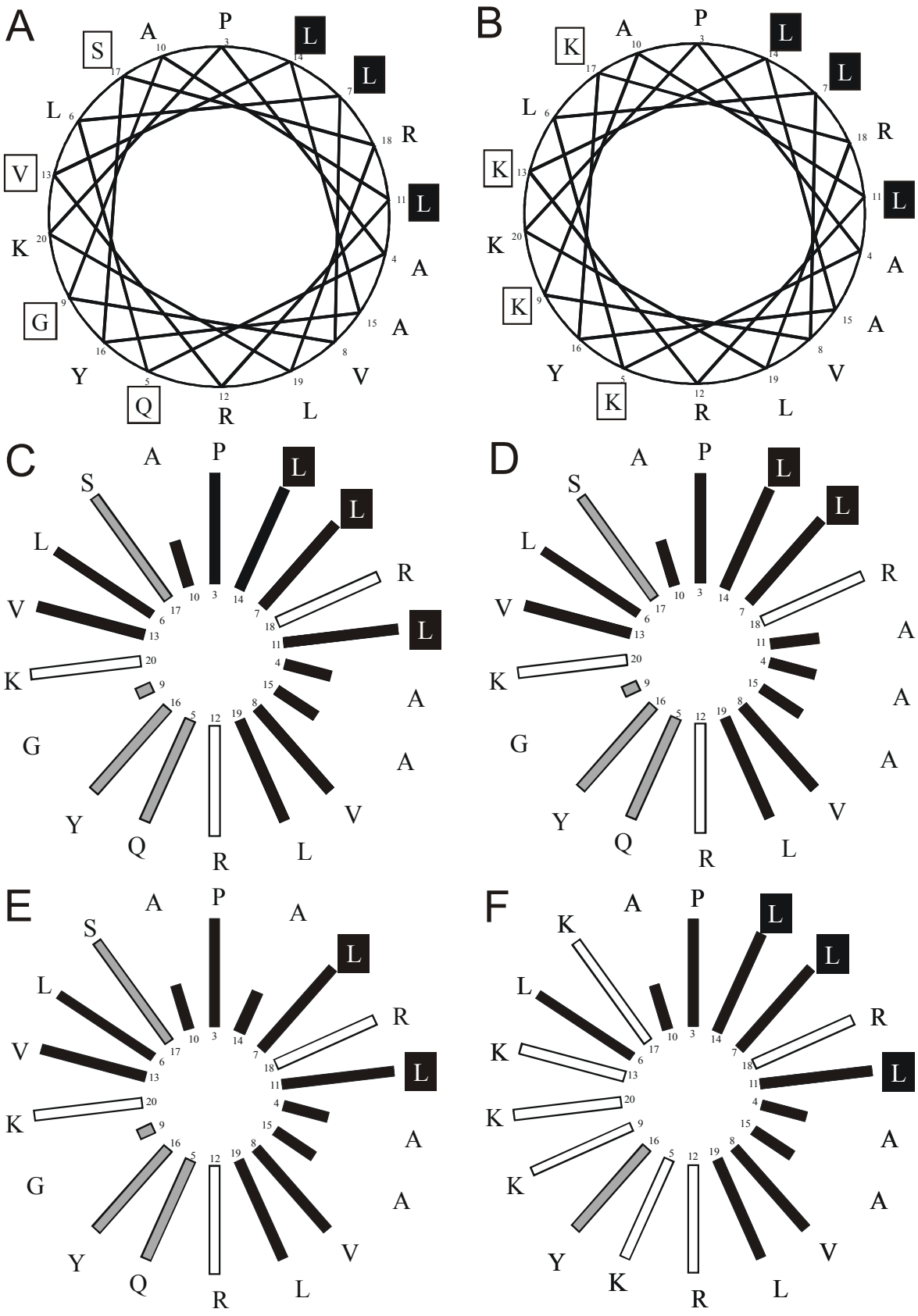

Figure 2.17 Schiffer Edmundson wheel projections of CD14-derived peptide amides. The helical wheel describes the order and position of amino acids along the axis of the α-helix. (A) Peptide corresponding to amino acids 83 to 100 of human CD14 and (B) peptide analogue containing

internal lysine substitutions. (C-F) Residues are schematically represented by bars with lengths that reflect the side-chain size and coloured white for highly hydrophilic, grey for moderate hydrophilic and black for hydrophobic characteristics. Shown are (C) the native sequence, (D,E) the alanine substitution mutants that failed to inhibit the LPS-induced cytokine secretion and (D) the derivative containing internal lysine substitutions.

In this conformation the relevant hydrophobic leucine residues are located at one side along the axis of the helix forming a hydrophobic face. This part might be involved in the binding of a hydrophobic domain of the LPS ligand. The derivative containing additional lysine residues (Figure 2.17B) exhibits an amphipathic structure with an opposite hydrophilic and a hydrophobic face of the helix. Analogues of CD14 (81-100) in which the relevant leucine residues are substituted by alanine residues exhibited strongly reduced inhibitory activity. This indicates that not only the hydrophobic character of the amino acid but also the length of the side chain might be responsible for the inhibitory activity of the peptide.

2.3.10 Inhibition of the cellular binding of FITC-LPS by CD14-derived peptides.

To further define the inhibitory mode of action of the CD14-derived peptides we determined whether these peptides prevented LPS from binding to cells or whether the LPS-peptide complexes could still bind but failed to activate the receptor. For this purpose, CD14-expressing CHO cells were incubated with FITC-conjugated LPS in the presence or absence of CD14-derived peptides and the cell-associated fluorescence was determined by flow cytometry (Figure 2.18). Peptide amides 30, 31 and 36 suppressed the binding of FITC-LPS by 70 to 80% at concentrations of 16, 6.5 and 2.5 μM, respectively. Peptides with enhanced amphipathicity (peptide 31 and 36) were more efficient in inhibiting the binding of FITC-LPS than the peptide corresponding to the native sequence of CD14 (81-100) (peptide 30). The highest activity was again observed for the peptide in which the proline residue at position 3 was exchanged by an alanine residue (peptide 36). In contrast, at a concentration of 2.5 μM peptide amides 34 (Leu11 to Gln) and 35 (Lys9 to Pro) had no inhibitory effect.

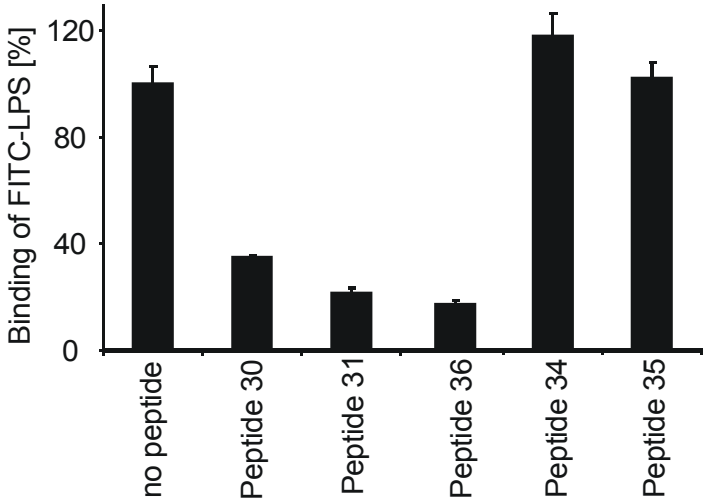

Figure 2.18 Effect of CD14-derived peptides on the binding of FITC-conjugated LPS to CHO cells. Cells were incubated with FITC-conjugated LPS (400 ng/ml) in the presence of peptide 30 (15 μM), peptide 31 (6.5 μM), peptide 36, peptide 34, peptide 35 (2.5 μM) for 3 h at 37°C. After washing the cells twice with medium, trypsinization and washing once with PBS, cellular fluorescence was determined by flow cytometry. Columns represent median fluorescence of vital cells relative to cells treated with FITC-LPS, only. Error bars represent the mean deviation of duplicates.

2.3.11 Antimicrobial activity of CD14-derived peptides.

Due to their homology to various α-helical antimicrobial peptides (see introduction) the antimicrobial activities of the CD14-derived peptides were investigated. For this purpose *E. coli* bacteria were grown in the presence or absence of peptide amides 31 and 38 (Table 2.7). Both peptide amides totally suppressed bacterial growth down to a concentration of 1.25 μM (peptide 31) and 0.6 μM (peptide 38) (Figure 2.19). The peptide 38 is an analogue containing a glutamine to lysine substitution in position 1 in order to enhance positive charge and amphipathicity. The enhanced amphipathicity of the peptide might be responsible for its enhanced antimicrobial activity compared to peptide 31.

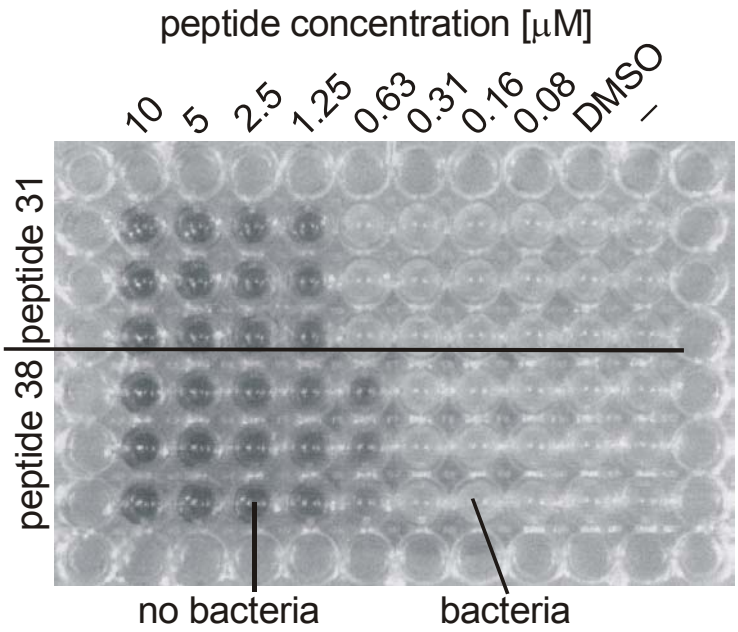

Figure 2.19 Impact of CD14-derived peptides on the growth of *E. coli*. Acetylated peptide amides were diluted in RPMI/10% FBS to the indicated concentrations. 10 μl of a suspension of the bacteria were then added to 200 μl of the corresponding peptide solution and incubated for 16 h at 37°C. The DMSO control contains 0.1% DMSO according to the amount of DMSO in the vial containing peptide at a concentration of 10 μM. Wells without bacteria appear dark, wells with bacteria bright.

2.4 Discussion

2.4.1 LPS-binding domain of CD14

Mapping of the full length human CD14 protein with synthetic 20-peptide amides which overlapped by 10 amino acids identified a single peptide amide with LPS-neutralizing activity corresponding to amino acids 81-100 of the mature protein. Using peptide-functionalized Sepharose beads it was shown that this peptide binds FITC-LPS from *E. coli* serotype O111:B4.

Recently a crystal structure of CD14, obtained in the absence of ligand, was published [178]. Amino acids 82-94 comprise an α-helix with one face oriented towards an intramolecular pocket and the other face directed outwards. The analysis of the structure-activity relationships of the peptide revealed that leucine residues corresponding to residues 87, 91 and 94 are required for biological activity. These residues are all located on the face of the helix that is directed into

the interior of the protein. The physiological significance of these residues for binding of LPS was confirmed by the failure of mutant proteins in which these residues were exchanged to either glutamine or proline residues to bind LPS. Our peptide mapping approach therefore provides strong evidence that the LPS-binding domain of CD14 is located in the interior of the protein and identifies residues directly involved in binding of LPS (Figure 2.9).

A hydrophobic binding pocket is able to shield hydrophobic determinants of an amphipatic molecule against the polar environment. Two proteins involved in binding and transport of hydrophobic molecules contain such a binding pocket. BPI complexes phosphatidylcholine within an apolar pocket formed by two amphipathic α-helices and two β-sheets [182]. Hydrophobic residues of an α-helix of this binding pocket are directly involved in the binding of the apolar acyl-chains of the phosphatidylcholine ligand (Figure 2.20).

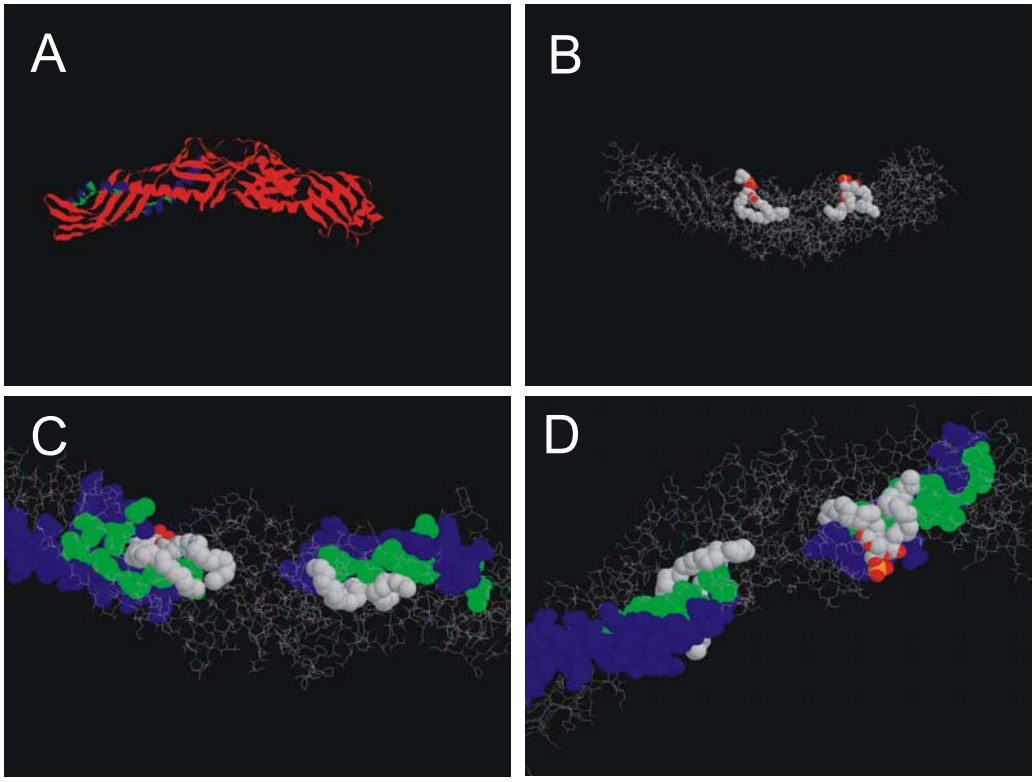

Figure 2.20 Crystal structure of BPI in complex with two phosphatidylcholine molecules (grey). Acyl chains of phosphatidylcholine are bound to hydrophobic amino acids (green) of an α-helix (blue) within BPI. Figures were created by Rasmol.

The bacterial lipopeptide localization factor LolA also contain a ligand binding pocket formed by a β-barrel in which lipoproteins are bound and transported across the membrane of the bacteria [183].

Several studies have focused on the identification of LPS-binding and -signal transducing domains of human CD14. The failure to detect the LPS-binding activity of amino acids 81 to 100, previously, may be due to the different strategies applied for the identification of the binding sites. For an LPS-binding domain formed by several separate binding sites, limited mutation of only one site may only slightly affect the affinity of the entire protein. However, based on our analysis of the structure-activity relationships for the peptide we were able to identify the amino acids involved in LPS binding and confirm their relevance for the full length protein by simultaneous site-specific mutation for amino acids with different physicochemical properties or conformational characteristics.

The reason why CD14 (81-100) was the only peptide exhibiting an LPS-neutralizing activity in our assays may be based on the fact that among those peptides corresponding to parts of the LPS-binding domain, this peptide may be the only one assuming a conformation similar to the one of the corresponding region in the native protein. CD spectroscopy confirmed that under relatively mild helix-inducing conditions CD14 (81-100) derived peptides possessed a considerable α-helix content, consistent with the secondary structure of this domain in the crystal structure.

Given the previous observation that mutations of residues 91 to 101 affected the signal transducing capacity we hypothesized that CD14 (81-100) might also have the ability to mimic the functional domain of CD14 responsible for binding to cellular receptors. However, when the fluorescein-labeled analogue of the peptide was incubated with signaling-competent THP-1 cells no binding could be detected.

The CD14 derived peptide with enhanced solubility (peptide 31) neutralized smooth LPS from different bacterial strains in the LAL assay but failed to inhibit the LAL reaction induced by rough LPS. This activity profile for the peptide is consistent with a recent report that CD14 does not only enhance the responsiveness of cells to LPS but also contributes to the discrimination of different types of LPS [184]. Removal of increasing amounts of carbohydrate decreased the activity and this residual activity was increasingly CD14-independent. Amino acids 81-100 might therefore interact with carbohydrates of

the O-antigen rather than the lipid A moiety of LPS and thereby contribute to the ligand specificity of CD14. In spite of the remarkable agreement of the activity profiles further experiments will be needed to determine, whether LPS is buried so deeply in the ligand-binding pocket.

Our data indicate that the CD14-derived peptides neutralize the cell stimulating and -binding properties of LPS by complex formation. We did not determine directly, to which degree the binding of LPS with LPS-binding molecules involved in the activation of TLR4 was inhibited or whether the peptide interfered with the activity once LPS was bound to one of these molecules. Effective molecular recognition of endotoxin requires the concerted action of several extracellular and cell surface proteins in addition to TLR4 which bind and transfer LPS. In serum, LPS micelles form complexes with the lipid transfer protein LBP. LBP potently enhances the agonistic activity of LPS [185;186] by accelerating the transfer of monomeric LPS molecules to CD14 [186-188]. CD14-bound endotoxin is then transferred to MD-2 and TLR4 [20;189]. Given this molecular mechanism it seems unlikely that LPS once bound to a cofactor is accessible to the LPS neutralizing peptides. In our experiments, we observed that the inhibitory activity of the CD14-derived peptides was enhanced when the dilution of the LPS stock solution to working concentrations was performed under serum-free conditions. Serum constitutes a source for LBP and complex formation between LPS and LBP during dilution in a serum-containing buffer, might therefore limit the inhibitory activity of the peptides. It was previously shown that several structurally diverse LPS-neutralizing cationic peptides inhibit the interaction of LPS with LBP [142]. Based on these and our observations we propose that our peptides might block the initial binding to LBP. However this has to be determined in future experiments.

2.4.3 Comparison of CD14 (81-100) with LPS-binding peptides from other proteins

Recent effords to develop molecules that neutralize endotoxin have concentrated on characterizing lipid A-binding regions from endotoxin-binding peptides and proteins. The crystal structure of LALF revealed a positively charged amphipathic loop with basic residues facing to one side that contributes to LPS-binding [163]. Similar motifs were proposed for other endotoxin-binding proteins, namely BPI, LBP [163;164], heparin-binding protein [190] and lactoferrin [191].

LPS-binding studies with synthetic peptides designed to mimic the putative LPS-binding site of these proteins showed that a stabilization of a β-turn conformation by disulfide bridges or insertion of β-turn-inducing amino acids was required for high affinity endotoxin binding and neutralization [162;164;168;170;191-194].

In addition to LPS-neutralizing molecules with β-sheet structure, some α-helical cationic peptides exhibit high LPS-binding and -neutralizing activity. These include antimicrobial peptides derived from silk moth cecropin and bee mellitin [127;129], human CAP18 [107;128], and guinea pig CAP11 [195].

Our results obtained by the analysis of the structure-activity relationships and CD spectroscopy revealed that the CD14-derived LPS neutralizing peptides can be assigned to the class of α-helical peptides with antimicrobial activity. This was supported by the observation that the CD14-derived peptides inhibited bacterial growth down to a concentration of 1 μM (Figure 2.19).

The amino acid residues leucines 11 and 14 that are critical for biological activity are three residues apart. In addition, the lysine-substituted variant of the native sequence exhibits a pattern of aliphatic and cationic amino acid residues that is characteristic for cationic amphipathic α-helices. Similar properties have been reported for the LPS-binding and -neutralizing 18-amino acid peptide derived of the C-terminal part of CAP18 [128;171]. Further evidence for an α-helical conformation of CD14 (81-100) was obtained by removal or introduction of proline residues. Mutation of the proline residue to alanine in position 3 yielded a more potent peptide as shown by the significantly enhanced LPS-neutralizing activity in the LAL test. In contrast, the activity of the peptide was significantly reduced when lysine at position 9 was substituted by a proline residue.

To this end it was not possible to determine to which degree the increase in activity was due to the enhanced solubility of the lysine-substituted peptides or due to additional molecular interactions of the positively charged amino acid side chains with the negatively charged groups of LPS. The observation that the C-terminal elongation of the peptide increased the activity even stronger than the internal lysine substitutions indicates that the higher solubility was the major contribution to the higher activity.

This is the first report of a peptide with LPS-neutralizing activity derived from CD14. While previous analyses on LPS-neutralizing peptide motifs have stressed the significance of cationic residues, for CD14 (81-100) side chains with

substantial hydrophobicity proved to be essential for activity. For the inactive derivatives containing leucine to alanine substitutions the smaller and less hydrophobic alanine side chain is not able to sustain the inhibitory activity of the peptide. These side chains likely engage in interactions with LPS that also play a role for LPS binding in the entire protein. Due to the ability to generate CD14 (81-100) analogues with higher solubility we are confident that the CD14-derived peptide is a promising candidate for a further development of LPS-neutralizing peptides for use in the prevention and treatment of septic shock.

2.5 Materials and methods

2.5.1 Reagents

Lipopolysaccharide (phenol extracted and purified by ion-exchange chromatography) and fluorescein isothiocyanate-labeled lipopolysaccharide (FITC-LPS), both from *E. coli* serotype O111:B4, lipopolysaccharides from *Pseudomonas aeroginosa*, *Klebsiella pneumoniae*, *Salmonella friedenau*, *Salmonella typhimurium* and Rd-LPS from *E. coli*, 3-(4,5-dimethylthiazol-2-yl)-2,5-diphenyl tetrazolium bromide (MTT), and phorbol 12-myristate 13-acetate (PMA) were from Sigma (Taufkirchen, Germany), *Limulus* amebocyte lysate was from BioWhittaker (Walkersville, USA). Standard chemicals were from Fluka (Deisenhofen, Germany) and Merck (Darmstadt, Germany). Fmoc-amino acids were from Novabiochem, Senn Chemicals (Dielsdorf, Switzerland), and Orpegen Pharma (Heidelberg, Germany). The isomeric mixture of 5(6)-carboxyfluorescein was from Fluka. G418 was from Gibco (Karlsruhe, Germany) and Hygromycin from PAN Biotech (Aidenbach, Germany).

2.5.2 Peptide synthesis

Parallel peptide amide synthesis [196] was performed by solid-phase Fmoc/*tert.*-butyl chemistry using an automated peptide synthesizer for multiple peptide synthesis (Syro, MultiSynTech, Bochum, Germany). Peptide amides were synthesized on Rink amide resin (Rapp Polymere, Tübingen, Germany). Side chain-protecting groups of Fmoc-amino acids were *tert.*-butyl (Ser, Thr, Tyr, Glu, Asp), 2,2,4,6,7-pentamethyldihydrobenzofuran-5-sulfonyl (Arg), trityl (Asn, Gln,

Cys, His), *tert.*-butyloxycarbonyl (Trp, Lys). Fmoc-protected amino acids including Fmoc-8-amino-3,6-dioxaoctanoic acid (Fmoc-Ado-OH) (Neosystem, Strasbourg, France) were coupled by *in situ* activation using N,N'-diisopropylcarbodiimide/1-hydroxybenzotriazol for 90 min in 2 ml syringes. The removal of the Fmoc-protecting group was carried out by treatment with piperidine/DMF (1:4, v/v), twice for 8 min. The resin was washed with DMF (6x) after each coupling and deprotection step. Peptide amides were cleaved off the resin and side-chain-deprotected by treatment with trifluoroacetic acid/triisopropylsilane/ethanedithiol/ H_2O (92.5:2.5:2.5:2.5, v/v/v/v) for 4 h. Crude peptides were precipitated by adding cold diethyl ether (-20°C). The precipitated peptides were collected by centrifugation and resuspended in cold diethyl ether. This procedure was repeated twice. Finally peptides were dissolved in *tert.*-butyl alcohol/H_2O (4:1, v/v) and lyophilized three times.

2.5.3 Labeling of peptide amides with carboxyfluorescein

N-terminal labeling of the peptide amides with 5(6)-carboxyfluorescein was performed as described [176]: Fmoc-deprotected, resin-bound peptides were reacted with 5 equiv. of 5(6)-carboxyfluorescein, N,N'-diisopropylcarbodiimide, and 1-hydroxybenzotriazol each in DMF for 16 h. Reactions were stopped by washing the resins three times with DMF, methanol, dichloromethane and diethyl ether. Subsequently, peptides were treated with piperidine/DMF (1:4, v/v) for 20 min in order to remove ester-bound carboxyfluorescein. Completeness of labeling was confirmed by Kaiser-Test [197].

2.5.4 Labeling of peptide amides with S0387

S0387 was covalently attached to the deprotected N-terminus using 5 equiv. of DIC (11.7 μl, 75 μmol), 5 equiv. of HOBt (11.5 mg, 75 μmol) and 1.5 equiv. of S0387 (15.9 mg, 22,5 μmol) in DMF twice for 16 h. Reactions were stopped by washing the resins three times with DMF, methanol, dichloromethane and diethyl ether. Completeness of labeling was confirmed by Kaiser-Test

2.5.5 Biotinylation of resin-bound peptide amides.

Conjugation of biotin to the N-terminus of resin-bound peptides was performed using 5 equiv. biotin, 5 equiv. 2-(1*H*-benzotriazol-1-yl)-1,1,3,3-tetramethyluronium tetrafluoroborate, 5 equiv. 1-hydroxybenzotriazol, and 10 equiv. N,N'-diisopropylethylamine in N-methylpyrrolidone for 16 h. Completeness of biotinylation was confirmed by Kaiser-Test.

2.5.6 Acetylation of resin-bound peptide amides

N^{α}-Acetylation was performed in the presence of acetic anhydride, N,N'-diisopropylethylamine, and DMF (1:1:8, v/v/v) for 2 x 30 min. Completeness of N^{α}-acetylation was confirmed by Kaiser-Test.

2.5.7 HPLC

Peptides and conjugates were analyzed by analytical RP-HPLC. Gradient: water/0.1% TFA (solvent A) and acetonitrile/0.1% TFA (solvent B) (Waters 600 System (Eschborn, Germany)), detection at 214 nm. The samples were analyzed on an analytical HPLC column (Nucleosil 100, 250 x 2 mm, C18 column, 5 μm particle diameter; Grom, Herrenberg, Germany), using a linear gradient from 10% B to 100% B within 30 min (flow rate: 0.3 ml/min). Peptides were purified by preparative RP-HPLC (Nucleosil 300, 250 x 20 mm, C18 column, 10 μm particle diameter; Grom, Herrenberg, Germany) on a Gilson preparative system (Bad Camberg, Germany, equipped with a 321 Pump and a 156 UV/Vis Detector, flow rate: 10 ml/min). Gradients were adjusted according to the elution profiles and peak profiles obtained from the analytical HPLC chromatograms.

2.5.8 Mass spectrometry of synthetic peptides

1 μl of 2,6-dihydroxyacetophenone matrix (20 mg of 2,6-dihydroxyacetophenone and 5 mg of ammonium citrate in 1 ml of isopropyl alcohol/H_2O (4:1, v/v)) were mixed with 1 μl of each peptide solution (dissolved in acetonitrile/water (1:1, v/v) at a concentration of 1 mg/ml) on a gold target. Measurements were performed using

a matrix-assisted laser desorption ionization (MALDI) time-of-flight mass spectrometer (G2025A, Hewlett-Packard, Waldbronn, Germany). For signal generation 20-50 laser shots were added up in the single shot mode.

2.5.9 Peptide stock solutions

Carboxyfluorescein-labeled peptides were dissolved in DMSO at concentrations of 10 mM. These stock solutions were further diluted 1:10 in *tert.*-butyl alcohol/H_2O (4:1). Peptide concentrations were determined by UV/VIS-spectroscopy of a further dilution (1:100) in Tris/HCl buffer (0.1 M, pH 8.8). Absorption was measured at a wavelength of 492 nm. Concentrations were calculated assuming a molar extinction coefficient of 75,000 l/(mol·cm).

2.5.10 Cell culture

The human myelomonocytic cell line THP-1 [198] was obtained from the Deutsche Sammlung von Mikroorganismen und Zellkulturen (DSMZ) (Braunschweig, Germany). The cells were cultured in RPMI 1640 medium (PAN Biotech, Aidenbach, Germany) supplemented with 10% FBS (PAN Biotech) in a 5% CO_2 humidified atmosphere at 37°C. HEK 293T cells were cultured in IMDM medium (PAN Biotech, Aidenbach, Germany) supplemented with 10% FBS. The generation of the CD14-expressing Chinese hamster ovary (CHO)-K1 reporter cell line CHO/CD14/TLR2.elam.tac has been described in detail previously [199]. The cells were grown in RPMI 1640 medium containing 10% FBS, 400 μg/ml G418 and 400 units/ml hygromycin B. Adherent cells were harvested with trypsin/EDTA (Biochrom, Berlin, Germany). Cells were passaged every third to fourth day.

2.5.11 IL-8 ELISA

THP-1 cells were suspended in RPMI medium containing 10% FBS and dispensed into 96-well culture plates (Sarstedt, Nürnbrecht, Germany) at a cell density of 4 x 10^4 cells per 200 μl of medium per well. Peptide amide stock solutions in DMSO were diluted 1:10 in *tert.*-butyl alcohol/H_2O (4:1) prior to the addition to the cells. The amount of *tert.*-butyl alcohol in the cell culture never exceeded 1% (v/v). Solutions of peptide amides with enhanced solubility (peptide

11-24) were prepared without an intermittent dilution step in *tert.*-butyl alcohol/H_2O (4:1). Cells were incubated with peptides at the indicated concentrations for 10 min at 37°C. Controls with peptide-free medium containing equal amounts of DMSO and *tert.*-butyl alcohol were included in each assay. Endotoxins were solubilized at a concentration of 5 mg/ml by sonication in endotoxin-free water for 7 min at 55°C. LPS was added to the samples at a concentration of 20 ng/ml. After further incubation for 5 h at 37°C cell-free supernatants were collected and stored at -80°C prior to the quantification of IL-8 secretion by matched-pair ELISA (clone G265-5 and clone G265-8, BDPharMingen, San Diego, USA) according to the protocol provided by the manufacturer.

2.5.12 TNF-α ELISA

PMA was added to a THP-1 cell suspension from a 0.1 mg/ml stock solution to a final concentration of 30 ng/ml [200]. Cells were plated immediately into 96-well microtiter plates at a density of 4 x 10^4 cells per 200 µl of medium and allowed to differentiate for 72 h at 37°C. Before addition of the peptides, the cells were washed twice with medium. Due to the enhanced solubility of peptides applied in these assays, peptides were diluted directly into medium without a predilution step in *tert.*-butyl alcohol/H_2O. After 10 min incubation with the indicated peptide LPS was added to the samples at a final concentration of 20 ng/ml. Supernatants were collected after 5 h incubation at 37°C and ELISA (clone MAb1 and clone MAb11, BDPharMingen) was performed according to the protocol provided by the manufacturer.

2.5.13 Cell viability assay

Cell viability was measured using the colorimetric 3-(4,5-dimethyl thiazol-2-yl)-2,5-diphenyl tetrazolium bromide (MTT) dye reduction assay. THP-1 cells were treated with the corresponding peptide amide and LPS for 5 h (see above). After removing 120 µl of the supernatant for ELISA analysis, cells were incubated with MTT (Sigma) at a concentration of 1 mg/ml for 4 h. The formazan product was solubilized with SDS (10% (m/v) in 10 mM HCl). The fraction of viable cells was determined by measuring the absorbance of each sample at 570 nm relative to the absorbance of untreated control cells using the microplate reader.

2.5.14 Detection of FITC-LPS-binding to biotinylated bead-immobilized peptides with laser scanning microscopy

A suspension (100 µl) of high performance streptavidin-Sepharose in ethanol (20%, v/v) (Amersham Bioscience, Uppsla, Sweden) was washed three times with PBS and resuspended in 1 ml of PBS. A stock solution (10 mM) of biotinylated peptides in DMSO (2 µl) was incubated with 1 ml of the streptavidin-bead suspension for 60 min at 4°C on a shaker. Unbound peptides were removed by washing the beads three times with PBS and beads were resuspended in 350 µl PBS. 50 µl of this suspension were diluted with 950 µl of PBS in a 1.5 ml reaction tube. *E. coli* FITC-LPS serotype O111:B4 was solubilized to a concentration of 2 mg/ml by sonication for 5 min at 50°C. 1 µl of this FITC-LPS solution was added to the 1 ml peptide loaded bead suspension and incubated for further 60 min at 4°C on a shaker. For competition experiments FITC-LPS was incubated with the beads in the presence of an unlabeled LPS-binding peptide (2 and 20 µM) or a 50-fold excess of unlabeled LPS. Subsequently the beads were washed three times with PBS/Tween20 (0.2%, v/v) and laser scanning microscopy was performed using an inverted LSM510 microscope (Carl Zeiss, Göttingen, Germany) equipped with a Plan-Apochromat 63 x 1.4 N. A.. Fluorescein was excited with a 488 nm argon-ion laser via an HFT 488 main beam-splitter. Fluorescence was detected with a BP 505 - 550 nm band pass filter.

2.5.15 Inhibition of the *Limulus* amebocyte lysate response to LPS

Endotoxins were prepared according to the manufacturer`s protocol in endotoxin-free water to a concentration of 2 endotoxin units/ml. Peptides were prepared at varying concentrations in endotoxin-free water and 25 µl of the respective peptide solution were mixed with 25 µl of the LPS solution in a 96-well microtiter plate (Becton Dickinson, Franklin Lakes, USA) and incubated at 37°C on a shaker. After 45 min 25 µl of *Limulus* amebocyte lysate was added to each well and incubated for further 15 min. 50 µl of chromogenic substrate, prepared according to manufacturer's specifications, were added and the reaction was stopped after 10 min by adding 100 µl of acetic acid (25%, v/v) to each well. Absorbance at 405 nm was determined using a microplate reader.

2.5.16 Inhibition of the cellular binding of FITC-LPS by CD14-derived peptides

200 µl of RPMI 1640 containing FITC-conjugated LPS (1.2 µg/ml) was incubated either in the absence or presence of CD14-derived peptide amides for 5 min at 37°C. Subsequently, 50 µl of these mixtures were added to CHO-CD14 cells seeded at a density of 1 x 10^6 cells/ml in 100 µl serum-containing RPMI 1640 in a 96-well plate. After incubation, cells were washed twice with ice-cold medium, detached by trypsinization, suspended in ice-cold PBS and washed once in ice-cold PBS. Binding of FITC-conjugated LPS to the cells was analysed by flow cytometry (BD FACSCalibur System, Becton Dickinson, Heidelberg, Germany). In each case, the median fluorescence intensity of 8,000 vital cells was determined. Vital cells were gated based on sideward and forward scatter.

2.5.17 Determination of peptide conformation by CD-spectroscopy

CD spectra were measured on a JASCO J-720 dicrograph spectrometer (Jasco, Easton, MD, U.S.A.). Spectra were recorded at room temperature from 195 to 250 nm at 0.2 nm intervals, with a spectral band width of 1 nm, and a scan speed of 20 nm/min. Stock solutions of the peptide amides (1 mM) were prepared in 1,1,1,3,3,3-hexafluoro-2-propanol and diluted to a concentration of 10 µM in 10 mM sodium phosphate buffer, pH 7.4 or 10 mM sodium phosphate buffer (pH 7.4) diluted with trifluoroethanol (TFE) to yield 20% TFE (v/v). The spectra were corrected for buffer alone and the mean molar residual ellipticity ([Θ]) was plotted versus wavelength. The fractional helical content was estimated from the JFIT spectral deconvolution method (Lawrence Livermore National Laboratory, Livermore, CA).

2.5.18 Site-directed mutagenesis

The full length CD14 ORF was cloned into the pcDNA3 vector. Site-directed mutagenesis was performed using the QuikChange II site-directed Mutagenesis Kit (Stratagene Europe, Amsterdam, NL) according to the manufacturer's instructions using the following primers: for the triple L to P exchange: 5'-ctcagctaccggtaggcgccccgcgtgtgccagcgtactc-3', 5'-gagtacgctggcacacgcggggcgcctaccggtagctgag-3'; for the triple L to Q exchange: 5'-

ctcagctacaggtaggcgcccagcgtgtgcaagcgtactc-3', 5'-gagtacgcttgcacacgctgggcgcctacctgtagctgag-3' (obtained from biomers.net, Ulm, Germany). The correct sequences were verified by sequencing. The plasmid DNA was purified using the Endofree Plasmid Maxi Kit from Qiagen (Hilden, Germany).

2.5.19 Analysis of the binding of FITC-LPS to HEK cells expressing wild type and mutant CD14.

For transfection, HEK 293T cells were harvested with trypsin/EDTA washed with medium and suspended in medium containing the indicated plasmid. Cells were electroporated in 4 mm cuvettes (Peqlab, Erlangen, Germany) at a density of 2 x 10^6 cells/ml, using a 15 millisecond pulse of 330 V and 1700 μF maximal resistance (Fischer Electroporator, Heidelberg, Germany). After electroporation, cells were incubated in the cuvettes for further 30 min and seeded at a density of 500,000 cells per well in 6-well plates (Sarstedt) or 40,000 cells per well in 8-well chambered cover glasses (Nunc, Wiesbaden, Germany) for further analysis.

For flow cytometry, after 16 h at 37°C cells were trypsinized and seeded at a density of 100,000 per well in 96-well plates in serum-containing RPMI 1640. Cells were washed with medium, resuspended in 200 μl medium containing FITC-LPS (1 μg/ml) and incubated for 1 h at 4°C. Subsequently, cells were washed three times with medium, followed by incubation in 50 μl of ice-cold PBS/0.1% BSA (v/w) containing a polyclonal sheep anti-human CD14 antibody (5 μg/ml) (R & D Systems, Minneapolis, U.S.A) for 1 h at 4°C. After washing three times in ice-cold PBS/0.1% BSA cells were incubated with 50 μl PBS/0.1% BSA containing a phycoerythrin-conjugated donkey anti-sheep secondary antibody (Dianova, Hamburg, Germany) (1:100 dilution) for 1 h at 4°C. Cells were washed three times with ice-cold PBS/0.1% BSA, suspended in ice-cold PBS/0.1% BSA, and measured immediately by flow cytometry (BD FACSCalibur System, Becton Dickinson, Heidelberg, Germany). In each case, the fluorescence of 10,000 vital cells was acquired. Vital cells were gated based on sideward and forward scatter.

For confocal microscopy, electroporated HEK 293T cells were seeded at a density of 40,000/well in 8-well chambered cover glasses. One day later, cells were washed once with serum-containing RPMI 1640, followed by incubation with medium containing FITC-LPS on ice and stained for CD14 by indirect

immunofluorescence using the same reagents as described above. After staining living cells were imaged immediately. For double detection of FITC-LPS and phycoerythrin-labeled antibody the 488 nm line of an argon ion laser and the light of a 543 nm helium/neon laser were directed over an HFT UV/488/543/633 beam splitter and fluorescence was detected using an NFT 545 and an NFT 635 VIS beam splitter in combination with a BP 505-530 band pass filter for fluorescein detection and a BP 560-615 band pass filter for phycoerythrin detection.

3 Ratiometric fluorescence-based LPS-sensing element

This chapter was adapted from a manuscript in preparation. The author performed all experiments. Sensing element 1 was synthesized Dr. Rainer Fischer.

3.1 Summary

Lipopolysaccharide (LPS), the major compound of the outer leaflet of the cell wall of Gram-negative bacteria, is known to be responsible for the initiation of severe immunological disorders, such as sepsis and septic shock. We developed a novel FRET-based sensing element for detection of lipopolysaccharide. The sensing element is composed of the LPS-binding peptide corresponding to the amino acid sequence 81-100 of human CD14 terminally attached by tetramethylrhodamine (Tamra) and fluorescein (Fluo) residues serving as donor/acceptor pair for fluorescescence resonance energy transfer (FRET). Upon addition of LPS a FRET-based increase of Tamra fluorescence emission upon fluorescein excitation was observed and the ratio of the maximum fluorescence emission of the tetramethylrhodamine and fluorescein was determined for LPS-detection. Discrimination of LPS versus other lipids was achieved by the comparison of the peptide and an analogue with distinct specificity due to alterations in the physicochemical properties using a detailed analysis of the fluorescence emission profile for both molecules.

3.2 Introduction

Lipopolysaccharide, released from the outer membrane of Gram-negative bacteria when bacteria die or multiply, initiates a signaling cascade that induces the expression of inflammatory cytokines that may lead to Gram-negativ sepsis and septic shock [143]. Due to the high toxicity of LPS continuous effort is directed to the development of specific LPS-detection systems that are able to trace smallest amounts of LPS. Currently, the enzymatic *Limulus* amebocyte lysate (LAL) assay is used most widely to detect and quantify endotoxin in clinical and non clinical samples. However, there are several limitations of this method. The LAL assay, as most enzymatic tests are, is very sensitive but highly susceptible to changes in temperature and pH. Moreover, carbohydrate derivatives other than LPS, like β-glucans also react positively in this assay [201]. A variety of alternatives to or modifications of the LAL assay have been developed but none of them has established for biomedical applications, because of poor sensitivity or inconvenience [202].

Ideally, a biomedical assay should enable the highly sensitive and specific detection of the analyte and be robust to changes in the molecular environment and prolonged storage. Sensors based on synthetic small molecules are considered a highly promising strategy for this purpose. A moiety for recognition is linked to a transducer that reports on the binding of the analyte. Förster resonance energy transfer (FRET) provides a sensitive fluorescence-based read-out for recognition elements in which binding of the analyte induces a conformational change. [203-208].

For peptide-based recognition elements, a random coil to helix transition strongly changes the relative orientation of fluorophores attached to both ends of the helix thereby affecting the rate of energy transfer. For the detection of lipids a sensor based on a recombinant fusion protein in which the lipid-binding peptide derived from ActA was flanked by cyan and yellow fluorescent proteins at both ends was recently presented [209]. Binding of polyphosphorylated phosphoinositides induces a random coil to helix transition leading to a decrease of the FRET signal which is observed in the absence of the ligand.

For the α-helical antimicrobial peptide magainine with LPS-binding properties such a random coil to helix transition has also been described [210]. Recently, we identified a novel LPS-binding peptide from the LPS receptor CD14. We could show that in aqueous buffers this peptide is present as a random coil. Upon addition of trifluoroethanol (TFE), a helix promoting organic solvent, the peptide assumes an α-helical conformation corresponding to the conformation of the corresponding segment in the crystallized protein [178]. The peptide exhibited a strong LPS neutralizing activity in inhibiting the induction of the expression inflammatory cytokines. Moreover, an analogue with amino acid substitutions that increased the solubility had an IC_{50} value of about 10 μM in the LAL test.

We therefore reasoned that the CD14-derived LPS-binding peptide and its analogue would provide promising recognition elements for the rational design of small molecule LPS sensing elements using FRET for the detection of binding. As fluorophores, carboxytetramethylrhodamine (Tamra) was attached to the N-terminus and carboxyfluorescein to the C-terminus. It has been reported previously, that for this combination of fluorophores, when attached to a conformationally unconstrained peptide, the fluorescence of both fluorophores is quenched by a mechanism involving dimer formation [211]. Any conformational change of the peptide that induces the separation of the fluorophores decreases the quenching so that FRET may be detected. Based on this principle, binding of an antibody to a 13-peptide epitope labeled with these fluorophores was detected.

We here demonstrate that a doubly labeled CD14-derived peptide as well a similar ligand-depended increase in FRET was observed. The CD14-derived peptide and its analogue were synthesized using optimized protocols for the generation of doubly labeled peptides [176]. In the presence of LPS both fluorescent peptides alter their spectral characteristics. Selectivity of these sensing elements was established by probing the response to a series of lipid and lipopeptides. Detection of LPS was achieved for as little as 150 nM of LPS, thereby exceeding previously published LPS sensors by a factor of about 100 [212].

3.3 Results

3.3.1 Development of a fluorescence-based LPS-sensing element

The native sequence of the CD14-derived peptide and an analogue with higher solubility were selected as recognition elements for a small molecule LPS sensing element (Table 3.1).

Table 3.1 Doubly labeled fluorescent peptides used as FRET-based LPS-sensing elements (SE). SE 1 corresponds to the amino acid positions 81-100 of mature human CD14. SE 2, an analogue of SE 1 containing amino acid substitutions at positions 3, 5, 9, 13, 17 was designed to enhance sensor solubility and sensitivity. 5(6)-Carboxyfluorescein is attached via the α-amino group of the C-terminal lysine residue and the peptide was assembled on the ε-amino group [176]. Carboxytetramethylrhodamine was attached to the N-terminus of the peptide amides.

Peptide	Sequence
SE 1	Tamra-QVPAQLLVGALRVLAYSRLK-εK(αFluo)-NH_2
SE 2	Tamra-QVAAKLLVKALRKLAYKRLK-εK(αFluo)-NH_2
SE 3	Tamra-QVPAQLLVGALRVLAYSRLK-NH_2

The native sequence corresponds to amino acids 81-100 of human CD14. In the analogue, residues 5, 9, 13, 17 of the native peptide (Voss et al., 2005) were mutated for lysine residues and residue 3 for a proline residue. It was shown by an alanine scan that these residues were not required for the LPS-neutralizing activity. We reasoned that the increased solubility would be beneficial to the application of this peptide as a sensor. Furthermore, we were interested to learn whether both molecules exhibited different sensitivity for LPS and possibly also different specificity for related amphiphilic ligands, due to the enhanced positive net charge of SE 2.

When performing fluorescence spectrometry in buffer, both molecules displayed a two-peak spectrum upon excitation at 492 nm (excitation of fluorescein) (Figure 3.1A and 3.1B). Upon addition of lipopolysaccharide (*E.coli*, serotype O111:B4) both sensing elements altered their spectral characteristics leading to a reduced fluorescence emission at 520 nm and a significantly enhanced emission at 588 nm, indicating an increase in FRET. For the lipid sensor based on ActA the fluorophore separation due to ligand binding resulted in a decrease in FRET [209].

The spectral changes in the presence of LPS should therefore be a consequence of dimer dequenching due to spatial separation of fluorophores and due to environment-dependent changes in fluorescence quantum yield caused by interaction of the fluorophores with the ligand. The latter possibility was addressed by the synthesis of a SE 1 analogue (SE 3) that lacks the fluorescein moiety (Figure 3.1C). In spite of the absence of a potential energy donor, in the ligand-free state SE 3 exhibited a stronger rhodamine emission than SE 1, demonstrating that the rhodamine fluorescence was nearly completely quenched due to dimer formation. The presence of environment-dependent effects on quantum yield was confirmed by the increase in fluorescence upon addition of LPS.

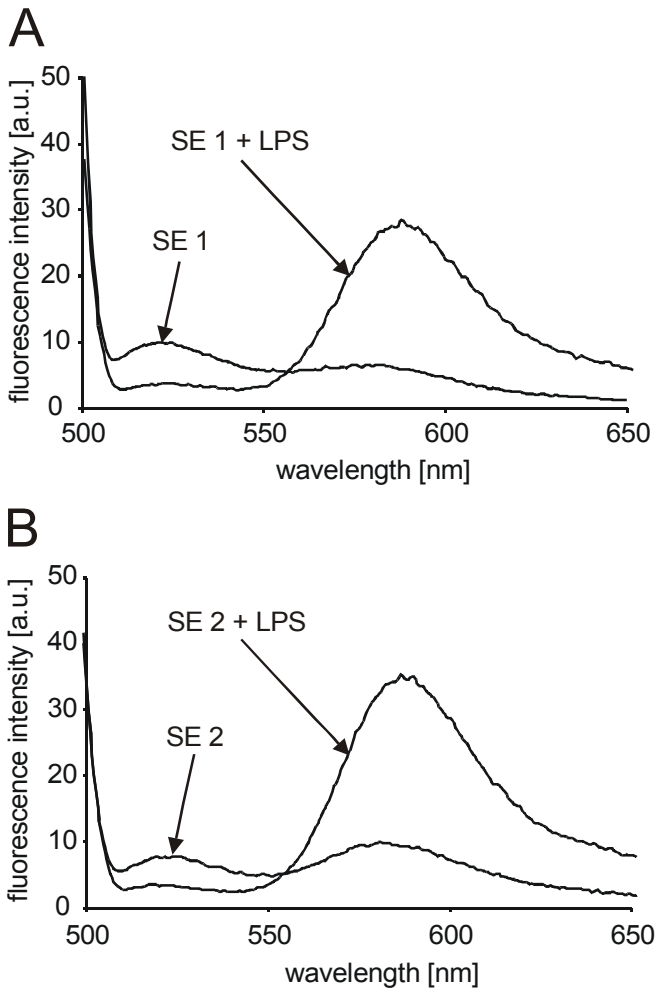

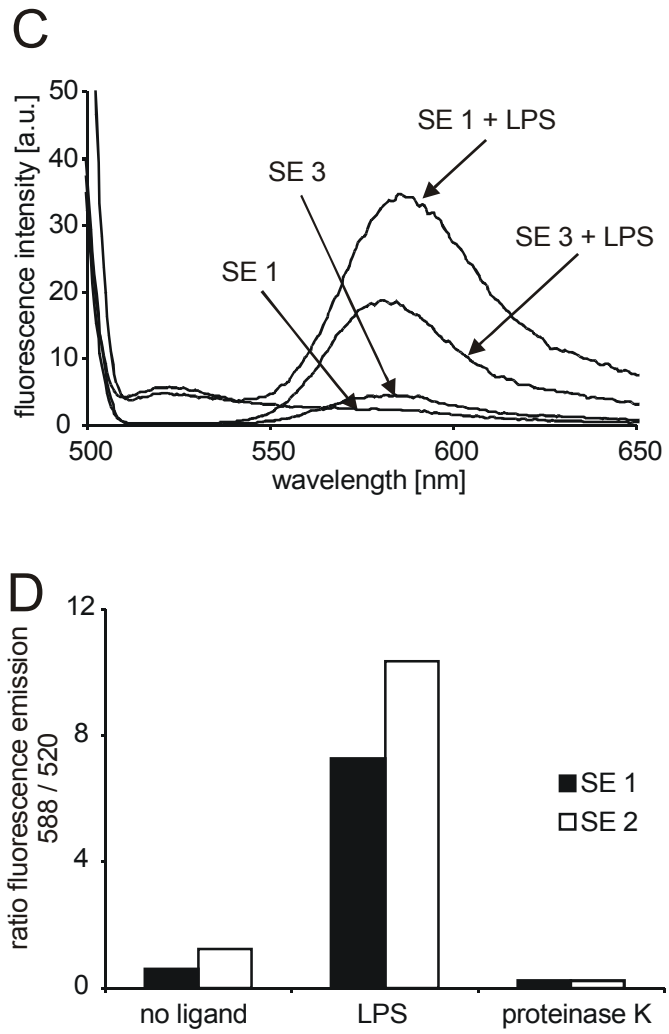

Figure 3.1 Spectral characteristics of the small molecule LPS sensing elements. Fluorescence emission spectra of sensor 1 (A) and 2 (B) (100 nM) in PBS in the absence and presence of LPS (2 μM). (C) Fluorescence emission spectra of SE 1 and 3 (100 nM) in PBS in the absence and presence of LPS (2 μM). Probes were excited at 492 nm and an emission spectrum was recorded as described in the method section. (D) Ratio of the fluorescence emissions at 588 and 520 nm of SE 1 and 2 in PBS alone, in the presence of LPS and after proteinase K treatment (10 μg/ml).

To determine the maximal loss of quenching of fluorescein fluorescence and to obtain further information on the dimer induced quenching of rhodamine fluorescence SE 1 was digested by proteinase K (Figure 3.2). Proteolysis induced a strong increase in the intensity of the fluorescein emission at 520 nm (Figure 3.2A).

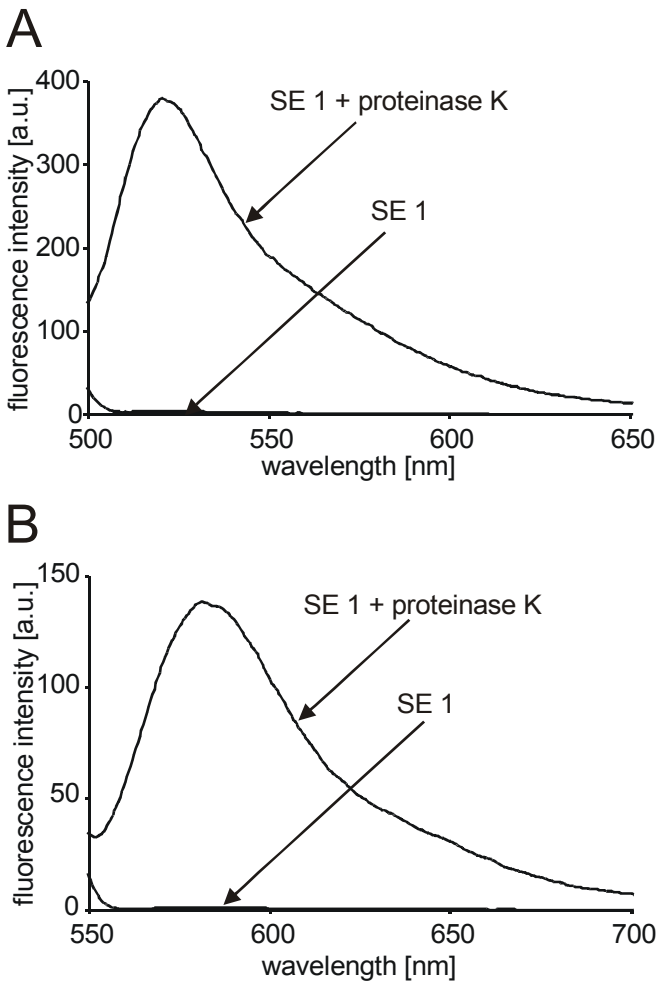

Figure 3.2 Fluorescence emission spectra of SE 1 (100 nM) in PBS in the absence and presence of proteinase K (10 μg/ml). The digestion was carried out at 37°C for 3 h. The spectra were measured in PBS. Probes were excited at 492 nm (A) or 541 nm (B) which represent the excitation optima for fluorescein and tetramethylrhodamine, respectively. The emission spectra were recorded and described in the method section.

The maximum emission intensity of Tamra was achieved when the proteinase K digested sample was excited at 541 nm (Figure 3.2B), the excitation maximum of this dye. This value is about three times higher than the value of the undigested SE 1 in the presence of 2 μM LPS.

For the single labeled peptide, binding of LPS already led to an environment-dependent increase in fluorescence quantum yield. However, a determination of the LPS-binding due to a mere increase in fluorescence intensity is little robust to changes of the sensor concentration. In contrast, for doubly labeled sensing elements a specific ratiometric value of the emission intensities could be obtained

for each of the functional states of the sensing elements (ligand-free or LPS-bound) which is independent on the sensor concentration (Figure 3.1D). Interestingly, the maximum emission ratios for both sensing elements in the LPS-free as well as in the LPS-bound state also differed significantly. For SE 2 the ratio was larger than for SE 1.

A putative mechanism for the detection of LPS is shown schematically in Figure 3.3. The efficiency of FRET is highly sensitive to the distance between the fluorophores, and an eicosapeptide is sufficiently long to maintain fluorophore separation.

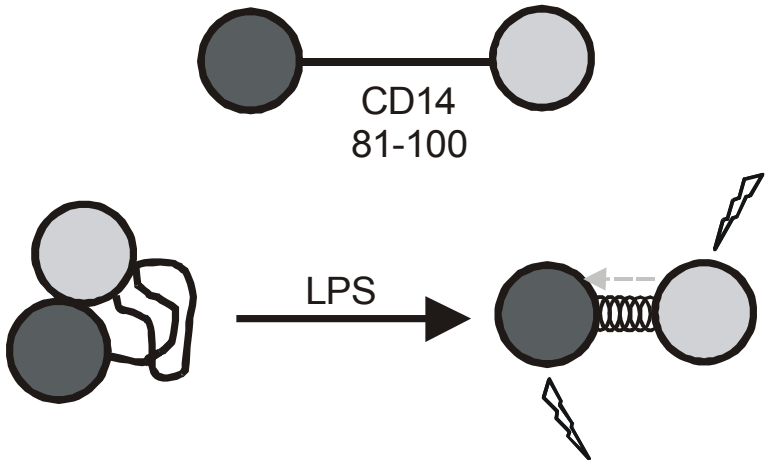

Figure 3.3 Schematic representations of the SE and its putative conformational states in the absence and presence of LPS. The SE is composed of a 20-peptide moiety, corresponding to the LPS-binding site of CD14 (amino acids 81-100), flanked by N-terminal Tamra and C-terminal fluorescein. Without ligand, both fluorophores form an intramolecular dimer resulting in a significant quenching of the fluorescence emission. The LPS-induced structural change leads to a fluorophore separation so that fluorescence resonance energy transfer could be observed.

Next, the dependence of the LPS-induced increase in the emission ratios on the concentration of LPS was determined (Figure 3.4). For SE 1 the ratio increased linearly with concentration over a concentration range of up to 1.5 μM LPS. Saturation was observed at concentrations higher than 2 μM. The detection limit of LPS was about 150 nM. SE 2 exhibited a steeper increase in the ratiometric values, at concentrations between 0.5 and 1.5 μM and larger maximum ratiometric values, but also a higher detection limit (about 0.5 μM) compared to SE 1 (Figure 3.4C).

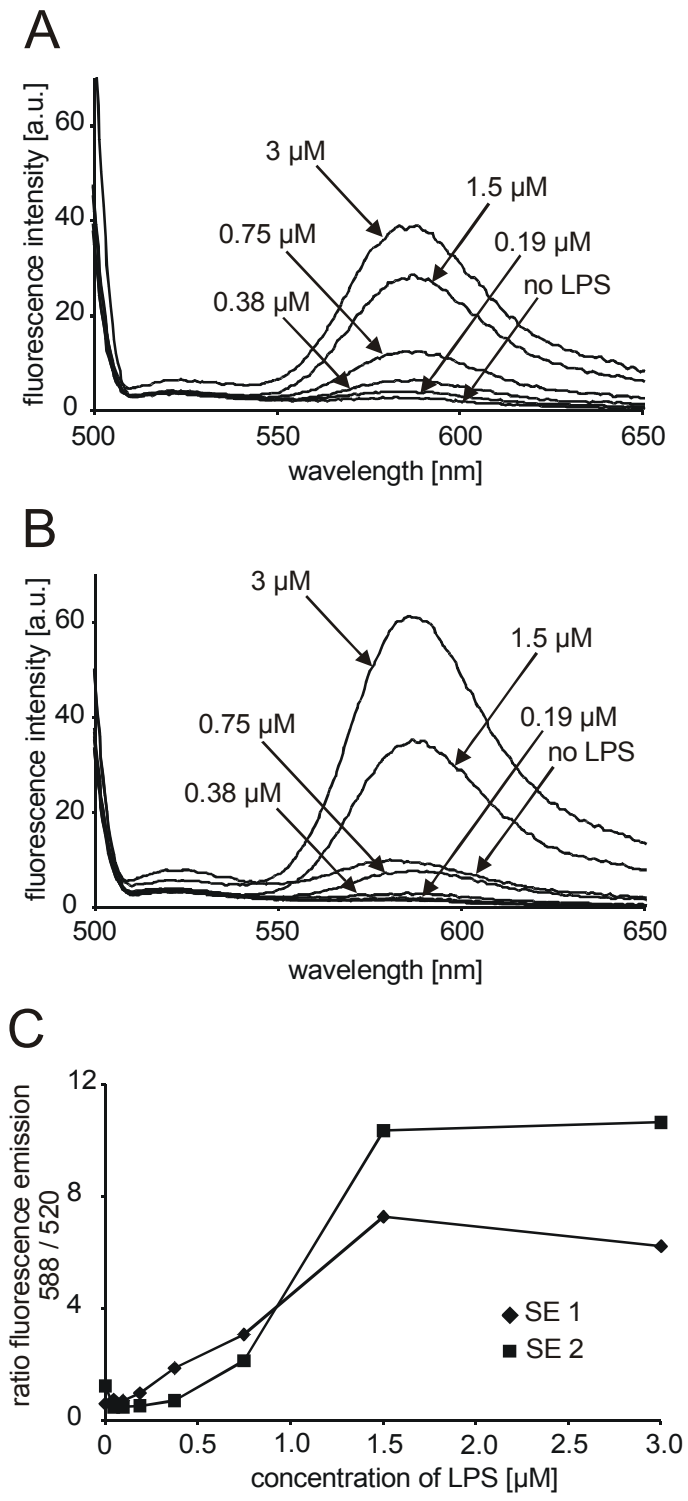

Figure 3.4 Fluorescence emission spectra of SE 1 (A) and SE 2 (B) (100 nm) in the presence of varying concentrations of LPS (0, 0.094, 0.188, 0.375, 0.75, 1.5, and 3 μM). (C) Ratios of the fluorescence emissions at 588 and 520 nm of SE 1 and 2. Probes were incubated for 1 h at 37°C on a shaker and excited at 492 nm in PBS. The emission spectra were recorded as described in the method section.

3.3.2 Determination of the specificity of sensing elements 1 and 2

Beside sensitivity, a sensor is characterized by its specificity enabling the recognition of the ligand without interference by molecules with similar physicochemical characteristics. To determine whether the sensing elements were able to specifically detect LPS, their fluorescence emission spectra were recorded in the presence of increasing concentrations of several amphipathic lipids. These include LPS from *Escherichia coli*, the neutral and negatively charged phospholipids POPC and POPG, and di- and triacylated lipopeptides (Table 3.2). Latter were selected due to their high immune-stimulating properties [28;78-81;87;213] and outstanding relevance as immune adjuvants [83-85;89;214-219] such as the water soluble lipopeptide $Pam_3Cys\text{-}SK_4$ [82;220-224].

Table 3.2 Amphipathic compounds tested in the presence of SE 1 and 2.

Lipid compound	Sequence / denotation
LPS	*E. coli* O111:B4
$Pam_3Cys\text{-}SK_4$	Pam_3Cys-SKKKK
BCI-009	$Pam_3Cys\text{-}(VPGVG)_4VPGKG\text{-}NH_2$
MALP2	Pam_2Cys-GNNDESNISFKEK
POPC	phosphatidylcholine
POPG	phosphatidylglycerol

Since both sensing elements exhibit characteristic differences in the recognition of varying concentrations of LPS (Figure 3.2) we hypothesized that the sensing elements also differentially recognize different lipids. Figure 3.5 shows the fluorescence emission ratios of SE 1 and 2 as a function of lipid concentration. For both sensing elements, the steepest increase and the highest ratiometric values were obtained in the presence of LPS and the lipopeptide $Pam_3Cys\text{-}SK_4$. In contrast, the maximum values evoked by BCI-009, MALP-2 and the phospholipid POPC were significantly lower (3, 4 and 1, respectively) and the curves exhibited a flatter increase. Interestingly, POPG was differentially recognized by the sensing elements. Whereas SE 2 exhibited a steeper increase of the ratiometric values and a higher maximum value, SE 1 exhibited a curve comparable to that for MALP-2. In contrast, the neutral phospholipid POPC was detected neither by SE 1 nor by SE 2.

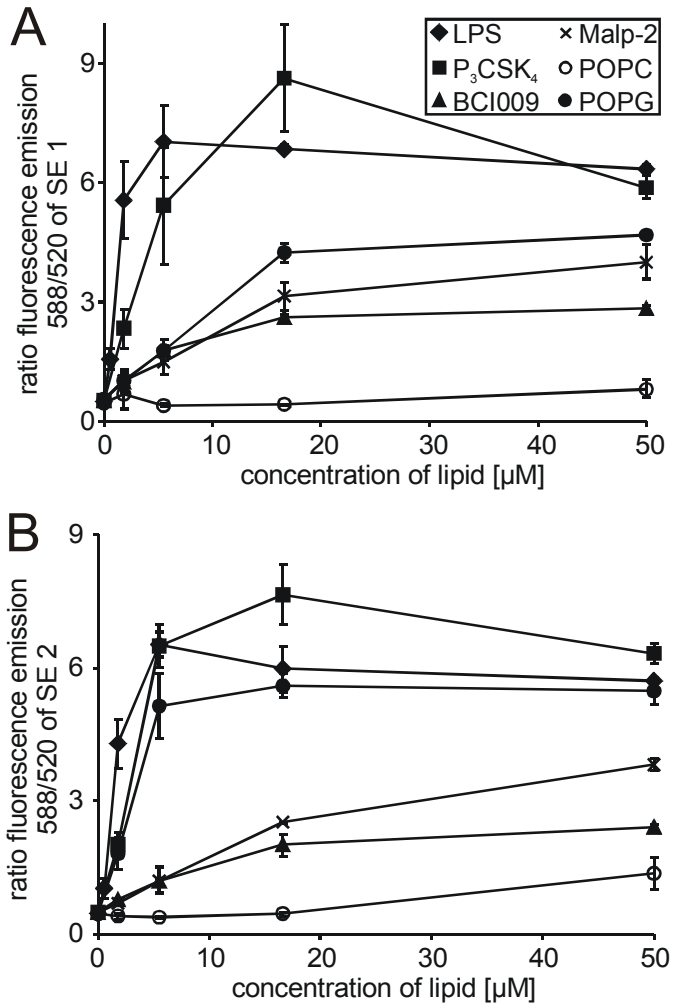

Figure 3.5 Dependence of the fluorescence emission ratios of SE 1 (100 nM) (A) and 2 (B) on concentration for various amphipathic compounds. The spectra were measured in PBS. Probes were excited at 492 nm and an emission spectrum was recorded as described in the methods section.

Next, we plotted the ratiometric values as a function of the fluorescence emission at 588 nm (Figure 3.6) to reveal whether the concentration dependent alterations of the ratio and the corresponding fluorescence emission at 588 nm behave in a distinctive manner. The obtained curves can be consulted for ligand discrimination if they are sufficiently separated.

LPS evoked the steepest increase in the ratio values in comparison to all other lipids resulting in a separation of its curves from that of POPC, POPG, Malp-2 and BCI-009 when using SE 1. For lipopeptide BCI-009, the curve is even separated from all other lipids, due to a significant weaker increase in the emission ratio. In

contrast, intersection was observed between LPS and $Pam_3Cys\text{-}SK_4$. However the lipopeptide exhibited a weaker increase and significantly enhanced emission values at 588 nm at higher concentrations resulting in a pronounced right shift of the curve, compared to that from LPS.

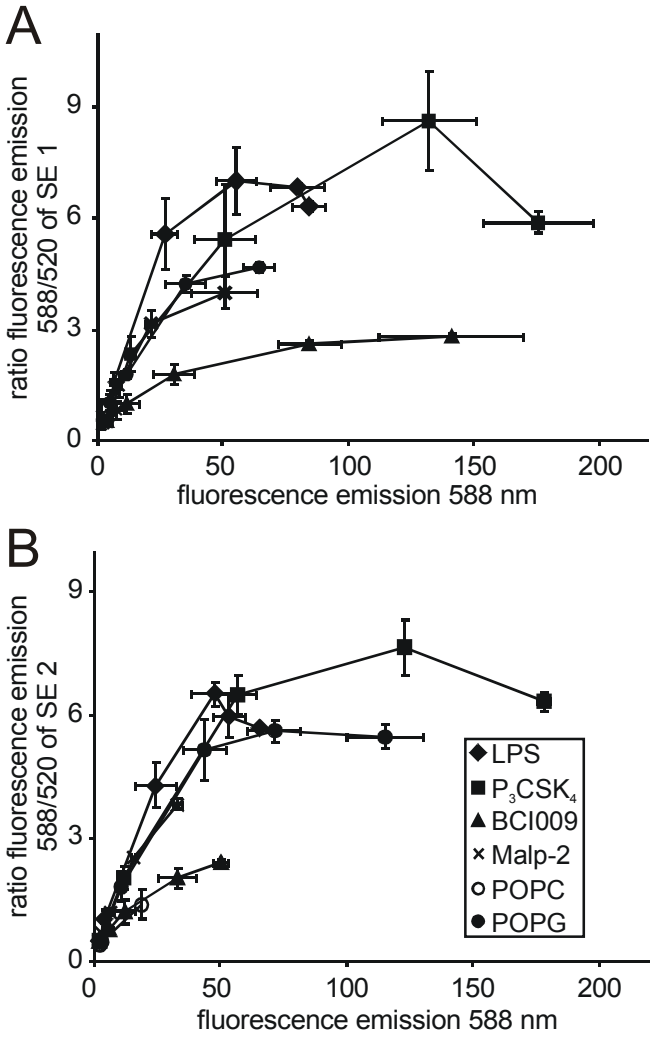

Figure 3.6 Ratio of the fluorescence emission of (A) SE 1 and (B) SE 2 (100 nM) in the presence of increasing concentrations of lipids as a function of the fluorescence emission at 588 nm. The spectra were measured in PBS. Probes were excited at 492 nm and an emission spectrum was recorded as described in the methods section.

To attain further discrimination the ratiometric values evoked by increasing concentrations of lipids of SE 1 and 2 were plotted against each other (Figure 3.7). For most lipids both sensing elements exhibited a comparable ratiometric signal which was represented by a linear increase of the respective curve. However, for POPG the sensitivity of SE 2 was significantly enhanced compared to SE 1 which

is represented by a steeper increase of the fluorescence ratio at POPG concentrations below 5 μM.

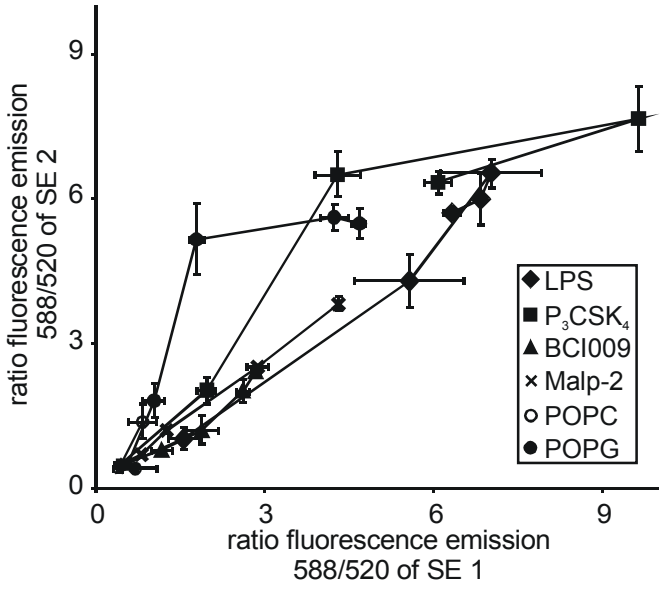

Figure 3.7 Fluorescence emission ratios of SE 1 plotted versus the flurescence emission ratio of SE 2 in the absence or presence of increasing concentration of lipid compounds.

3.4 Discussion

The peptide corresponding to amino acid 81 to 100 of human CD14 tagged N-terminally with Tamra and C-terminally with fluorescein exhibited a significant change in FRET in the presence of LPS and therefore could be applied as a FRET-based sensing element for LPS. Previously, we identified a part of LPS-binding domain of the LPS-receptor CD14. The corresponding peptide was able to bind to LPS from *E. coli*, serotype O111:B4, thereby neutralizing the LPS-induced cytokine expression of THP-1 cells. Three leucines at positions 7, 11 and 14 were found to be essential residues. Under mild secondary structure inducing conditions (20% TFA) this peptide exhibited an α-helical conformation which is also observed for other LPS-binding peptides when binding to LPS. In this report we show, that the binding of LPS to the doubly labeled peptide and to an analogue with enhanced amphipathicity caused a change of the fluorescence emission spectrum. The ratio from the fluorescence emissions at 588 nm and 520 nm was determined and selected for ligand recognition.

Although several other lipids induced an increase in this ratiometric signal of our sensing molecules we observed distinct spectral characteristics for these compounds which were selected for specific ligand detection. The lipopeptide $Pam_3Cys\text{-}SK_4$, for instance induced concentration-dependent changes of the ratiometric signals of SE 1 and 2 comparable to that of LPS. However, in contrast to LPS, the lipopeptide evoked a significantly enhanced fluorescence emission at 588 nm at high ligand concentrations, which resulted in a significant separation of the curve in Figure 3.6. In comparison to LPS and $Pam_3Cys\text{-}SK_4$, the hydrophobic lipopeptide BCI-009 as well as the diacylated lipopeptide MALP-2 evoked significantly lower ratiometric values. When the ratio of the fluorescence emission of the analyzed lipids was plotted against the excitation at 588 nm (Figure 3.6) discrimination between the two hydrophobic lipopeptides BCI-009 and MALP-2 and LPS was possible in a range between 5 and 50 μM.

For most lipids tested the spectral changes for SE 1 and 2 were similar. However, for POPG, SE 2 exhibited higher ratiometric signals at low POPG concentrations than SE 1 resulting in a characteristic curve when the ratiometric values of SE 1 were plotted against those of SE 2. As shown in section 2, hydrophobic residues contribute to the interaction between LPS and the CD14-derived peptides. The enhanced sensitivity of SE 2 for POPG as well as the inability for both sensing elements to detect the neutral phospholipid POPC might therefore indicate that electrostatic rather than hydrophobic interactions are involved in the recognition of phospholipids by our sensing element. Due to these properties it might be possible to distinguish between the effects of negative and neutral phospholipids. In addition, our observations demonstrate that alterations of the physicochemical properties of the sensing element influence its sensitivity and specificity.

It is known that LPS evokes immune responses when injected at nanogram quantities [99]. Since the LAL assay is able to detect these small amounts of LPS it represents an appropriate method for LPS detection in this concentration range. However, the usage of the LAL assay is compromised by limited specificity. Despite of the lower sensitivity of our CD14-derived sensing system, sensors in which the recognition element consists of a peptide have the advantage that their specificity can be varied easily by altering the binding-sequence, as we could

show in this study. Therefore, the peptide based sensing element constitutes a starting point for the development of further, more sensitive and selective sensors.

In addition to LPS, CD14 also contributes to the activation of cells by lipopeptides [44;150] and binds to a variety of lipid compounds, including phosphatidylinositides [225]. We cannot completely exclude whether the corresponding binding region in the native CD14 might also be involved in the recognition of ligands other than LPS. For this reason, the CD14-derived peptides might also interact with other CD14-binding molecules in addition to LPS. However, as revealed by *in vitro* assays, the peptide amide CD14 (81-100) showed only weak inhibitory activity against the lipopeptide $Pam_3Cys\text{-}SK_4$ indicating for an LPS-specific recognition element.

The peptide-based sensing system provides a novel opportunity to detect and distinguish lipids. By applying SE 1 we were not able to specifically recognize LPS, because several other lipids were able to evoke signals almost comparable to that of LPS. However, specific LPS recognition in the concentration range of 5 to 50 μM was achieved by the application of two sequentially differing sensing elements SE 1 and SE 2 which exhibit distinct physicochemical properties and by analysing the data in a way that considers the characteristics spectral changes evoked by the induced by the individual lipid compounds.

3.5 Materials and methods

3.5.1 Reagents

Lipopolysaccharide from *E. coli* (phenol extracted and purified by ion-exchange chromatography) was from Sigma (Taufkirchen, Germany). Three synthetic lipopeptides were from EMC microcollections (Tübingen, Germany): The water soluble *S*-[2,3-bis(palmitoyloxy)-(2*RS*)-propyl]-*N*-palmitoyl-(*R*)-cysteinyl-(S)-seryl-tetralysine (Pam_3Cys-SKKKK), *S*-[2,3-bis(palmitoyloxy)-(2*RS*)-propyl]-*N*-palmitoyl-(*R*)-cysteinyl-$(VPGVG)_4VPGKG\text{-}NH_2$ ($Pam_3Cys\text{-}(VPGVG)_4VPGKG\text{-}NH_2$) (BCI-009) and the diacylated lipopeptide *S*-[2,3-bis(palmitoyloxy)-(2*RS*)-propyl]-(*R*)-cysteinyl-GNNDESNISFKEK (Pam_2Cys-GNNDESNISFKEK) with the sequence of MALP-2 [75]. Standard chemicals were from Fluka (Deisenhofen, Germany) and Merck (Darmstadt, Germany). Fmoc-amino acids were purchased from

Novabiochem (Läufelfingen, Schweiz), Senn Chemicals (Dielsdorf, Switzerland), and Orpegen Pharma (Heidelberg, Germany). Fmoc-Lys(Dde)-OH was from Novabiochem. The mixtures of the isomers of 5(6)-carboxyfluorescein (Fluo) and 5(6)-carboxytetramethylrhodamine (Tamra)-N-succinimidylester were from Fluka. 1-Palmitoyl-2-oleoyl-phosphatidylcholine and 1-palmitoyl-2-2-oleoyl-phosphatidylglycerol were from Avanti Polar Lipids / Otto Nordwald GmbH (Hamburg, Germany).

3.5.2 Solid-phase synthesis of Tamra-CD14 (81-100)-Fluo.

The doubly labeled peptides Tamra-QVPAQLLVGALRVLAYSRLK-εK(αFluo)-NH_2 and Tamra-QVAAKLLVKALRKLAYKRLK-εK(αFluo)-NH_2 (Table 3.1) were synthesized using a previously described (Fluo(Trt)-Lys-Rink amide resin [176]. The carboxyfluorescein is attached to the N^{α}–amino group of the resin bound lysine and the peptide was assembled on the N^{ε}–amino group of the lysine residue. The resin-bound and side-chain protected peptide (5 μmol) was then reacted with 5(6)-carboxytetramethylrhodamine-N-succinimidyl ester (10 μmol, 5.3 mg) in DMF (200 μl) containing DIPEA (2 μmol, 4.3 μl). After 16 h, the resin was thoroughly washed. Peptides were cleaved off the resin and side chains deprotected by treatment with trifluoroacetic acid/triisopropylsilane/H_2O (92.5:2.5:2.5:5, v/v/v/v) for 4 h. Crude peptides were precipitated by adding cold diethyl ether (-20°C). The precipitated peptides were collected by centrifugation and resuspended in cold diethyl ether. This procedure was repeated twice. Finally the peptides listed in Table 3.1 were dissolved in ACN/water, lyophilized and analyzed by HPLC and MALDI-MS. Tamra-QVPAQLLVGALRVLAYSRLK-εK(αFluo)-NH_2: purity 80% (HPLC, 214 nm), calc. $[M+H]^+$ = 3094.7 Da, exp. $[M+H]^+$ = 3094.6 Da. Tamra-QVAAKLLVKALRKLAYKRLK-εK(αFluo)-NH_2: purity 80% (HPLC, 214 nm), calc. $[M+H]^+$ = 3209.9 Da, exp. $[M+H]^+$ = 3209.5 Da (Table 3.3). The fluorescent peptide was then purified by preparative HPLC for spectroscopic characterization.

Table 3.3 Characterization of sensing elements 1 and 2 by MALDI-TOF MS and HPLC.

Sensing element	Sequence	$[M+H]^+$ [Da]	Retention time [min]
SE 1	Tamra-QVPAQLLVGALRVLAYSRLK-εK(αFluo)-NH_2	3094.6	26.0
SE 2	Tamra-QVAAKLLVKALRKLAYKRLK-εK(αFluo)-NH_2	3209.5	23.2

3.5.3 HPLC

Peptides and conjugates with fluorophores (Table 3.1) were analyzed by analytical RP-HPLC (Waters 600 System, Eschborn, Germany) with a solvent system gradient: water/0.1% TFA (solvent A) and acetonitrile/0.1% TFA (solvent B) using an analytical HPLC column (Nucleosil 100, 250 x 2 mm, C18 column, 5 μm particle diameter; Grom, Herrenberg, Germany) with a linear gradient from 10% B to 100% B within 30 min (flow rate: 0.3 ml/min) and detection at 214 nm. Peptides were purified by preparative RP-HPLC (Nucleosil 300, 250 x 20 mm, C18 column, 10 μm particle diameter; Grom, Herrenberg, Germany) on a Gilson preparative system (Bad Camberg, Germany), equipped with a 321 Pump and a 156 UV/Vis detector at a flow rate of 10 ml/min. Gradients were adjusted according to the elution profiles and peak profiles obtained from the analytical HPLC chromatograms. Peptide purities of all peptides used in this study were >98% (214 nm, HPLC).

3.5.4 MALDI-TOF MS

1 μl of DHAP matrix (20 mg of DHAP, 5 mg of ammonium citrate in 1 ml of isopropyl alcohol/H_2O (4:1, v/v)) was mixed with 1 μl of each sample (dissolved in ACN/water (1:1) at a concentration of 1 mg/ml) on a gold target. Measurements were performed using a MALDI time-of-flight system (G2025A, Hewlett-Packard, Waldbronn, Germany). For signal generation 20-40 laser shots were added up in the single shot mode.

3.5.5 Peptide stock solutions

Doubly-labeled peptides (Table 3.3) were dissolved in DMSO at concentrations of 10 mM. Peptide concentrations were determined by UV/VIS-spectroscopy of a further dilution (1:100) in MeOH. Absorptions were measured at a wavelength of 540 nm (ε = 95,000 l/(mol·cm)).

3.5.6 Preparation of lipids and fluorescence spectroscopy.

Lipopeptides were suspended in DMSO (10 mM), lipopolysaccharides in water (5 mg/ml) and phospholipids in chloroform (32 mM). All lipids were sonicated at 40 W using a Sonorex Super RK 510H sonicator (Bandelin, Berlin, Germany) until solubilization as indicated by a clear solution. Doubly-labeled peptides were diluted in PBS to a concentration of 100 nM. The doubly-labeled peptide solution (400 μl) was transferred to an Eppendorf reaction tube and lipids (Table 3.2) were added to a final concentration of 2 μM. Titration experiments were performed in 96-well round bottom microtiter plates. The samples were incubated for 10 min on ice and subsequently for at least 45 min at 37°C on a shaker. After incubation probes were subjected to fluorescence spectrometry performed in quartz cuvettes using an LS 50B luminescence spectrometer (Perkin-Elmer, Norwalk, CT, USA). The excitation wavelength was set to 492 nm; emission scans from 450 to 800 nm were recorded, and the ratio of emission intensities of 588 versus 520 was determined. For proteinase K treatment, a 100 nM solution of sensing element 1 (SE 1, Table 3.3) was incubated with 10 μg/ml of proteinase K for 3 h. Aliquots were taken and the emission spectra of the sample were recorded immediately

4 The state of aggregation determines the bioactivity of lipopeptides

This chapter was adapted from a manuscript submitted to *European Journal of Immunology*. The author of this thesis performed all experiments. Lipopeptides used for the experiments were from EMC microcollections (Tübingen, Germany).

4.1 Summary

Lipoproteins are major components of the cell wall of Gram-positive and -negative bacteria and activate cells of the innate immune system via heterodimers of Toll-like receptor (TLR) 2 with either TLR1 or TLR6. In spite of the progress in understanding TLR-dependent signal transduction and the pathophysiological relevance of TLR2, the molecular basis of ligand recognition by this receptor is only poorly defined. The bioactivity of lipopeptides strongly depends on the dilution protocol. Analysis of fluorescently labeled analogues of the synthetic amphiphilic lipohexapeptide Pam_3Cys-Ser-Lys_4 by fluorescence correlation spectroscopy revealed that these compounds form aggregates in solution. Dilution into protein-and serum-free buffers leads to a complete loss of activity due to formation of large and highly heterogeneous aggregates. When diluted into BSA or serum-containing buffers, the size of the aggregates was strongly reduced and indicative of an interaction of the lipopeptides with protein. Moreover, the aggregate size depended on the peptide moiety and correlated negatively with the bioactivity of the peptide. Dilution of DMSO stock solutions of lipopeptides with *tert.*-butyl alcohol/H_2O (4:1) prior to the preparation of the final working solutions eliminated these peptide-dependent differences in aggregate size resulting in comparable bioactivities. This result is highly relevant for the analysis of structure-activity relationships of lipopeptide-dependent TLR2 activation.

4.2 Introduction

Due to the highly repetitive structure and complex physicochemical and conformational properties of most TLR ligands, the exact nature of the molecular interaction between receptors and agonists has remained elusive for all TLR subtypes as did the molecular mechanism of receptor activation. For lipopeptide and lipopolysaccharide ligands, amphiphilicity leads to the rapid insertion of these molecules into cellular membranes [226-228].

For TLR2-dependent signal transduction, synthetic lipopeptides provide a rich source of highly diverse structures to explore the structure-activity relationships of TLR2-dependent activation. Analogues of the well known synthetic adjuvants *S*-[2,3-bis(palmitoyloxy)-(2*RS*)-propyl]-*N*-palmitoyl-(*R*)-cysteinyl (Pam_3Cys) peptides [79;82;216] with modifications of the lipid as well as the peptide moiety can be efficiently generated by combinatorial solid-phase organic chemistry [94;196].

When testing the induction of expression of the cytokine IL-8 by synthetic lipopeptides that differed with respect to their peptide moiety we discovered that the dissolution protocol affected the bioactivity of some lipopeptides. It had been described previously, that Pam_3Cys-conjugates form vesicular or tubular aggregates of different size in aqueous solutions depending on the configuration of the glycerol moiety and the head group [229]. We therefore wondered, whether the observed dissolution-dependent differences correlated with a differential tendency of the respective analogues to form aggregates. For LPS it was shown, that the aggregation as well as the type of aggregate structure is essential for activity and cell binding properties [230-234].

To detect the presence of aggregates in solution confocal fluorescence correlation spectroscopy (FCS) [235] was applied to a limited set of fluorescently labeled lipopeptide analogous. FCS is a highly sensitive tool to derive information on molecular interactions, particle size and the number of fluorescent particles from the time-correlated analysis of fluctuations of a fluorescence signal. For example, fluorescence fluctuation spectroscopy was formerly used to detect e.g. aggregation between oligonucleotides and polycationic polymers [236]. In addition, FCS provides a quick and simple method for the determination of aggregates in solution.

Using FCS our experiments revealed that the observed dissolution-dependent differences were in fact due to the formation of aggregates of different size. Introduction of an additional dilution step in *tert.*-butyl alcohol/H_2O (4:1) decreased the aggregate size and increased the biological activity. The optimized dissolution protocol eliminates a major uncertainty in comparing the biological activity of TLR2 ligands. Therefore, our results generate a solid experimental basis for the analysis of structure-activity relationships that reliably reflect the capacity of the ligands to activate the receptor.

4.3 Results

4.3.1 Dissolution-dependent biological activity of lipopeptides..

It had been shown previously for a collection of synthetic lipohexapeptide analogues carrying the head group agonist Pam_3Cys, that the peptide moiety has little influence on the TLR2 agonistic bioactivity [94]. When testing two different Pam_3Cys peptide analogues LP1 and LP2 with respect to the induction of IL-8 expression in THP-1 cells, we were therefore surprised to find that LP1 showed little agonistic activity whereas LP2 exhibited significant activity (Figure 4.1). LP1 contains the ovalbumine derived epitope of the MHC-I-complex H-$2K^b$ and a proline spacer between the lipid and the epitope whereas LP2 contains an arbitrarily constituted peptide sequence and a pentaproline spacer (Table 4.1)

Table 4.1 Lipopeptide analogues tested for agonistic activity. Fluorescently labeled derivatives of LP1 and LP2 (Rh-LP1 and Rh-LP2) were in addition investigated by FCS. Carboxytetramethylrhodamine (Tamra) was covalently linked to the ε-amino group of the lysine residue in the peptide moiety.

Lipopeptide	Sequence
LP1	P_3C-PPPPPSIINFEKL
LP2	P_3C-PPPPPPFEDIYKN
Rh-LP1	P_3C-PPPPPSIINFEK(Tamra)L
Rh-LP2	P_3C-PPPPPPFEDIYK(Tamra)N

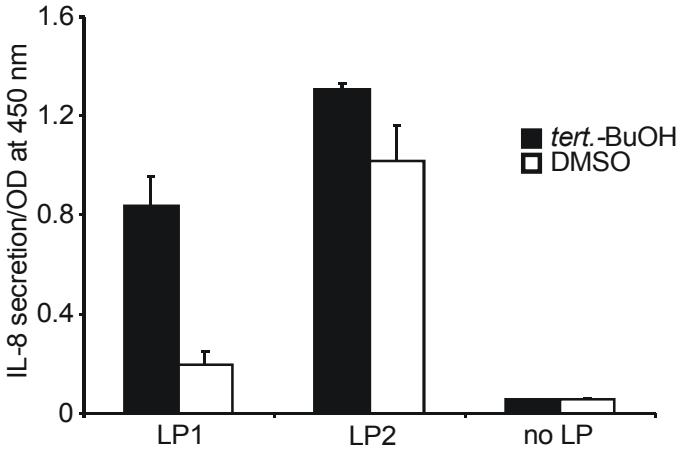

Figure 4.1 Agonistic activities of differently diluted lipopeptides. Lipopeptide stock solutions (1 mM in DMSO) were diluted either 1:20 in *tert.*-butyl alcohol/H_2O (4:1) or DMSO. These solutions were further diluted 1:500 with RPMI/10% FBS and subsequently 1:10 to a final concentration of 10 nM with medium containing THP-1 cells. THP-1 cells were incubated with LP1 (A) and LP2 (B) for 16 h. IL-8 secretion was measured by matched-paired ELISA. Error bars represent the mean deviations of triplicates.

It is well known that for amphiphilic molecules, the dissolution protocol is a critical first step. Even though clear solutions were prepared for both lipopeptides, we therefore suspected differences in the dissolution behaviour of these lipopeptides as the basis for this observation. As an alternative to the preparation of highly concentrated 1 mM DMSO stock solutions we had previously used a dilution of the DMSO stock solutions of lipopeptides into *tert.*-butyl alcohol/H_2O (4:1, v/v) as a dissolution protocol. When such solutions of fluorescently labeled lipopeptides were pipetted onto hydrophobic surfaces and dried, a highly homogeneous surface functionalization was obtained, indicative of a good dissolution of the lipopeptides [237]. We therefore introduced a further 1:20 dilution step of the DMSO stock solution into *tert.*-butyl alcohol/H_2O (4:1, v/v)). The agonistic activity of lipopeptide 1 (LP1) was in fact significantly enhanced using *tert.*-butyl alcohol/H_2O (4:1) as a solvent prior to its addition to the FBS-containing tissue culture medium. In contrast, for LP2, dilution into *tert.*-butyl alcohol/H_2O (4:1) yielded only a minor increase in bioactivity. DMSO and *tert.*-butyl alcohol possess cytotoxic activities when present in the cell culture medium at concentrations exceeding 0.2 or 2% respectively (own observations). In our experiments the amount of the solvents was two orders of magnitude below the toxic concentrations and did therefore not influence the viability of the THP-1 cells.

4.3.2 Aggregation of differently diluted LPs monitored by single molecule detection.

To determine whether the increase in bioactivity of the *tert.*-BuOH/H_2O treated LP1 was due to a change in aggregation, fluorescence correlation spectroscopy of 5(6)-carboxytetramethylrhodamine-labeled analogues of these lipopeptides (Rh-LP1 and Rh-LP2) was performed. Changes in the hydrodynamic radius of molecules, e. g. due to formation of molecular aggregates constitute themselves as a shift of the autocorrelation function towards longer diffusional autocorrelation times. However, as the diffusion constant D scales inversely with the cubic root of the molecular weight, detectable shifts require a substantial mass increase.

First, we investigated whether the fluorescently labeled lipopeptides exhibited the same dilution-dependent cell-activating properties as their non-fluorescent counterparts (Figure 4.2A). The agonistic activity of Rh-LP1, the fluorescently labeled analogue of LP1, strongly depends on the dilution protocol in correspondence to the unlabeled lipopeptide. In contrast, the dilution protocol did not influence the biological activity of Rh-LP2 as determined for its non-fluorescent analogue. For LPS it was shown that several proteins, including LPS-binding protein, sCD14 and albumin are involved in binding, transport and disaggregation of LPS aggregates prior receptor activation [185;187;188;238]. Due to the fact, that these LPS binding molecules are present in FBS we also investigated whether dilution of the lipopeptide solutions into buffer containing BSA alone yielded the same dependence of activity on the additional *tert.*-butyl alcohol/H_2O (4:1) dilution step. A high activity of LP demonstrated that addition of BSA to the buffer is sufficient to achieve an efficient lipopeptide-mediated activation of cells (Figure 4.2B) whereas the dilution of lipopeptides in buffer without protein completely abolishes lipopeptide activity (see Figure 4.6). Therefore BSA is a minimal requirement for an active state of the lipopeptides. The general effect of the dilution protocol (Figure 4.3) for both lipopeptides was the same and the overall activity of both lipopeptides was lower in the presence of BSA than in the presence of FBS.

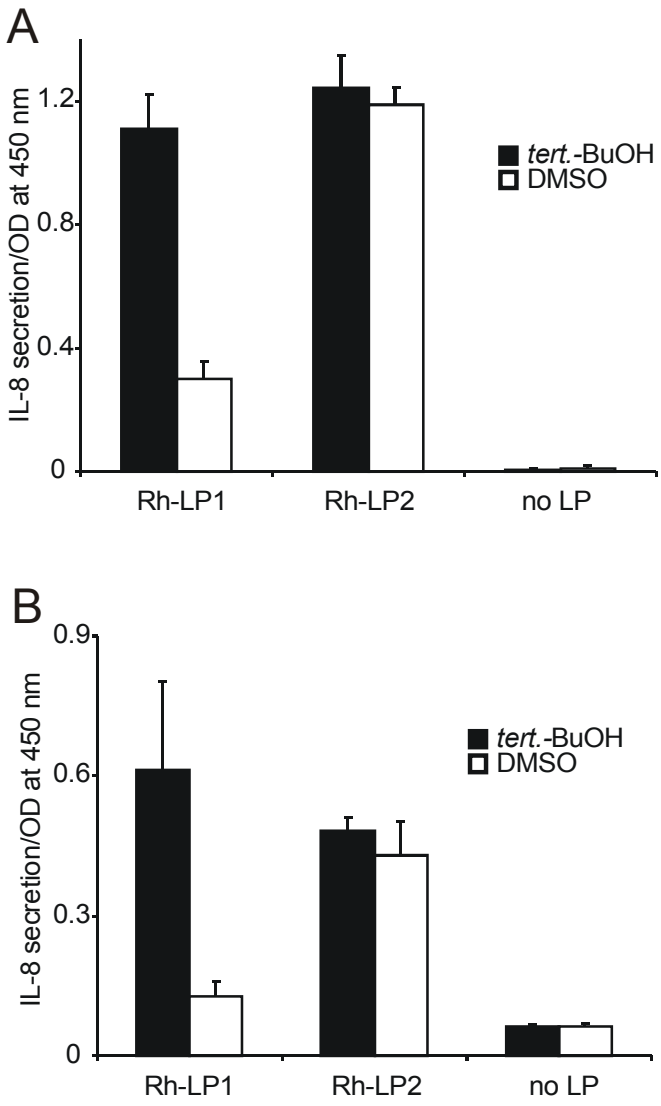

Figure 4.2 Determination of the agonistic activity of differently diluted Tamra-labeled analogues of lipopeptides LP1 and LP2. THP-1 cells were incubated with 10 nM of either *tert.*-butyl alcohol/H_2O (4:1)- or DMSO-diluted (Figure 4.3) Rh-LP1 and Rh-LP2 for 16 h. (A) Final dilution into PBS/FBS (10%), (B) into in PBS/BSA (0.1%). IL-8 secretion was measured by ELISA. Error bars represent mean deviations of triplicates.

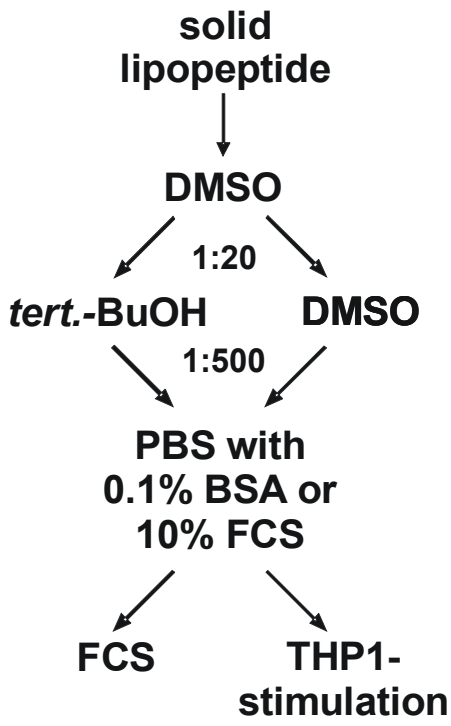

Figure 4.3 Dilution protocols for the preparation of lipopeptide solutions. First, lipopeptides were solubilized in DMSO as 1 mM stock solutions. Second, these stock solutions were either diluted 1:20 with *tert.*-butyl alcohol/H_2O (4:1) or DMSO. Third, a 1:500 dilution in PBS/BSA (0.1%) or PBS/FBS (10%) was subjected to fluorescence correlation spectroscopy or added 1:10 to THP-1 cells in order to determine the agonistic activity.

FCS experiments for aggregate detection of the differently diluted lipopeptides were conducted on the same day with aliquots of the same dilutions of lipopeptides in order to ensure maximum consistency of results. For any lipopeptide in any condition no large aggregates were detected (Figure 4.4).

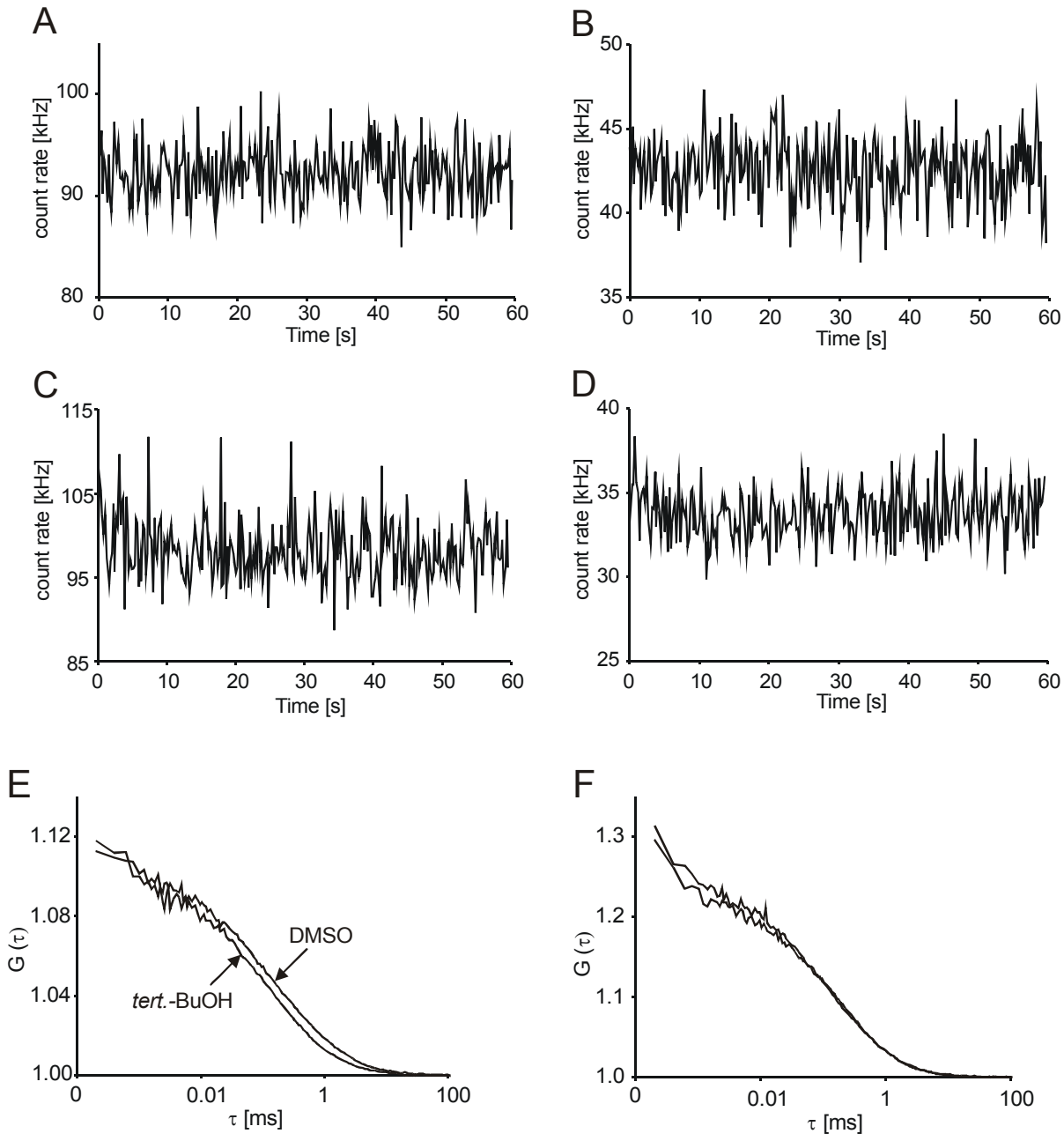

Figure 4.4 Dilution dependent aggregation determined by fluorescence correlation spectroscopy. *Tert.*-Butyl alcohol/H_2O (4:1) or DMSO diluted Rh-LP1 and Rh-LP2 were diluted 1:500 in PBS/BSA (0.1%) as described in material/methods and subjected to fluorescence correlation spectroscopy. (A-D) Fluorescence count traces F(t) of 60 s measurements of Rh-LP1 (A,C) and of Rh-LP2 (B,D) either treated with *tert.*-butyl alcohol/H_2O (4:1) (A,B) or DMSO (C,D). Autocorrelation functions of Rh-LP1 (E) and Rh-LP2 (F).

In the fluorescence count traces, such aggregates constitute themselves as large spikes of fluorescence and compromise the acquisition of autocorrelation

functions. The obtained count traces were characteristic for homogeneously solubilized molecules. Smooth autocorrelation functions with well defined diffusional autocorrelation times were obtained in all cases. However, for Rh-LP1 diluted only in DMSO the autocorrelation function was right-shifted towards longer autocorrelation times in contrast to the *tert.*-butyl alcohol/H_2O-diluted sample (Figure 4.4E). This finding indicates that the lipopeptide was present in aggregates of higher molecular weight. The autocorrelation functions of differently diluted Rh-LP2 were indistinguishable from each other, consistent with their comparable biological activities (Figure 4.4F). All autocorrelation functions could be fitted with a formalism including only one diffusing component, yielding the diffusional autocorrelation times τ_D. As mentioned above, the autocorrelation function allows conclusions about the aggregation state of the fluorescent molecules. Only a substantial mass increase of the particles results in a detectable shift of the autocorrelation function.

For Rh-LP1, treatment with *tert.*-butyl alcohol/H_2O reduced the diffusional autocorrelation time to 200 μs compared to 350 μs for the DMSO-diluted sample (Figure 4.5A). For Rh-LP2 for both conditions a diffusional autocorrelation time of about 200 μs was determined corresponding to the one of the *tert.*-butyl alcohol/H_2O-diluted Rh-LP1. Interestingly, while for the dilution into BSA and FBS-containing buffers the general observations were the same for both lipopeptides, in detail the diffusional autocorrelation times differed (Figure 4.5B). For Rh-LP2 diluted into FBS-containing buffer, for both dilution protocols the diffusional autocorrelation times were significantly longer, while for Rh-LP1 diluted directly from the DMSO stock solution, the diffusional autocorrelation time was shorter.

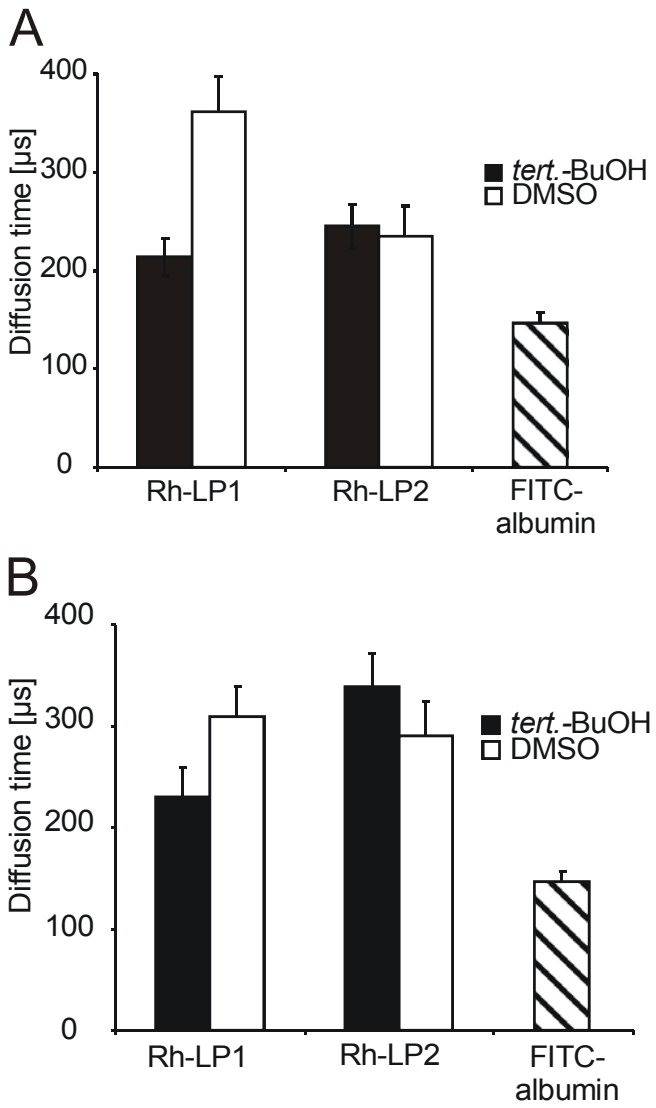

Figure 4.5 Diffusion times of fluorescently labeled lipopeptides determined by fluorescence correlation spectroscopy. Diffusional autocorrelation time (μs) of fluorescent labeled lipopeptides and FITC-BSA in (A) PBS/BSA (0.1%) or (B) PBS/FBS (10%) were obtained by fitting of the autocorrelation functions using the Confocor software. The values represent the median and standard deviation of the diffusion time of 10 measurement intervals of 60 s measurement time, each.

In order to obtain information on the size of these particles, FCS measurements were also performed for fluorescein-labeled BSA serving as a molecular size reference. For BSA a diffusional autocorrelation time of 150 μs was obtained, indicating that in any case the lipopeptides were present as aggregates significantly exceeding the size of BSA. Binding of a single lipopeptide molecule to BSA would not be expected to result in such an increase in molecular size. BSA has a hydrodynamic radius of about 4 nm [239]. Assuming a globular shape, the

radius of the lipopeptide-containing particles should therefore be in the range of 5 to 7 nm. Correlation of the FCS results with the induction of IL-8 expression therefore reveals a negative correlation of the size of the lipopeptide-containing particle and the biological activity.

So far, following established protocols, lipopeptides had been diluted into protein-containing media. When lipopeptides, either diluted only with DMSO or with *tert.*-butyl alcohol/H_2O, were diluted into BSA- and FBS-free PBS almost no agonistic activity was detected. In the fluorescence count trace large peaks were present, indicating the formation of large aggregates that were heterogeneous in size (Figure 4.6).

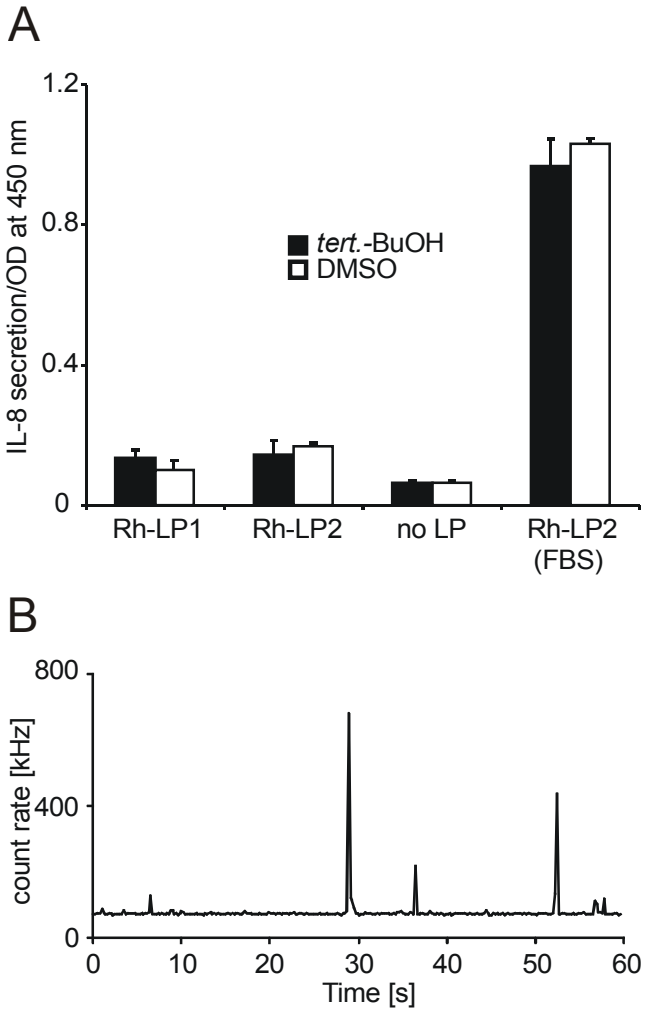

Figure 4.6 (A) Biological activity of Rh-LP1 and Rh-LP2 diluted in PBS without FBS and BSA in comparison to Rh-LP2 diluted in PBS/FBS (10%). (B) Fluorescence count trace of Rh-LP1 diluted into PBS alone.

Due to the heterogeneity of the size of the detected aggregates the calculation of the autocorrelation function was impossible.

4.4 Discussion

When testing different lipopeptides for their agonistic activity in a cellular assay, we observed for some compounds a strong dependence of the activity on the solvent applied during dilution onto working concentration. Especially dilution with *tert*-butyl alcohol treatment of some lipopeptides prior to the dilution into the cell containing medium significantly enhanced the agonistic activity. Aqueous buffers, required for cellular assays, force amphipathic molecules into an aggregated state which shields the hydrophobic moieties against the hydrophilic environment. For the *in vitro* testing of the agonistic activities of different amphipathic molecules, however, it is necessary to achieve comparability of the test scores. In this study we addressed the question if the aggregation state of a lipopeptides influences their agonistic activity and if dilution with different solvents results in different aggregation states of these amphiphilic molecules.

So far, little has been known about the molecular mechanism of TLR2 activation by lipopeptides. Definition of the molecular state of these molecules once they encounter a target cell is the first step for dissecting the molecular events leading to receptor activation. The observation that for some analogues of the synthetic Pam_3Cys lipopeptide the biological activity depended on the dissolution protocol prompted us to investigate whether these differences were due to differences in the molecular state, i. e. aggregation of these molecules. Solutions of fluorescently labeled lipopeptide analogues were analyzed by fluorescence correlation spectroscopy. Aggregates of similar size were obtained for both tested lipopeptides when the optimized dissolution protocol was employed. The finding that the autocorrelation functions could be fitted with one diffusive component indicates that these aggregates were not very heterogeneous in nature, however, it cannot be concluded that lipopeptides form well-defined oligomers. For polyethyleneimine-DNA complexes a very similar observation had been made [240].

Remarkably, in all cases the aggregates were larger in size than BSA. If no protein was present in the medium, very large and heterogeneous aggregates

were obtained. Apparently, the lipopeptide aggregates do not exist free in solution but associate with BSA or constituents of the FBS.

For the TLR4-agonist LPS, it has been reported that aggregates bind to membrane-bound LBP leading to the activation of cells [230;241]. In addition to LBP, albumine is involved in the LPS-dependent activation of cells. Prior to the binding to LBP, aggregated LPS forms a complex with albumin and mediates its solubility in aqueous solutions [238]. The formation of large and heterogeneous aggregates in PBS without added proteins (Figure 4.6), suggests that serum components may exert a similar solubilizing function for lipopeptides.

Several accessory molecules such as CD14 [44;150] or LBP [242] in addition to TLRs contribute to the lipopeptide dependent activation of cells. The involvement of these proteins indicates for an incorporation of lipopeptides into membrane associated proteins. For our experiments, FBS constitute a source of these proteins and we observed that lipopeptides diluted into buffer containing FBS exhibited an enhanced activity in comparison to lipopeptides which were diluted in buffer only containing BSA. Nevertheless, the addition of BSA to PBS was sufficient to achieve a solubilization state of the lipopeptides that renders the lipopeptides biologically active and enables the acquisition of defined autocorrelation functions by FCS. This dissolution protocol therefore generates a basis for the analysis of structure-activity relationships of lipopeptides under highly controlled conditions.

4.5 Materials and methods

4.5.1 Reagents

Standard chemicals were from Fluka (Deisenhofen, Germany) and Merck (Darmstadt, Germany). 1-Hydroxybenzotriazole, diisopropylethylamine, N,N´-diisopropylcarbodiimide, piperidine, dichloromethane, dimethylformamide were from Fluka. FITC-labeled albumin was from Sigma (Taufkirchen, Germany). Fmoc-amino acids were from Novabiochem (Läufelfingen, Switzerland), Senn Chemicals (Dielsdorf, Switzerland), and Orpegen Pharma (Heidelberg, Germany). Pam3Cys-OH was from EMC microcollections GmbH (Tübingen, Germany).

4.5.2 Lipopeptides

Pam_3Cys-P_5SIINFEKL-OH and Pam_3Cys-P_6FEDIYKN-OH and their 5(6)-carboxytetramethylrhodamine labeled analogues Pam_3Cys-P_5SIINFEK(N^{ε}Tamra)L-OH and Pam_3Cys-P_6FEDIYK(N^{ε}Tamra)N-OH were synthesized by fully automated solid phase chemistry [196] using the fluorenylmethoxycarbonyl-*t*-butyl strategy on TCP resins as described previously [243]. The *N*-palmitoyl-*S*-[2,3-bis(palmitoyloxy)-(2*RS*)-propyl]-(*R*)-cysteine residue was coupled to the free N-terminus of the resin-bound peptides in dimethylformamide/dichloromethane (1:1) with N,N´-diisopropylcarbodiimide/1-hydroxybenzotriazol in three-fold excess within 3 h. The coupling was monitored by Kaiser test. The lipopeptides were cleaved off the resins and side chains deprotected with trifluoroacetic acid : phenol : ethanedithiol : thioanisole : water (96 : 2 : 1 : 2 : 1, v/w/v/v/v) for 3 h. The products were filtered from the resins, which were washed once with dichloromethane. The solvents were evaporated and lipopeptides were precipitated at -20°C by the addition of diethylether. The precipitates were washed twice by sonication with diethylether and were lyophilized from water : *tert.*-butyl alcohol (1 : 4, v/v).

4.5.3 Labeling of lipopeptides with carboxytetramethylrhodamine

For selective fluorescent labeling of the side chain of the lysine residue the 4-methyltrityl group (Novabiochem) was deprotected by 0.5% TFA (v/v) in dichloromethane. After deprotection resin-bound lipopeptides were reacted with 3 eq. of 5(6)-carboxytetramethylrhodamine, O-(benzotriazol-1-yl)-N,N,N',N'-tetramethyluronium tetrafluoroborate, 1-hydroxybenzotriazol and 6 eq. N,N-diisopropylethylamine in DMF for 16 h. Reactions were stopped by washing the resins five times each with DMF, methanol and diethyl ether. Completeness of labeling was confirmed by Kaiser-Test. The identity of defined lipopeptides was determined by electrospray mass spectrometry [244]. All biological and spectroscopic studies should be performed with freshly prepared solutions max 1 h after performing the dilution protocol.

4.5.4 Dilution protocol

Lipopeptide solutions were prepared using a three-step dilution protocol (Figure 4.3): First, lipopeptides were solubilized to 1 mM stock solutions in DMSO. Second, these stock solutions were diluted 1:20 (v/v) either in *tert.*-butyl alcohol/H_2O (4:1, v/v) or in DMSO. Third, for non fluorescent lipopeptides these dilutions were further diluted 1:500 in RPMI medium (PAN Biotech, Aidenbach, Germany) containing 10% FBS (PAN Biotech) and finally added 1:10 to the THP-1 cell suspension. Fluorescent lipopeptides were diluted 1:500 in PBS, PBS containing 0.1% BSA or PBS containing 10% FBS. After incubation for 50 min at 37°C on a shaker samples were used for fluorescence correlation spectroscopy or for stimulation of THP-1 cells. Lipopeptide concentrations were determined by UV/VIS-spectroscopy. For this purpose the DMSO-stock solution was diluted (1:500) in MeOH. Absorption was measured at a wavelength of 540 nm. Concentrations were calculated using a molar extinction coefficient of 95,000 l/(mol·cm).

4.5.5 Aggregate analysis by single molecule detection.

FCS measurements were carried out on a ConfoCor2 fluorescence correlation spectroscope (Carl Zeiss, Jena, Germany) using a 400 µl sample volume in an 8-well chambered coverslip (Nunc, Wiesbaden, Germany). Fluorescein fluorescence was excited using the 488 nm line of an argon-ion laser and fluorescence detected using a BP 505 – 550 nm band pass filter; Tamra fluorescence was excited using a 543 nm HeNe-laser and fluorescence was detected with a 550 - 600 nm bandpass filter. For each experimental condition every sample was subjected to 10 measurement intervals of 60 s measurement time, each. Autocorrelation functions were calculated on-line using the ConfoCor 2 FCS software. Autocorrelations were fitted between 10 µs and 1 s with a formalism accounting for one diffusing species. For samples in which a large number of aggregates were present no defined autocorrelation functions could be obtained. Diffusion coefficients D were calculated from:

$$D = \frac{\omega_{xy}^{2}}{4\tau_{D}}$$

(ω_{xy} = radius of the detection volume in the xy-plane, τ_D = diffusional autocorrelation time). ω_{xy} was determined from τ_D of rhodamine-6-G ($D = 2.5 \cdot 10^{-6}$ cm^2 s^{-1}).

For PBS-diluted samples that exhibited signals originating from solution containing highly heterogeneous aggregates with strong heterogeneity evaluation of fluorescence fluctuations using autocorrelation analysis was not possible.

4.5.6 Cell culture

The human monocytic leukemia cell line THP-1 was obtained from the DSMZ (Braunschweig, Germany). The cells were cultured in RPMI 1640 medium supplemented with 10% FBS in a 5% CO_2 humidified atmosphere at 37°C. Cells were passaged every third to fourth day.

4.5.7 IL-8 ELISA

THP-1 cells were suspended in RPMI medium containing 10% fetal calf serum and dispensed into 96-well culture plates at a cell density of 5 x 10^4 cells per 180 µl of medium. The cells were then incubated for 1 h at 37°C in the incubator. 20 µl of the 1:500 diluted lipopeptides were then added to THP-1 cells and further incubated at 37°C for 16 h. Controls with peptide-free buffers containing equal amounts of DMSO and *tert*-butyl alcohol/H_2O in RPMI (10% fetal calf serum), PBS, PBS containing 0.1% BSA or PBS containing 10% fetal calf serum were included in each assay. Cell free supernatants were collected and stored at –80°C prior to the ELISA. Maxi-sorb 96-well plates (Nunc, Wiesbaden, Germany) were coated for 20 h with 100 µl per well of a solution of a mouse anti-human IL-8 antibody (clone G265-5, BDPharMingen, San Diego, USA) (1 µg/ml in PBS). After blocking with 200 µl of PBS/4% BSA per well, the plates were incubated with 100 µl of culture supernatants diluted 1:2 in PBS/4% BSA for 1 h at room temperature. Subsequently, 100 µl per well of a solution of a biotinylated mouse anti-human IL-8 antibody (clone G265-8, BDPharMingen) (0.5 µg/ml in PBS/4% BSA) was added

and incubated for 1 h, followed by a 1 h incubation with streptavidin horseradish peroxidase (Pierce, Bonn, Germany) (1:5,000 in PBS/4% BSA). For detection, the plates were incubated with 3,3´,5,5´-tetramethylbenzidine substrate (Pierce, Rockford, USA). The reaction was stopped by adding 100 µl H_2SO_4 (0.5 M) to each well and the absorbance was measured at 450 nm with a microplate reader (Molecular Devices SpectraMax 340, GMI, Albertville, USA). After each incubation, the plates were washed three times with PBS pH 7.2/0.2% Tween 20 (Sigma).

5 Lipolanthionine peptides act as inhibitors of TLR2-mediated IL-8 secretion

The chapter was adapted from a manuscript submitted to *Journal of Medicinal Chemistry*. The author of this thesis performed all experiments shown in Figure 5.2 to 5.5 Lipolanthionine peptides were synthesized and analysed by Dr. Tobias Seyberth.

5.1 Summary

Lipoproteins from Gram-positive and Gram-negative bacteria and from mycoplasma as well as shorter synthetic lipopeptide analogues activate cells of the innate immune system via Toll-like receptor TLR2/TLR1 or TLR2/TLR6 heterodimers. For this reason, these compounds constitute highly active adjuvants for vaccines either admixed or covalently linked. The lanthionine scaffold has structural similarity with the S-[2,3-dihydroxypropyl]-cysteine core structure of lipopeptides. Therefore, lanthionine-based lipopeptide amides were synthesized and probed for activity as potential TLR2 agonists and antagonists. A collection of analytically defined lipolanthionine peptide amides exhibited an inhibitory effect of the TLR2-mediated IL-8 secretion when applied in high molar excess to the agonistic synthetic lipopeptide Pam_3Cys-Ser-$(Lys)_4$-OH. Analysis of structure-activity relationships revealed the influence of the chirality of the two α-carbon-atoms, chain lengths of the attached fatty acids and fatty amines and of the oxidation level of the sulphur atom on the inhibitory activity of the lipolanthionine peptide amides.

5.2 Introduction

Lipoproteins are cell wall components of Gram-positive and Gram-negative bacteria [245;246] and mycoplasma [247;248]. The N-terminal cysteine residue of these bacterial membrane proteins is posttranslationally modified to S-[2,3-dihydroxypropyl]-cysteine (Dhc) which is acylated by three or two fatty acids. Lipoproteins and synthetic analogues such as the water-soluble lipohexapeptide Pam_3Cys-Ser-$(Lys)_4$-OH [90] stimulate B cell proliferation and possess very favorable adjuvant activities in the generation of T cell responses to vaccines [83;84;86;249;250].

Among PAMPs lipopeptides are the primary candidates for analysing the structure-activity relationships of immune modulators. The role of the peptide moiety, the number and structure of the fatty acids and the stereochemistry of lipopeptides based on Dhc for TLR activation have been analysed in great detail [94;251]. In contrast, variation of the Dhc core-structure has found little attention so far [252]. The apparent similarity of the scaffolds Dhc and lanthionine (Figure 5.1) led us to the assumption that lanthionine-based lipopeptide amides might show TLR2 agonistic activities similar to those of Pam_3Cys-peptides [83;84;86;90;249;250] or, due to their structural differences, inhibitory activities.

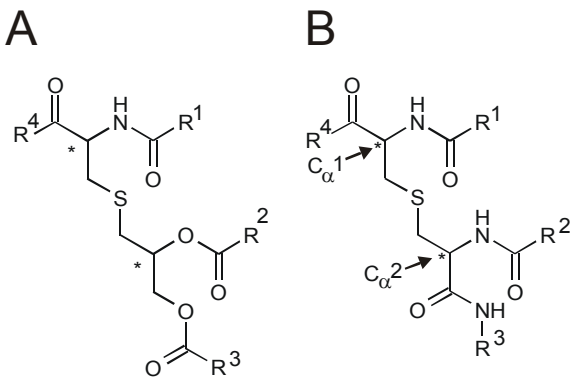

Figure 5.1 Structures of the natural thioether amino acid scaffolds Dhc (A) and lanthionine (Lan) (B)**.** Because of the structural relationship lanthionine is an interesting scaffold for lipopeptides with potential TLR2 agonistic or antagonistic activity. R^1, R^2 and R^3 are long chain alkyl residues; R^4 correspond to the peptide moiety.

TLR agonists and antagonists are potential candidates for the treatment of various immune-associated diseases [253]. TLR2 antagonists have been suggested to have beneficial effects in chronic inflammation, acute inflammation, skin diseases such as acne, and treatment of sepsis. In order to explore these therapeutic options there is an imminent need for synthetically accessible TLR agonistic and antagonistic compounds. Recently it was demonstrated in a sepsis model that lethal shock-like syndromes could be prevented by treatment of mice with the TLR2 antagonistic antibody mAB T2.5 prior to lipopeptide or *Bacillus subtilis* challenge [110]. No synthetic low molecular weight compounds with inhibitory activity against TLR2 have been described so far.

Lanthionine was first discovered in alkaline hydrolysates of wool. Moreover, this molecule was found in human hair, and keratin. In human lenses the photo-oxidative degradation of cystine residues may also result in the formation of lanthionine, accompanied by protein cross-bridging that leads to increased tissue rigidity and hardening of the lens. Another highly interesting natural occurrence of lanthionine is the class of bioactive lantibiotics [254].

For the synthesis of lipolanthionine a new preparation method for N,N-bis-(Fmoc)-lanthionine with orthogonally protected carboxy groups was formulated by Seyberth et al. (2005). A representative collection of lipolanthionine peptides with variations in the length of the fatty acid, the fatty amine as well as the oxidation level of the sulfur and the stereoconfigurations was tested for biological activity, revealing an ability of these compounds to inhibit the TLR2-mediated IL-8 secretion.

5.3 Results

5.3.1 Structure-activity relationships

A representative collection of analytically defined single lipolanthionine peptide amides (Table 5.1) was tested for agonistic activity and for their ability to inhibit the TLR2-mediated IL-8 secretion.

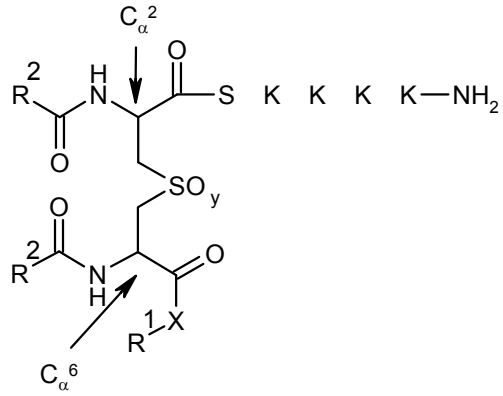

Figure 5.2 Core-structure of the synthesized lipolanthionine peptide amides: Definition of the residues and abbreviations for Table 5.1 (R^1, R^2 alkyl chains / y = 0; sulfide; y = 1, sulfoxide; y = 2 sulfone / configurations $C_\alpha{}^2$,$C_\alpha{}^6$: 2R,6R; 2R,6S; 2S,6R; 2S,6S / X = NH, O).

Table 5.1 Lipolanthionine peptides test for agonistic and inhibitory activity.

	R^1	X	R^2	SO_y	$C_\alpha{}^2$	$C_\alpha{}^6$
1	C_6H_{13}	NH	$C_{13}H_{27}$	0	R	R
2	C_8H_{17}	NH	$C_{13}H_{27}$	0	R	R
3	$C_{10}H_{21}$	NH	$C_{13}H_{27}$	0	R	R
4	$C_{12}H_{25}$	NH	$C_{13}H_{27}$	0	R	R
5	$C_{14}H_{29}$	NH	$C_{13}H_{27}$	0	R	R
6	$C_{16}H_{33}$	NH	$C_{13}H_{27}$	0	R	R
7	$C_{18}H_{37}$	NH	$C_{13}H_{27}$	0	R	R
10	$C_{16}H_{33}$	NH	C_5H_{11}	0	R	R
11	$C_{16}H_{33}$	NH	C_7H_{15}	0	R	R
12	$C_{16}H_{33}$	NH	C_9H_{19}	0	R	R
13	$C_{16}H_{33}$	NH	$C_{11}H_{23}$	0	R	R

14	$C_{16}H_{33}$	NH	$C_{15}H_{31}$	0	R	R
15	$C_{16}H_{33}$	NH	$C_{17}H_{35}$	0	R	R
16	$C_{16}H_{33}$	NH	$C_{19}H_{39}$	0	R	R
20	$C_{16}H_{33}$	NH	$C_{13}H_{27}$	0	R	S
21	$C_{16}H_{33}$	NH	$C_{13}H_{27}$	0	S	R
22	$C_{16}H_{33}$	NH	$C_{13}H_{27}$	0	S	S
30	H	O	$C_{13}H_{27}$	0	R	R
31	H	O	$C_{13}H_{27}$	0	R	S
32	H	O	$C_{13}H_{27}$	0	S	R
33	H	O	$C_{13}H_{27}$	0	S	S
40	$C_{16}H_{33}$	NH	$C_{15}H_{31}$	1	R	R
41	$C_{16}H_{33}$	NH	$C_{15}H_{31}$	2	R	R

To test the inhibitory activity of the lipolanthionine peptides, the well-studied agonist Pam_3Cys-Ser-$(Lys)_4$-OH was used for stimulation of THP-1 cells. The synthesized lipolanthionine compounds enabled the analysis of the structure-activity relationships for the (i) fatty amine chain length, (ii) fatty acid chain length, (iii) stereochemical properties and (iv) the oxidation level of the sulphur.

First, the influence of the fatty amine chain length was investigated using the derivatives based on the bis-myristoylated (2R,6R)-lanthionine lipopeptide amides (**1-7**). At concentrations of 25 μM only for the hexylamine derivative (**1**) a weak agonistic activity was observed.

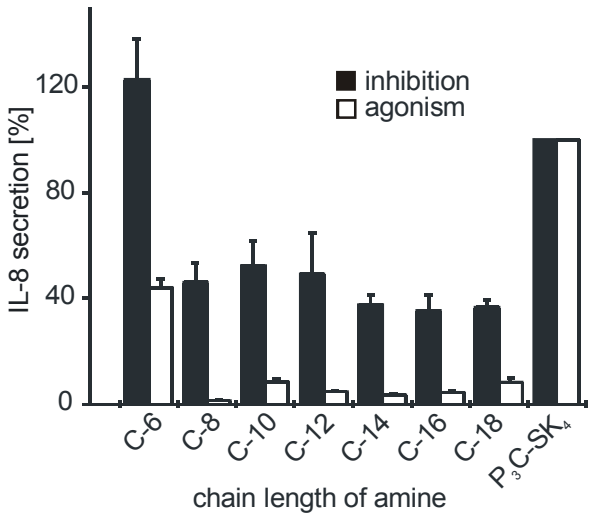

Figure 5.2 Inhibitory activities of $Myr_2Lan(R^1)$-SK_4-NH_2 with varying fatty amine residue R^1. THP-1 cells were incubated with lipolanthionine peptides (25 μM) in the absence or presence of the agonistic lipohexapeptide Pam_3Cys-SK_4-OH (50 nM) for 5 h. The secretion of IL-8 was detected by

ELISA in cell free supernatants. The $Pam_3Cys\text{-}SK_4$-OH induced IL-8 secretion is shown in relation to a sample that was incubated with $Pam_3Cys\text{-}SK_4$-OH in the presence of the same amount of solvent as the lipolanthionine-containing samples. Error bars represent the standard deviation of triplicates in one representative experiment.

Interestingly, except for the hexylamine derivative (**1**) all analogues of lipolanthionine peptide amides exhibited a pronounced and comparable TLR2 inhibitory activity (Figure 5.2). When applied in a 500-fold excess (25 μM) over the highly potent $Pam_3Cys\text{-}Ser\text{-}(Lys)_4$-OH TLR2 agonist (50 nM), IL-8 expression was reduced by 48 to 65 %. Therefore, given a minimum length of 8 carbon atoms, the length of the fatty amine chain seemed to be of minor significance. Except for the octadecylamine derivative (**7**) no cell toxic properties were observed at the tested concentration as determined by MTT-test. The derivative containing the hexadecylamine residue was arbitrarily selected for further tests.

Next the influence of the variation of the amide-bound fatty acid moieties was studied. In this case, only for the caprylic acid derivative (C-8, **11**) an agonistic activity was observed. The derivatives containing lauric (C-12, **13**), myristic (C-14, **6**) and palmitic acid (C-16, **14**) had the highest inhibitory effect on the lipopeptide-induced IL-8 secretion (Figure 5.3). The analogues with short fatty acids (C-6 – C-10, **10-12**) exhibited less inhibitory activities.

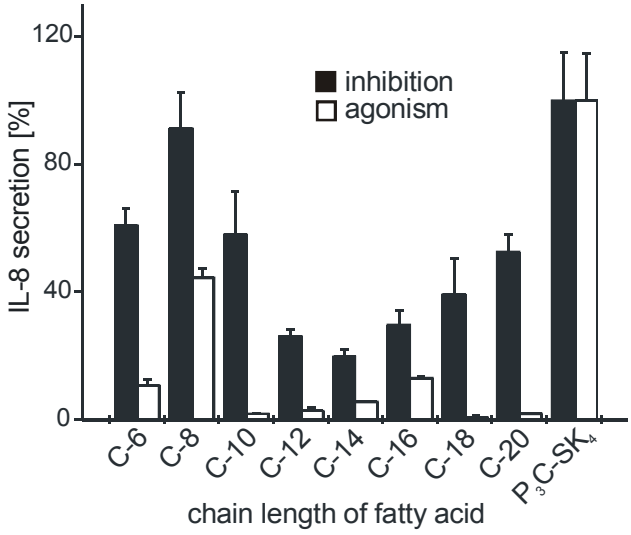

Figure 5.3 Inhibitory activities of $(R^2)_2Lan(Hda)\text{-}SK_4\text{-}NH_2$ with varying fatty acid residue R^2. THP-1 cells were incubated with lipolanthionine peptides (25 μM) in the absence or presence of

Pam_3Cys-SK_4-OH (50 nM) for 5 h. The secretion of IL-8 was detected by ELISA in cell-free supernatants.

For two of the most active inhibitors (**6**, **14**), the concentration dependence of the inhibitory activity was determined. For both compounds a concentration-dependent decrease in IL-8 expression was observed (Figure 5.4).

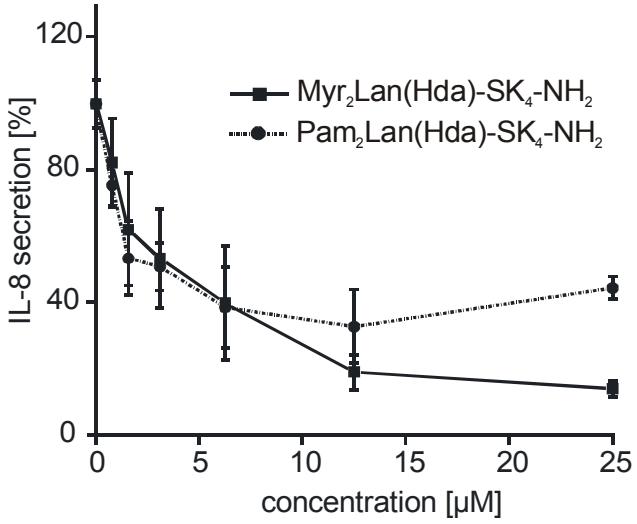

Figure 5.4 Concentration dependence of the inhibitory activity of $Myr_2Lan(Hda)$-SK_4-NH_2 (**6**) and $Pam_2Lan(Hda)$-SK_4-NH_2 (**14**). THP-1 cells were incubated with lipolanthionine peptides (0, 0.78, 1.56, 3.13, 6.25, 12.5, 25 µM) in the presence of Pam_3Cys-SK_4-OH (50 nM) for 5 h. The secretion of IL-8 was detected by ELISA in cell free supernatants. Error bars represent the standard deviation of triplicates.

For the myristic acid derivative, IL-8 expression was reduced by up to 86% for the palmitic acid derivative by up to 68%. Both compounds exhibited IC_{50} values of about 5 µM. However, the inhibitory activity of compounds 17 and 18 varied between several experiments (38, 18 and 14% residual activity for compound **17**, respectively 30 and 42% for compound **18**).

The agonistic activity of Pam_3Cys-Ser-$(Lys)_4$-OH and even of lipopeptide vaccines is dependent on the configuration of the S-glyceryl-cysteine scaffold [255]. Therefore the four stereoisomers of the bis-myristoylated hexadecylamide derivative, the most active inhibitor identified so far were tested. The agonistic activity negatively correlated with the inhibitory activity. The (2R,6R)-lanthionine

peptide showed the highest inhibitory activity, closely followed by the (2S,6R) derivative (**6** and **21**; Figure 5.5).

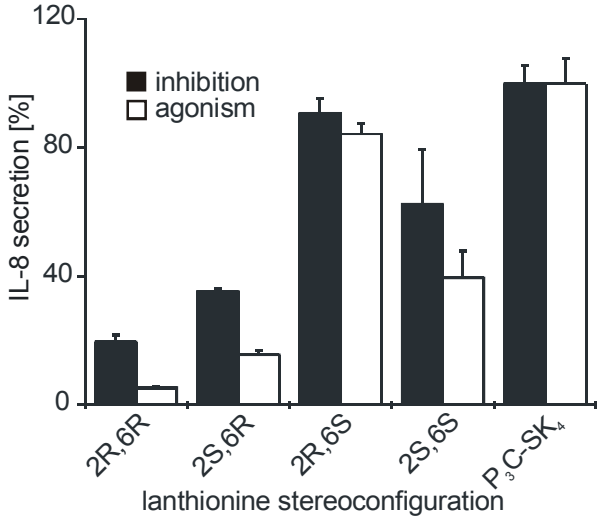

Figure 5.5 Dependence of the inhibitory activities of $Myr_2Lan(Hda)$-SK_4-NH_2 (17) on the configuration of the lanthionine scaffold. THP-1 cells were incubated with lipolanthionine peptides (25 μM) in the absence or presence of Pam_3Cys-SK_4-OH (50 nM) for 5 h. The secretion of IL-8 was detected by ELISA in cell-free supernatants. Error bars represent the standard deviation of triplicates. For inhibition high bars indicate low activity, while for agonism high bars indicate high activity.

In contrast, a change of the configuration in the C-6 stereocenter led to a loss of the inhibitory and to an increase of the agonistic activity. The agonistic activity of the (2R,6S) was higher than that of the (2S,6S) derivative. Therefore, only the configuration of C-6 strongly influences the TLR2 inhibitory activity of the compounds whereas the configuration at C-2 seems to be of minor significance.

Lipolanthionine peptide amides containing free carboxy functions (**30-33**) were unable to suppress the Pam_3Cys-Ser-$(Lys)_4$-OH-induced IL-8 secretion. Interestingly, the methyl ester derivatives possessed cell toxic properties (MTT-test, data not shown). The $Pam_2LanHda$-Ser-$(Lys)_4$-NH_2 oxides (**40** and **41**) showed no significant alteration of the observed inhibitory effect (data not shown).

5.4 Discussion

So far, analyses of structure-activity relationships of the well characterized lipopeptide and highly active TLR2 agonist Pam_3Cys-Ser-$(Lys)_4$-OH have focused mainly on the periphery of the natural core scaffold (Dhc), i. e. variations of the peptide and/or of the fatty acids. In order to vary the scaffold, we substituted the Dhc by the structurally related thioether amino acid lanthionine. The lanthionine scaffold possesses the same number of functional groups, suitable for the introduction of structural diversity for lipopeptide synthesis, as the Dhc scaffold. Two lipolanthionine peptide amides were tested for their capacity to influence the IL-8 secretion induced by the TLR2 agonist Pam_3Cys-Ser-$(Lys)_4$-OH. These *in vitro* tests revealed concentration-dependent and saturable TLR2 inhibitory rather than agonistic activities of the lipolanthionine peptides.

Detailed analyses of the structure-activity relationship for the fatty acid and fatty amine moieties were conducted for the (2R,6R) configuration. The chain length of the amide-bound fatty acid had a strong influence on the activity, whereby the myristic acid derivative (**6**) was the most effective inhibitor of the lipopeptide induced IL-8 secretion. In contrast, the chain length of the amide-bound fatty amine residue had no influence on the inhibitory activity for chain lengths from C-8 to C-16 (**2**-**6**). The C-6 derivative (**10**) exhibited some agonistic activity.

The configuration at the C-6 position of the lanthionine proved to be crucial for inhibitory activity whereas the C-2 configuration showed little influence. In conclusion, the lipolanthionine peptide amide (2R,6R)-Myr_2LanHda-Ser-$(Lys)_4$-NH_2 (**6**) exhibited the strongest TLR2 inhibitory activity.

Several possibilities exist in which way the lipolanthionine peptide amides might influence the TLR2-mediated IL-8 secretion. First, the inhibitor may interact with the agonist preventing receptor recognition and initiation of signal transduction [168]. Second, the inhibitor may influence the TLR2 and/or a coreceptor directly, by interacting with the respective ligand binding site. Third, the lipolanthionine peptides could inhibit the assembly of the TLR2 receptor complex by integrating into cell membrane domains like lipid rafts. For TLR4 it was demonstrated that LPS induces the co-clustering of CD14 and TLR4 in the lipid rafts [256;257]. Recently it was shown that oxidized phospholipid products inhibited the LPS-induced translocation of TLR4 to lipid rafts [258]. It was also reported, that n-3

unsaturated fatty acids caused the alteration of fatty acid composition in membrane lipid rafts, resulting in the inhibition of T cell activation [259].

A direct inhibition by selective blocking of the TLR2 receptor and/or either the TLR1 or TLR6 coreceptor seems to be rather unlikely, since the lipolanthionine peptides also inhibited the LPS-induced, TLR4-mediated IL-8 secretion (data not shown).

On the other hand, the inhibitory potential of the lipolanthionine peptides was strongly dependent on the configuration of the lanthionine C-6 position, an observation that favours a mechanism of inhibition based on the interaction with a receptor molecule. It is moreover remarkable that the agonistic activity of the lanthionine peptides negatively correlated with their inhibitory activity. Therefore, a non-specific mode of action by insertion of the lipolanthionine peptides into membrane domains such as lipid rafts seems to be unlikely. Instead of directly interacting with any TLR, the lipolanthionine peptides may bind to CD14, a coreceptor which is shared by LPS and lipopeptides for activation of their respective TLR [44]. Still, the high concentrations necessary for the inhibitory activity of the lipolanthionine peptides suggest a direct interaction with the agonists. For example, the agonist Pam_3Cys-Ser-$(Lys)_4$-OH might be integrated into micelles composed of lipolanthionine peptides. Future studies will have to elucidate whether the lipolanthionine peptide-mediated IL-8 inhibition follows one of the above-described mechanisms.

5.5 Materials and methods

5.5.1 Reagents

Lipolanthinonine peptides were synthesized by Tobias Seyberth. Standard chemicals were from Fluka (Deisenhofen, Germany) and Merck (Darmstadt, Germany). Pam3Cys-Ser-$(Lys)_4$-OH was from EMC microcollections GmbH (Tübingen, Germany).

5.5.2 Cell culture

The human myelomonocytic cell line THP-1 (ATCC number: TIB-202) was obtained from the Deutsche Sammlung von Mikroorganismen und Zellkulturen (DSMZ) (Braunschweig, Germany). The cells were cultured in RPMI 1640 medium (PAN Biotech, Aidenbach, Germany) supplemented with 10% FCS (PAN Biotech) in a 5% CO_2 humidified atmosphere at 37°C. Cells were passaged every third to fourth day.

5.5.3 IL-8 ELISA

THP-1 cells were dispensed into 96-well culture plates at a cell density of 4 x 10^4 cells per 200 µL of medium per well. Stock solutions of lipolanthionine peptides and Pam_3Cys-SK_4-OH (EMC microcollections, Tübingen, Germany) in DMSO were prepared at a concentration of 10 mM. Cells were incubated with lipolanthionine peptides at the indicated concentrations for 10 min at 37°C. Controls with lipolanthionine-free medium containing equal amounts of DMSO were included in each assay. The agonist Pam_3Cys-SK_4-OH was added to the samples at a concentration of 50 nM. After a further incubation for 5 h at 37°C cell-free supernatants were collected and stored at -80°C prior to the quantification of IL-8 secretion by matched-pair ELISA (clone G265-5 and clone G265-8, BDPharMingen, San Diego, USA) according to the protocol provided by the manufacturer.

5.5.4 Cell viability assay

Cell viability was measured using the colorimetric 3-(4,5-dimethyl thiazol-2-yl)-2,5-diphenyl tetrazolium bromide (MTT) dye reduction assay. THP-1 cells were treated with the corresponding lipolanthionine peptides and Pam_3Cys-SK_4-OH for 5 h (see above) and after removing 120 µl of the supernatant for ELISA analysis, cells were incubated with MTT (Sigma) at a concentration of 1 mg/ml for 4 h. The formazan product was solubilized with SDS (10% (m/v) in 10 mM HCl). The fraction of viable cells was determined by measuring the absorbance of each

sample at 570 nm relative to the absorbance of untreated control cells using the microplate reader.

6 Conclusions

The successful treatment of patients with sepsis and septic shock might be hampered by the outstanding immune stimmulating properties of bacterial cell wall components, such as lipopeptides and lipopolysaccharides. Injections of only nanogram quantities of endotoxin are sufficient to evoke systemic inflammatory responses in humans and up to now, efforts to efficiently block these properties *in vivo* were insufficient.

This work presents (i) novel agents that block lipopolysaccharide- and lipopeptide-induced TLR activation (ii) the identification of a LPS-binding domain of human CD14, (iii) a novel FRET-based LPS-sensing element (iv) investigations of lipopeptide aggregation as well as (v) a dilution protocol to reliably test lipopeptides in cellular assays.

Chapter 2 and 5 of the thesis deal with the identification of molecules that interfere with LPS- and lipopeptide-induced cytokine secretion. Several possibilities exist to generate inhibititory molecules, such as random screening of compound libraries, rational design of inhibitors using receptor ligands as templates, or by mapping proteins that are critically involved in signal generation onto small peptides or peptidomimetics.

The latter possibility was selected by using CD14, a central PRR in innate immuity, as a template for the generation of 20-peptides. The CD14-derived peptides were tested for their ability to inhibit the cytokine secretion of LPS-stimulated monocytes. One peptide of this screen was found to bind and neutralize LPS. In contrast to formerly identified LPS-binding and -neutralizing peptides, hydrophobic residues were shown to be critical for this activity of the CD14-peptide, and, as identified by site-directed mutagenesis, for the LPS-binding capacity of the entire protein. Therefore, the combination of peptide chemistry with cell biology and molecular biology enabled the identification of a novel ligand binding pocket as well as of specific residues involved in the LPS binding of human CD14. Interestingly, as revealed by comparison with the crystal structure of human CD14, this binding site is located in the interior of the protein.

The major purpose for the design of LPS-binding and –neutralizing peptides derived from CD14 was their potential application as drugs for the treatment of sepsis and septic shock. The CD14-derived peptides exhibited an IC_{50} value *in*

vitro in the low μM range which corresponds to that of other LPS-neutralizing peptides. However, the CD14-peptides lack to completely block the agonistic activity of LPS. In addition, highly charged analogues of the native sequence exhibited cell lytic as well as immune stimulating properties at concentrations higher than 5 μM. Despite of these limitations, the ability of CD14-derived peptides to encounter sepsis and septic shock *in vivo* has been investigated using the septic model of galactosamine-sensitized mice. Neither the peptide corresponding to the native sequence nor the analogue with enhanced solubility inhibited the LPS-induced death of the animals but rather enhanced the mortality of the mice. Interestingly, lethality was exclusively observed when the peptides were administered intraperitoneally in the presence of LPS. This effect might be due to the property of cationic peptides to amplify the immune-stimulatory properties of LPS. These and other attributes of peptide-based drugs, such as short half times in serum, poor transport properties from the intestine to the blood and across the blood-brain barrier, as well as rapid excretion through the liver and/or kidney might limit the applicability of the CD14-derived peptides and LPS-neutralizing peptides in general as drugs for the treatment of sepsis. Still, the CD14-derived peptides and the knowledge of their exact molecular mechanism of action may represent a starting point for the rational design of peptidomimetics and non-peptide analogues that overcome these limitations.

Sepsis is usually induced by a mixture of various microorganisms rather than one pathogen and therefore LPS neutralization might be insufficient in most cases of sepsis. Additionally, LPS neutralization may be effective only in a very early phase of sepsis and may come too late at a time when multi-organ failure is already in progress. For these reasons, LPS-neutralizing peptides might be effective in preventing sepsis especially when applied together with agents that release LPS from the bacterial cell wall, as is the case for many antibiotics.

Based on the LPS-binding peptide from CD14 a fluorescence-based LPS-sensing element was designed and applied for LPS-detection *in vitro*. The sensing element containing the native sequence (CD14 (81-100)) did not enable specific recognition of LPS, because several other lipids evoked signals that were almost comparable to that evoked by LPS. However, when two different fluorescently labeled peptides with distinct physicochemical properties were combined and the data analysed in a way that considered the several aspects of characteristic

spectral changes evoked by the individual lipid compounds, specificity for LPS was achieved in the concentration range between 5 to 50 μM of ligand.

In contrast to LPS, little is known whether the activity of lipopeptides is influenced by their aggregation state. For LPS, aggregates activate cells more efficiently than single molecules and several plasma and cellular proteins are required for the activation of cells by these complexes. As shown in chapter 4, the agonistic properties of some lipopeptides were highly dependent on the dissoluon protocol. Fluorescence correlation spectroscopy with fluorescently labeled analogues revealed that the solvent dependent activity was due to the property of the lipopeptides to form aggregates. Dilution into protein- and serum-free buffers led to a complete loss of activity due to formation of large and highly heterogeneous aggregates. In contrast, dilution into BSA- or serum-containing buffers strongly reduced the size of the aggregates. This indicates for an interaction of lipopeptides with serum compounds. Moreover, peptide-dependent differences in aggregate formation and activity were eliminated by introducing an additional dilution step in *tert.*-butyl alcohol/H_2O (4:1). Due to fact that the dilution-dependent activity might compromise biological screens these results are highly relevant for analyzing structure-activity relationships of lipopeptide-dependent TLR2 activation and contribute to a better understanding in which way the aggregation state of lipopeptides is critical for TLR2 activation.

7 References

1. Hashimoto,C., Hudson,K.L., and Anderson,K.V.**,** *Cell* 1988. **52**: 269-279.
2. Lemaitre,B., Nicolas,E., Michaut,L., Reichhart,J.M., and Hoffmann,J.A.**,** *Cell* 1996. **86**: 973-983.
3. Medzhitov,R., Preston-Hurlburt,P., and Janeway,C.A.**,** *Nature* 1997. **388**: 394-397.
4. Rock,F.L., Hardiman,G., Timans,J.C., Kastelein,R.A., and Bazan,J.F.**,** *Proc. Natl. Acad. Sci. USA* 1998. **95**: 588-593.
5. Takeuchi,O., Kawai,T., Sanjo,H., Copeland,N.G., Gilbert,D.J., Jenkins,N.A., Takeda,K., and Akira,S.**,** *Gene* 1999. **231**: 59-65.
6. Chuang,T. and Ulevitch,R.J.**,** *Biochim. Biophys. Acta* 2001. **1518**: 157-161.
7. Du,X., Poltorak,A., Wei,Y., and Beutler,B.**,** *Eur Cytokine Netw.* 2000. **11**: 362-371.
8. Chuang,T.-H. and Ulevitch,R.J.**,** *Eur. Cytokine Netw.* 2000. **11**: 372-378.
9. Zhang,D., Zhang,G., Hayden,M.S., Greenblatt,M.B., Bussey,C., Flavell,R.A., and Ghosh,S.**,** *Science* 2004. **303**: 1522-1526.
10. Slack,J.L., Schooley,K., Bonnert,T.P., Mitcham,J.L., Qwarnstrom,E.E., Sims,J.E., and Dower,S.K.**,** *J. Biol. Chem.* 2000. **275**: 4670-4678.
11. Bell,J.K., Mullen,G.E., Leifer,C.A., Mazzoni,A., Davies,D.R., and Segal,D.M.**,** *Trends Immunol.* 2003. **24**: 528-533.
12. Poltorak,A., He,X., Smirnova,I., Liu,M.Y., Van Huffel,C., Du,X., Birdwell,D., Alejos,E., Silva,M., Galanos,C., Freudenberg,M., Ricciardi-Castagnoli,P., Layton,B., and Beutler,B.**,** *Science* 1998. **282**: 2085-2088.
13. Qureshi,S.T., Lariviere,L., Leveque,G., Clermont,S., Moore,K.J., Gros,P., and Malo,D.**,** *J. Exp. Med.* 1999. **189**: 615-625.
14. Ulevitch,R.J. and Tobias,P.S.**,** *Annu. Rev. Immunol.* 1995. **13**: 437-457.
15. Wright,S.D., Ramos,R.A., Tobias,P.S., Ulevitch,R.J., and Mathison,J.C.**,** *science* 1991. **252**: 1321-1322.
16. Frey,E.A., Miller,D.S., Jahr,T.G., Sundan,A., Bazil,V., Espevik,T., Finlay,B.B., and Wright,S.D.**,** *J. Exp. Med.* 1992. **176**: 1665-1671.
17. Pugin,J., Schürer-Maly,C.-C., Leturcq,D., Moriarty,A., Ulevitch,R.J., and Tobias,P.S.**,** *Proc. Natl. Acad. Sci. USA* 1993. **90**: 2744-2748.

18. Pugin,J., Ulevitch,R.J., and Tobias,P.S., *J. Exp. Med.* 1993. **178**: 2193-2200.
19. Jiang,Q., Akashi,S., Miyake,K., and Petty,H.R., *J. Immunol.* 2000. **165**: 3541-3544.
20. da Silva Correia,J., Soldau,K., Christen,U., Tobias,P.S., and Ulevitch,R.J., *J. Biol. Chem.* 2001. **276**: 21129-21135.
21. Shimazu,R., Akashi,S., Ogata,H., Nagai,Y., Fukudome,K., Kensuke,M., and Kimoto,M., *J. Exp. Med.* 1999. **189**: 1777-1782.
22. Akashi,S., Shimazu,R., Ogata,H., Yoshinori,N., Takeda,K., Kimoto,M., and Miyake,K., *J. Immunol.* 2000. **164**: 3471-3475.
23. Kawasaki,K., Akashi,S., Shimazu,R., Yoshida,T., Miyake,K., and Nishijima,M., *J. Biol. Chem.* 2000. **275**: 2251-2254.
24. Kurt-Jones,E.A., Popova,L., Kwinn,L., Haynes,L.M., Jones,L.P., Tripp,R.A., Walsh,E.E., Freeman,M.W., Golenbock,D.T., Anderson,L.J., and Finberg,R.W., *Nat. Immunol.* 2000. **1**: 398-401.
25. Rassa,J.C., Meyers,J.L., Zhang,Y., Kudaravalli,R., and Ross,S.R., *Proc. Natl. Acad. Sci. USA* 2002. **99**: 2281-2286.
26. Ohashi,K., Burkart,V., Flohe,S., and Kolb,H., *J. Immunol.* 2000. **164**: 558-561.
27. Gallucci,S. and Matzinger,P., *Curr. Opin. Immunol.* 2001. **13**: 114-119.
28. Aliprantis,A.O., Yang,R.-B., Mark,M.R., Suggett,S., Devaux,B., Radolf,J.D., Klimel,G.R., Godowski,P.J., and Zychlinsky,A., *Science* 1999. **285**: 736-739.
29. Brightbill,H.D., Libraty,D.H., Krutzik,S.R., Yang,R.-B., Belisle,J.T., Bleharski,J.R., Maitland,M., Norgard,M.V., Plevy,S.E., Smale,S.T., Brennan,P.J., Bloom,B.R., Godowski,P.J., and Modlin,R.L., *Science* 1999. **285**: 732-736.
30. Lien,E. and Golenbock,D.T., *J. Biol. Chem.* 1999. **274**: 33419-33425.
31. Hirschfeld,M., Kirschning,C.J., Schwandner,R., Wesche,H., Weis,J.H., Wooten,R.M., and Weis,J.J., *J. Immunol.* 1999. **163**: 2382-2386.
32. Schwandner,R., Dziarski,R., Wesche,H., Rothe,M., and Kirschning,C.J., *J. Biol. Chem.* 1999. **274**: 17406-17409.
33. Means,T.K., Wang,S., Lien,E., Yoshimura,A., Golenbock,D.T., and Fenton,M.J., *J. Immunol.* 1999. **163**: 3920-3927.

34. Campos,M.A., Almeida,I.C., Takeuchi,O., Akira,S., Valente,E.P., Procopio,D.O., Travassos,L.R., Smith,J.A., Golenbock,D.T., and Gazzinelli,R.T.**,** *J. Immunol.* 2001. **167**: 416-423.
35. Hajjar,A.M., O´Mahony,D.S., Ozinsky,A., Underhill,D.M., Aderem,A., Klebanoff,S.J., and Wilson,C.B.**,** *J. Immunol.* 2001. **166**: 15-19.
36. Underhill,D.M., Ozinsky,A., Hajjar,A.M., Stevens,A., Wilson,C.B., Bassetti,M., and Aderem,A.**,** *Nature* 1999. **401**: 811-815.
37. Opitz,B., Schröder,N.W.J., Spreitzer,I., Michelsen,K.S., Kirschning,C.J., Hallatschek,W., Zähringer,U., Hartung,T., Göbel,U.B., and Schumann,R.R.**,** *J. Biol. Chem.* 2001. **276**: 22041-22047.
38. Massari,P., Henneke,P., Ho,Y., Latz,E., Golenbock,D.T., and Wetzler,L.M.**,** *J. Immunol.* 2002. **168**: 1533-1537.
39. Hirschfeld,M., Weis,J.J., Toshchakov,V., Salkowski,C.A., Cody,M.J., Ward,D.C., Qureshi,N., Michalek,S.M., and Vogel,S.N.**,** *Infect. Immun.* 2001. **69**: 1477-1482.
40. Werts,C., Tapping,R.I., Mathison,J.C., Chuang,T.-H., Kravchenko,V., Girons,I.S., Haake,D.A., Godowski,P.J., Hayashi,F., Ozinsky,A., Underhill,D.M., Kirschning,C.J., Wagner,H., Aderem,A., Tobias,P.S., and Ulevitch,R.J.**,** *Nat. Immunol.* 2001. **2**: 286-288.
41. Takeuchi,O., Sato,S., Horiuchi,T., Hoshino,K., Takeda,K., Dong,Z., Modlin,R.L., and Akira,S.**,** *J. Immunol.* 2002. **169**: 10-14.
42. Takeuchi,O., Kawai,T., Mühlradt,P.F., Morr,M., Radolf,J.D., Zychlinsky,A., Takeda,K., and Akira,S.**,** *Int. Immunol.* 2001. **13**: 933-940.
43. Buwitt-Beckmann,U., Heine,H., Wiesmüller,K.H., Jung,G., Brock,R., Akira,S., and Ulmer,A.J.**,** *Eur. J. Immunol.* 2005. **35**: 282-289.
44. Manukyan,M., Triantafilou,K., Triantafilou,M., Mackie,A., Nilsen,N., Espevik,T., Wiesmüller,K.H., Ulmer,A.J., and Heine,H.**,** *Eur. J. Immunol.* 2005. **35**: 911-921.
45. Hemmi,H., Takeuchi,O., Kawai,T., Kaisho,T., Sato,S., Sanjo,H., Matsumoto,M., Hoshino,K., Wagner,H., Takeda,K., and Akira,S.**,** *Nature* 2000. **408**: 740-745.
46. Wagner,H.**,** *Immunity* 2001. **14**: 499-502.
47. Alexopoulou,L., Holt,A.C., Medzhitov,R., and Flavell,R.A.**,** *Nature* 2001. **413**: 732-738.

48. Diebold,S.S., Kaisho,T., Hemmi,H., Akira,S., and Reis e Sousa,C., *Science* 2004. **303**: 1529-1531.
49. Heil,F., Hemmi,H., Hochrein,H., Ampenberger,F., Kirschning,C.J., Akira,S., Lipford,G., Wagner,H., and Bauer,S., *Science* 2004. **303**: 1526-1529.
50. Hemmi,H., Kaisho,T., Takeuchi,O., Sato,S., Sanjo,H., Hoshino,K., Horiuchi,T., Tomizawa,H., Takeda,K., and Akira,S., *Nat. Immunol.* 2002. **3**: 196-200.
51. Jurk,M., Heil,F., Vollmer,J., Schetter,C., Krieg,A.M., Wagner,H., Lipford,G., and Bauer,S., *Nat. Immunol.* 2002. **3**: 499.
52. Scheel,B., Teufel,R., Probst,J., Carralot,J.P., Geginat,J., Radsak,M., Jarrossay,D., Wagner,H., Jung,G., Rammensee,H.-G., Hoerr,I., and Pascolo,S., *Eur. J. Immonol.* 2005. **35**: 1557-1566.
53. Hayashi,F., Smith,K.D., Ozinsky,A., Hawn,T.R., Yi,E.C., Goodlett,D.R., Eng,J.K., Akira,S., Underhill,D.M., and Aderem,A., *Nature* 2001. **410**: 1099-1103.
54. Yarovinsky,F., Zhang,D., Andersen,J.F., Bannenberg,G.L., Serhan,C.N., Hayden,M.S., Hieny,S., Sutterwala,F.S., Flavell,R.A., Ghosh,S., and Sher,A., *Science* 2005. **308**: 1626-1629.
55. Dunne,A., Ejdebäck,M., Ludidi,P.L., O´Neill,L.A.J., and Gay,N.J., *J. Biol. Chem.* 2003. **278**: 41443-4141.
56. Li,S., Strelow,A., Fontana,E.J., and Wesche,H., *Proc. Natl. Acad. Sci. USA* 2002. **99**: 5567-5572.
57. Bradley,J.R. and Pober,J.S., *Oncogene* 2001. **20**: 6482-6491.
58. Wang,C., Deng,L., Hong,M., Akkaraju,G.R., Inoue,J., and Chen,Z.J., *Nature* 2001. **412**: 346-351.
59. Karin,M. and Ben-Neriah,Y., *Annu. Rev. Immunol.* 2000. **18**: 621-663.
60. Kawai,T., Adachi,O., Ogawa,T., Takeda,K., and Akira,S., *Immunity* 1999. **11**: 115-122.
61. Kawai,T., Takeuchi,O., Fujita,T., Inoue,J., Mühlrath,P.F., Sato,S., Hoshino,K., and Akira,S., *J. Immunol.* 2001. **167**: 5887-5894.
62. Horng,T., Barton,G.M., Flavell,R.A., and Medzhitov,R., *Nature* 2002. **420**: 329-333.
63. Yamamoto,M., Sato,S., Hemmi,H., Uematsu,S., Hoshino,K., Kaisho,T., Takeuchi,O., Takeda,K., and Akira,S., *Nat. Immunol.* 2003. **4**: 1144-1150.

64. Yamamoto,M., Sato,S., Mori,K., Hoshino,K., Takeuchi,O., Takeda,K., and Akira,S., *J. Immunol.* 2002. **169**: 6668-6672.
65. Akira,S. and Takeda,K., *Nat. Rev. Immunol.* 2004. **4**: 499-511.
66. Zhang,G. and Ghosh,S., *J. Biol. Chem.* 2002. **277**: 7059-7065.
67. Kobayashi,K., Hernandez,L.D., Galan,J.E., Janeway,Jr.C.A., Medzhitov,R., and Flavell,R.A., *Cell* 2002. **110**: 191-202.
68. Burns,K., Janssens,S., Brissoni,B., Olivos,N., Beyaert,R., and Tschopp,J., *J. Exp. Med.* 2003. **197**: 263-268.
69. Wald,D., Qin,J., Zhao,Z., Qian,Y., Naramura,M., Tian,L., Towne,J., Sims,J.E., Stark,G.R., and Li,X., *Nat. Immunol.* 2003. **4**: 920-927.
70. Brint,E.K., Xu,D., Liu,H., Dunne,A., McKenzie,A.N., O´Neill,L.A.J., and Liew,F.Y., *Nat. Immunol.* 2004. **5**: 373-379.
71. Visintin,A., Mazzoni,A., Spitzer,J.H., Wyllie,D.H., Dower,S.K., and Segal,D.M., *J. Immunol.* 2001. **166**: 249-255.
72. Akira,S., Takeda,K., and Kaisho,T., *Nat. Immunol.* 2001. **2**: 675-680.
73. Gomez-Miguel,M.J., Moriyon,I., Alonso-Urmeneta,B., Riezu-Boj,J.I., and Diaz,R., *Infect. Immun.* 1988. **56**: 716-718.
74. Herrmann,A., Schlosser,A., Schmid,R., and Schneider,E., *Res Microbiol.* 1996. **147**: 733-737.
75. Muhlradt,P.F., Kiess,M., Meyer,H., Sussmuth,R., and Jung,G., *J. Exp. Med.* 1997. **185**: 1951-1958.
76. Melchers,F., Braun,V., and Galanos,C., *J. Exp. Med.* 1975. **142**: 473-482.
77. Norgard,M.V., Arndt,L.L., Akins,D.R., Curetty,L.L., Harrich,D.A., and Randolf,J.D., *Infect. Immun.* 1996. **64**: 3845-3852.
78. Kreutz,M., Ackermann,U., Hauschildt,S., Krause,S.W., Riedel,D., Bessler,W.G., and Andreesen,R.A., *Immunology* 1997. **92**: 396-401.
79. Wiesmüller,K.H., Bessler,W.G., and Jung,G., *Hoppe Seyler´s Z. Physiol. Chem.* 1983. **364**: 593-606.
80. Bessler,W.G., Cox,M., Lex,A., Suhr,B., Wiesmüller,K.H., and Jung,G., *J. Immunol.* 1985. **135**: 1900-1905.
81. Hoffmann,P., Heinle,S., Schade,U.F., Loppnow,H., Ulmer,A.J., Flad,H.D., Jung,G., and Bessler,W.G., *Immunobiology* 1988. **177**: 158-170.

82. Wiedemann,F., Link,R., Pumpe,K., Jacobshagen,U., Schaefer,H.E., Wiesmüller,K.H., Hummel,R.P., Jung,G., Bessler,W.G., and Böltz,T., *J. Pathol.* 1991. **164**: 265-271.
83. Wiesmüller,K.H., Bessler,W.G., and Jung,G., *Int. J. Pept. Protein. Res.* 1992. **40**: 255-260.
84. Wiesmüller,K.H., Jung,G., and Hess,G., *Vaccine* 1989. **7**: 29-33.
85. Hoffmann,P., Loleit,M., Mittenbühler,K., Beck,W., Wiesmüller,K.H., Jung,G., and Bessler,W.G., *FEMS Immunol Med Microbiol.* 1997. **17**: 225-234.
86. Deres,K., Schild,H., Wiesmüller,K.H., Jung,G., and Rammensee,H.-G., *Nature* 1989. **342**: 561-564.
87. Prass,W., Ringsdorf,H., Bessler,W.G., Wiesmüller,K.H., and Jung,G., *Biochim. Biophys. Acta* 1987. **900**: 116-121.
88. Hoffmann,P., Wiesmüller,K.H., Metzger,J., Jung,G., and Bessler,W.G., *Biol. Chem. Hoppe Seyler* 1989. **370**: 575-582.
89. Reitermann,A., Metzger,J., Wiesmüller,K.H., Jung,G., and Bessler,W.G., *Biol. Chem. Hoppe Seyler* 1989. **370**: 343-352.
90. Metzger,J., Wiesmüller,K.H., Schaude,R., Bessler,W.G., and Jung,G., *Int. J. Pept. Protein. Res.* 1991. **37**: 46-57.
91. Metzger,J., Wiesmüller,K.H., and Jung,G., *Int. J. Pept. Protein. Res.* 1991. **38**: 545-554.
92. Kleine,B., Rapp,W., Wiesmüller,K.H., Edinger,M., Beck,W., Metzger,J., Ataulakhanov,R., Jung,G., and Bessler,W.G., *Immunobiology* 1994. **190**: 53-66.
93. Bessler,W.G., Baier,W., vd Esche,U., Hoffmann,P., Heinevetter,L., Wiesmüller,K.H., and Jung,G., *Behring Inst. Mitt.* 1997. **98**: 390-399.
94. Spohn,R., Buwitt-Beckmann,U., Brock,R., Jung,G., Ulmer,A.J., and Wiesmüller,K.H., *Vaccine* 2004. **22**: 2494-2499.
95. Takeuchi,O., Kaufmann,A., Grote,K., Kawai,T., Hoshino,K., Morr,M., Muhlradt,P.F., and Akira,S., *J. Immunol.* 2000. **164**: 554-557.
96. Bone,R.C., Balk,R.A., Cerra,F.B., Dellinger,R.P., Fein,A.M., Knaus,W.A., Schein,R.M., and Sibbald,W.J., *Chest* 1992. **101**: 1644-1655.
97. Angus,D.C., Linde-Zwirble,W.T., Lidicker,J., Clermont,G., Carcillo,J., and Pinsky,M.R., *Crit. Care Med.* 2001. **29**: 1303-1310.

98. Van Amersfoort,E.S., Van Berkel,T.J.C., and Kuiper,J., *Clin. Microbiol. Rev.* 2003. **16**: 379-414.
99. Marshall,J.C., *Nat. Rev. Drug Discov.* 2003. **2**: 391-405.
100. Bone,R.C., Fisher,C.J.Jr., Clemmer,T.P., Slotman,G.J., Metz,C.A., and Balk,R.A., *N. Engl. J. Med.* 1987. **317**: 653-658.
101. Ziegler,E.J., Fisher,C.J.Jr., Sprung,C.L., Straube,R.C., Sadoff,J.C., Foulke,G.E., Wortel,C.H., Fink,M.P., Dellinger,R.P., and Teng,N.N., *N. Engl. J. Med.* 1991. **324**: 429-436.
102. Fisher,C.J.Jr., Agosti,J.M., Opal,S.M., Lowry,S.F., Balk,R.A., Sadoff,J.C., Abraham,E., Schein,R.M., and Benjamin,E., *N. Engl. J. Med.* 1996. **334**: 1697-1702.
103. Abraham,E., Wunderink,R., Silverman,H., Perl,T.M., Nasraway,S., Levy,H., Bone,R., Wenzel,R.P., Balk,R., and Alfred,R., *JAMA* 1995. **273**: 934-941.
104. Fisher,C.J.Jr., Slotman,G.J., Opal,S.M., Pribble,J.P., Bone,R.C., Emmanuel,G., Ng,D., Bloedow,D.C., and Catalano,M.A., *Crit. Care Med.* 1994. **22**: 12-21.
105. Bernard,G.R., Vincent,J.L., Laterre,P.F., LaRosa,S.P., Dhainaut,J.F., Lopez-Rodriguez,A., Steingrub,J.S., Garber,G.E., Helterbrand,J.D., Ely,E.W., and Fisher,C.J.Jr., *N. Engl. J. Med.* 2001. **344**: 699-709.
106. Giroir,B.P., Quint,P.A., Barton,P., Kirsch,E.A., Kitchen,L., Goldstein,B., Nelson,B.J., Wedel,N.J., Carroll,S.F., and Scannon,P.J., *Lancet* 1998. **350**: 1439-1443.
107. Larrick,J.W., Hirata,M., Balint,R.F., Lee,J., Zhong,J., and Wright,S.C., *Infect. Immun.* 1995. **63**: 1291-1297.
108. Christ,W.J., Asano,O., Robidoux,A.L., Perez,M., Wang,Y., Dubuc,G.R., Gavin,W.E., Hawkins,L.D., McGuinness,P.D., and Mullarkey,M.A., *Science* 1995. **268**: 80-83.
109. Iwami,K.I., Matsuguchi,T., Masuda,A., Kikuchi,T., Musikacharoen,T., and Yoshikai,Y., *J. Immunol.* 2001. **165**: 6682-6686.
110. Meng,G., Rutz,M., Schiemann,M., Metzger,J., Grabiec,A., Schwandner,R., Luppa,P.B., Ebel,F., Busch,D.H., Bauer,S., Wagner,H., and Kirschning,C.J., *J. Clin. Invest.* 2004. **113**: 1473-1481.
111. Bartfai,T., Behrens,M.M., Gaidarova,S., Pemberton,J., Shivanyuk,A., and Rebek,Jr.J., *Proc. Natl. Acad. Sci. USA* 2003. **100**: 7971-7976.

112. Abraham,E., Glauser,M.P., Butler,T., Garbino,J., Gelmont,D., Laterre,P.F., Kudsk,K., Bruining,H.A., Otto,C., Tobin,E., Zwingelstein,C., Lesslauer,W., and Leighton,A.**,** *JAMA* 1997. **277**: 1531-1538.
113. Reinhart,K. and Karzai,W.**,** *Crit. Care Med.* 2001. **29**: 121-125.
114. Hotchkiss,R.S. and Karl,I.E.**,** *N. Engl. J. Med.* 2003. **348**: 138-150.
115. Annane,D., Sebille,V., Charpentier,C., Bollaert,P.E., Francois,B., Korach,J.M., Capellier,G., Cohen,Y., Azoulay,E., Troche,G., Chaumet-Riffaut,P., and Bellissant,E.**,** *JAMA* 2002. **288**: 862-871.
116. Hagberg,L., Briles,D.E., and Eden,C.S.**,** *J. Immunol.* 1985. **134**: 4118-4122.
117. Shenep,J.L., Barton,R.P., and Mogan,K.A.**,** *J. Infect. Dis.* 1985. **151**: 1012-1018.
118. Hurley,J.C.**,** *Clin. Infect. Dis.* 1992. **15**: 840-854.
119. Cooperstock,M.S.**,** *Antimicrob. Agents Chemother.* 1974. **6**: 422-425.
120. Elsbach,P. and Weiss,J.**,** *Immunobiology* 1993. **187**: 417-429.
121. Hancock,R.E.W. and Lehrer,R.**,** *Trends Biotechnol.* 1998. **16**: 82-88.
122. Boheim,G., Janko,K., Leibfritz,D., Ooka,T., König,W.A., and Jung,G.**,** *Biochim. Biophys. Acta* 1976. **433**: 182-199.
123. Hanke,W., Methfessel,C., Wilmsen,H.U., Katz,E., Jung,G., and Boheim,G.**,** *Biochim. Biophys. Acta* 1983. **727**: 108-114.
124. Matsuzaki,K., Harada,M., Handa,T., Funakoshi,S., Fujii,N., Yajima,H., and Miyajima,K.**,** *Biochim. Biophys. Acta* 1989. **981**: 130-134.
125. Matsuzaki,K., Sugishita,K., Harada,M., Fujii,N., and Miyajima,K.**,** *Biochim. Biophys. Acta* 1997. **1327**: 119-130.
126. Pouny,Y., Rapaport,D., Mor,A., Nicolas,P., and Shai,Y.**,** *Biochemistry* 1992. **31**: 12416-12423.
127. Gough,M., Hancock,R.E.W., and Kelley,N.M.**,** *Infect. Immun.* 1996. **64**: 4922-4927.
128. Kirikae,T., Hirata,M., Yamasu,H., Kirikae,F., Tamura,H., Kayama,F., Nakatsuka,K., Yokochi,T., and Nakano,M.**,** *Infect. Immun.* 1998. **66**: 1861-1868.
129. Scott,M.G., Yan,H., and Hancock,R.E.W.**,** *Infect. Immun.* 1999. **67**: 2005-2009.
130. Zasloff,M.**,** *Proc. Natl. Acad. Sci. USA* 1987. **84**: 5449-5453.

131. Zasloff,M., Martin,B., and Chen,H.C., *Proc. Natl. Acad. Sci. USA* 1988. **85**: 910-913.
132. Dathe,M., Nikolenko,H., Meyer,J., Beyermann,M., and Bienert,M., *FEBS Lett.* 2005. **501**: 146-150.
133. Meyer,C.E. and Reusser,F., *Experientia* 1967. **23**: 85-86.
134. Rink,T., Bartel,H., Jung,G., Bannwarth,W., and Boheim,G., *Eur. Biophys. J.* 1994. **23**: 155-165.
135. Nakamura,T., Furunaka,H., Miyata,T., Tokunaga,F., Muta,T., Iwanaga,S., Niwa,M., Takao,T., and Shimonishi,Y., *J. Biol. Chem.* 1988. **263**: 16709-16713.
136. Hirakura,Y., Kobayashi,S., and Matsuzaki,K., *Biochim. Biophys. Acta* 2002. **1562**: 32-36.
137. Yonezawa,A., Kuwahara,J., Fujii,N., and Sugiura,Y., *Biochemistry* 1992. **31**: 2998-3004.
138. Straubitz,P., Peschel,A., Nieuwenhuizen,W.F., Otto,M., Götz,F., Jung,G., and Jack,R.W., *J. Pept. Sci.* 2001. **7**: 552-564.
139. Selsted,M.E., Novotny,M.J., Morris,W.L., Tang,Y.Q., Smith,W., and Cullor,J.S., *J. Biol. Chem.* 1992. **267**: 4292-4295.
140. Falla,T.J., Karunaratne,D.N., and Hancock,R.E.W., *J. Biol. Chem.* 1996. **271**: 19298-19303.
141. Fehlbaum,P., Bulet,P., Chernysh,S., Briand,J.P., Roussel,J.P., Letellier,L., Hetru,C., and Hoffmann,J.A., *Proc. Natl. Acad. Sci. USA* 1996. **93**: 1221-1225.
142. Scott,M.G., Vreugdenhil,A.C., Buurman,W.A., Hancock,R.E.W., and Gold,M.R., *J. Immunol.* 2000. **164**: 549-553.
143. Ulevitch,R.J., *Adv. Immunol.* 1993. **53**: 267-289.
144. Yu,B., Hailman,E., and Wright,S.D., *J. Clin. Invest.* 1997. **99**: 315-324.
145. Tobias,P.S., Soldau,K., Gegner,J.A., Mintz,D., and Ulevitch,R.J., *J. Biol. Chem.* 1995. **270**: 10482-10488.
146. Zhang,Y., Doerfler,M., Lee,T.C., Guillemin,B., and Rom,W.N., *J. Clin. Invest.* 1993. **91**: 2076-2083.
147. Pugin,J. and Ulevitch,R.J., *Immunity* 1994. **1**: 509-516.

148. Weidemann,B., Schletter,J., Dziarski,R., Kusumoto,S., Stelter,F., Rietschel,E.T., Flad,H.-D., and Ulmer,A.J., *Infect. Immun.* 1997. **65**: 858-864.

149. Cleveland,M.G., Gorham,J.D., Murphy,T.L., Tuomanen,E., and Murphy,K.M., *Infect. Immun.* 1996. **64**: 1906-1912.

150. Sellati,T.J., Bouis,D.A., Norgard,M.V., and Randolf,J.D., *J. Immunol.* 1998. **160**: 5455-5464.

151. Juan,T.S.C., Kelley,M.J., Johnson,D.A., Busse,L.A., Hailman,E., Wright,S.D., and Lichenstein,H.S., *J. Biol. Chem.* 1995. **270**: 1382-1387.

152. Viriyakosol,S. and Kirkland,T.N., *Infect. Immun.* 1996. **64**: 653-656.

153. Viriyakosol,S. and Kirkland,T.N., *J. Biol. Chem.* 1995. **270**: 361-368.

154. Viriyakosol,S., Mathison,J.C., Tobias,P.S., and Kirkland,T.N., *J. Biol. Chem.* 1999. **275**: 3144-3149.

155. Cunningham,M.D., Shapiro,R.A., Seachord,C., Ratcliffe,K., Cassiano,L., and Darveau,R.P., *J. Immunol.* 2000. **164**: 3255-3263.

156. Shapiro,R.A., Cunningham,M.D., Ratcliffe,K., Seachord,C., Blake,J., Bajorath,J., Aruffo,A., and Darveau,R.P., *Infect. Immun.* 1997. **65**: 293-297.

157. McGinley,M.D., Narhi,L.O., Kelley,M.J., Davy,E., Robinson,J., Rohde,M.F., Wright,S.D., and Lichenstein,H.S., *J. Biol. Chem.* 1995. **270**: 5213-5218.

158. Juan,T.S.C., Hailman,E., Kelley,M.J., Busse,L.A., Davy,E., Emping,C.J., Narhi,L.O., Wright,S.D., and Lichenstein,H.S., *J. Biol. Chem.* 1995. **270**: 5219-5224.

159. Stelter,F., Bernheiden,M., Menzel,R., Jack,R.S., Witt,S., Fan,X., Pfister,M., and Schütt,C., *Eur. J. Biochem.* 1997. **243**: 100-109.

160. Stelter,F., Bernheiden,M., Menzel,R., Witt,S., Jack,R.S., Grunwald,U., Fan,X., and Schütt,C., *Prog. Clin. Biol. Res.* 1998. **397**: 301-313.

161. Stelter,F., Loppnow,H., Menzel,R., Grunwald,U., Bernheiden,M., Jack,R.S., Ulmer,A.J., and Schütt,C., *J. Immunol.* 1999. **163**: 6035-6044.

162. Kloczewiak,M., Black,K.M., Loiselle,P., Cavaillon,J.M., Wainwright,N., and Warren,H.S., *J. Infect. Dis.* 1994. **170**: 1490-1497.

163. Hoess,A., Watson,S., Siber,G.R., and Liddington,R., *EMBO J.* 1993. **12**: 3351-3356.

164. Ried,C., Wahl,C., Miethke,T., Wellnhofer,G., Landgraf,C., Schneider-Mergener,J., and Hoess,A., *J. Biol. Chem.* 1996. **271**: 28120-28127.

165. Little,R.G., Kelner,D.N., Lim,E., Burke,D.J., and Conlon,P.J., *J. Biol. Chem.* 1994. **269**: 1865-1872.

166. Zhang,G.-H., Mann,D.M., and Tsai,C.-H., *Infect. Immun.* 1999. **67**: 1353-1358.

167. Taylor,A.H., Heavner,G., Nedelman,M., Sherris,D., Brunt,E., Knight,D., and Ghrayeb,J., *J. Biol. Chem.* 1995. **270**: 17934-17938.

168. Rustici,A., Velucchi,M., Faggioni,R., Sironi,M., Ghezzi,P., Quataert,S., Green,B., and Porro,M., *Science* 1993. **259**: 361-365.

169. Iwagaki,A., Porro,M., and Pollack,M., *Infect. Immun.* 2000. **68**: 1655-1663.

170. Mayo,K.H., Haseman,J., Ilyina,E., and Gray,B., *Biochim. Biophys. Acta* 1998. **1425**: 81-92.

171. Nagaoka,I., Hirota,S., Niyonsaba,F., Hirata,M., Adachi,Y., Tamura,H., Tanaka,S., and Heumann,D., *Clin. Diagn. Lab. Immunol.* 2002. **9**: 927-982.

172. Porro,M., *Trends Microbiol.* 1994. **2**: 65-67.

173. Giacometti,A., Cirioni,O., Ghiselli,R., Mocchegiani,F., Del Prete,M.S., Viticchi,C., Kamysz,W., Lempicka,E., Saba,V., and Scalise,G., *Antimicrob. Agents Chemother.* 2002. **46**: 2132-2136.

174. Hanasawa,K., *Ther. apher.* 2002. **6**: 290-295.

175. Zimmermann,N., Beck-Sickinger,A.G., Folkers,G., Krickl,S., Müller,I., and Jung,G., *Eur. J. Biochem.* 1991. **200**: 519-521.

176. Fischer,R., Mader,O., Jung,G., and Brock,R., *Bioconjugate Chem.* 2003. **14**: 653-660.

177. Mader,O., Reiner,K., Egelhaaf,H.-J., Fischer,R., and Brock,R., *Bioconj. Chem.* 2004. **15**: 70-78.

178. Kim,J.I., Lee,C.J., Jin,M.S., Lee,C.H., Paik,S.G., Lee,H., and Lee,J.O., *J. Biol. Chem.* 2005. **280**: 11347-11351.

179. Beutler,B., Milsark,I.W., and Cerami,A.C., *Science* 1985. **229**: 869-871.

180. Tracey,K.J., Fong,Y., Hesse,D.G., Manogue,K.R., Lee,A.T., Kuo,G.C., Lowry,S.F., and Cerami,A., *Nature* 1987. **330**: 662-664.

181. Tossi,A., Sandri,L., and Giangaspero,A., *Biopolymers* 2000. **55**: 4-30.

182. Beamer,L.J., Carroll,S.F., and Eisenberg,D., *Science* 1997. **276**: 1861-1864.

183. Takeda,K., Miyatake,H., Yokota,N., Matsuyama,S., Tokuda,H., and Miki,K., *EMBO J.* 2003. **22**: 3199-3209.

184. Gangloff,S.C., Zähringer,U., Blondin,C., Guenounou,M., Silver,J., and Goyert,S.M., *J. Immunol.* 2005. **175**: 3940-3945.
185. Schumann,R.R., Leong,S.R., Flaggs,G.W., Gray,P.W., Wright,S.D., Mathison,J.C., Tobias,P.S., and Ulevitch,R.J., *Science* 1990. **249**: 1429-1431.
186. Mathison,J.C., Tobias,P.S., Wolfson,E., and Ulevitch,R.J., *J. Immunol.* 1992. **149**: 200-206.
187. Wright,S.D., Ramos,R.A., Tobias,P.S., Ulevitch,R.J., and Mathison,J.C., *Science* 1990. **249**: 1431-1433.
188. Hailman,E., Lichenstein,H.S., Wurfel,M.M., Miller,D.S., Johnson,D.A., Kelley,M., Busse,L.A., Zukowski,M.M., and Wright,S.D., *J. Exp. Med.* 1994. **179**: 269-277.
189. Gioannini,T.L., Teghanemt,A., Zhang,D., Coussens,N.P., Dockstader,W., Ramaswamy,S., and Weiss,J.P., *Proc. Natl. Acad. Sci. USA* 2004. **101**: 4186-4191.
190. Iversen,L.F., Kastrup,J.S., Bjorn,S.E., Rasmussen,P.B., Wiberg,F.C., Flodgaard,H.J., and Larsen,I.K., *Nat. Struct. Biol.* 1997. **4**: 265-268.
191. Elass-Rochard,E., Roseanu,A., Legrand,D., Trif,M., Salmon,V., Motas,C., Montreuil,J., and Spik,G., *Biochem. J.* 1995. **312**: 839-845.
192. Dankesreiter,S., Hoess,A., Schneider-Mergener,J., Wagner,H., and Miethke,T., *J. Immunol.* 2000. **164**: 4804-4811.
193. Uknis,M.E., Wasiluk,K.R., Acton,R.D., Klaerner,H.G., Dahlberg,P.S., Ilyina,E.E., Haseman,J.R., Gray,B.H., Mayo,K.H., and Dunn,D.L., *Surgery* 1997. **122**: 380-385.
194. Pereira,H.A., Erdem,I., Pohl,J., and Spitznagel,J.K., *Proc. Natl. Acad. Sci. USA* 1993. **90**: 4733-4737.
195. Nagaoka,I., Hirota,S., Niyonsaba,F., Hirata,M., Adachi,O., Tamura,H., and Heumann,D., *J. Immunol.* 2001. **167**: 3329-3338.
196. Jung,G., *Combinatorial Peptide and Nonpeptide libraries.* Wiley-VCH, Weinheim, 1996.
197. Sarin,V.K., Kent,S.B., Tam,J.P., and Merrifield,R.B., *Anal. Biochem.* 1981. **117**: 147-157.
198. Tsuchiya,S., Yamabe,M., Yamaguchi,Y., Kobayashi,Y., Konno,T., and Tada,K., *Int. J. Cancer* 1980. **26**: 171-176.

199. Yoshimura,A., Lien,E., Ingalls,R.R., Toumanen,E., Dziarski,R., and Golenbock,D.T.**,** *J. Immunol.* 1999. **163**: 1-5.

200. Tsuchiya,S., Kobayashi,Y., Goto,Y., Okumura,H., Nakae,S., Konno,T., and Tada,K.**,** *Cancer Res.* 1982. **42**: 1530-1536.

201. Roslansky,P.F. and Novitsky,T.J.**,** *J. Clin. Microbiol.* 1991. **29**: 2477-2483.

202. Cohen,J.**,** *Intensive Care Med.* 2000. **26**: 51-56.

203. Miyawaki,A., Llopis,J., Heim,R., McCaffery,J.M., Adams,J.A., Ikura,M., and Tsien,R.Y.**,** *Nature* 1997. **388**: 882-887.

204. Sato,M., Ozawa,T., Inukai,K., Asano,T., and Umezawa,Y.**,** *Nat. Biotech.* 2002. **20**: 287-294.

205. Ting,A.Y., Kain,K.H., Klemke,R.L., and Tsien,R.Y.**,** *Proc. Natl. Acad. Sci. USA* 2001. **98**: 15003-15008.

206. Honda,A., Adams,S.R., Sawyer,C.L., Lev-Ram,V., Tsien,R.Y., and Dostmann,W.R.G.**,** *Proc. Natl. Acad. Sci. USA* 2001. **98**: 2437-2442.

207. Nagai,Y., Miyazaki,M., Aoki,R., Zama,T., Inouye,S., Hirose,R., Iino,M., and Hagiwara,M.**,** *Nat. Biotech.* 2000. **18**: 313-316.

208. Kurokawa,K., Mochizuki,N., Ohba,Y., Miuzno,H., Miyawaki,A., and Matsuda,M.**,** *J. Biol. Chem.* 2001. **276**: 31305-31310.

209. Cicchetti,G., Biernacki,M., Farquharson,J., and Allen,P.G.**,** *Biochemistry* 2004. **43**: 1939-1949.

210. Matsuzaki,K., Sugishita,K., and Miyajima,K.**,** *FEBS Lett* 1999. **449**: 221-224.

211. Wei,A.-P., Blumenthal,D.K., and Herron,J.N.**,** *Anal. Chem.* 1994. **66**: 1500-1506.

212. Rangin,M. and Amit,B.**,** *JACS* 2004. **126**: 5038-5039.

213. Kleine,B., Sprenger,R., Martinez-Alonso,C., and Bessler,W.G.**,** *Immunology* 1987. **61**: 29-34.

214. Mittenbühler,K., Loleit,M., Baier,W., Fischer,B., Sedelmeier,E., Jung,G., Winkelmann,G., Jacobi,C., Weckesser,J., Erhard,M.H., Hofmann,A., Bessler,W.G., and Hoffmann,P.**,** *Int J. Immunopharmacol.* 1997. **19**: 277-287.

215. Baier,W., Masihi,N., Huber,M., Hoffmann,P., and Bessler,W.G.**,** *Immunobiology* 1999. **201**: 391-405.

216. Bessler,W.G., Suhr,B., Bühring,H.J., Müller,C.P., Wiesmüller,K.H., Becker,G., and Jung,G., *Immunobiology* 1985. **170**: 239-244.
217. Lex,A., Wiesmüller,K.H., Jung,G., and Bessler,W.G., *J. Immunol.* 1986. **137**: 2676-2681.
218. Böltz,T., Hummel,R.P., Tröger,W., Rübsamen-Waigmann,H., Biesert,L., Müller-Lantzsch,N., Koch,P., Bessler,W.G., and Jung,G., *J. Virol. Methods* 1988. **22**: 173-182.
219. Höhlich,B.-J., Wiesmüller,K.H., Haas,B., Gerner,W., Correa,R., Hehnen,H.-R., Schlapp,T., Pfaff,E., and Saalmüller,A., *J Gen Virol.* 2003. **84**: 3315-3324.
220. Hoffmann,P., Jiminez-Diaz,M., Loleit,M., Tröger,W., Wiesmüller,K.H., Metzger,J., Jung,G., Kaiser,I., Stöcklin,S., and Lenzner,S., *Hum. Antibodies Hybridomas* 1990. **1**: 137-144.
221. Seifert,R., Schultz,G., Richter-Freund,M., Metzger,J., Wiesmüller,K.H., Jung,G., Bessler,W.G., and Hauschildt,S., *Biochem. J.* 1990. **267**: 795-802.
222. Berg,M., Offermanns,S., Seifert,R., and Schultz,G., *Am. J. Physiol.* 1994. **266**: 1684-1691.
223. Hioe,C.E., Qui,H., Chend,P.D., Bian,Z., Li,M.L., Li,J., Singh,M., Kuebler,P., McGee,P., O´Hagan,D., Zamb,T., Koff,W., Allsopp,C., Wang,C.Y., and Nixon,D.F., *Vaccine* 1996. **14**: 412-418.
224. Mittenbühler,K., Baier,W., Esche,U., Heinevetter,L., Wiesmüller,K.H., and Jung,G., *Curr Top Pept Protein Res.* 1997. **2**: 125-135.
225. Gupta,D., Kirkland,T.N., Viriyakosol,S., and Dziarski,R., *J. Biol. Chem.* 1996. **271**: 23310-23316.
226. Uhl,B., Wolf,B., Schwinde,A., Metzger,J., Jung,G., Bessler,W.G., and Hauschildt,S., *J. Leukoc. Biol.* 1991. **50**: 10-18.
227. Metzger,J., Sawyer,C.L., Wille,B., Biesert,L., Bessler,W.G., and Jung,G., *Biochim. Biophys. Acta* 1993. **1149**: 29-39.
228. Wolf,B., Hauschildt,S., Uhl,B., Metzger,J., Jung,G., and Bessler,W.G., *Immunology Letters* 1989. **20**: 121-126.
229. Reichel,F., Roelofsen,A.M., Geurts,H.P.M., Hämäläinen,T.I., Feiters,M.C., and Boons,G.-J., *J. Am. Chem. Soc.* 1999. **121**: 7989-7997.
230. Müller,M., Lindner,B., Kusumoto,S., Fukase,K., Schromm,A.B., and Seydel,U., *J. Biol. Chem.* 2004. **279**: 26307-26313.

231. Takayama,K., Din,Z.Z., Mukerjee,P., Cooke,P.H., and Kirkland,T.N., *J. Biol. Chem.* 1990. **265**: 14023-14029.
232. Takayama,K., Mitchell,D.H., Din,Z.Z., Mukerjee,P., Li,C., and Coleman,D.L., *J. Biol. Chem.* 1994. **269**: 2241-2244.
233. Kitchens,R.L. and Munford,R.S., *J. Immunol.* 1998. **160**: 1920-1928.
234. Brandenburg,K., Andra,J., Müller,M., Koch,M.H., and Garidel,P., *Carbohydr. Res.* 2005. **338**: 2477-2489.
235. Rigler,R., Mets,Ü., Widengren,J., and Kask,P., *Eur. Biophys. J.* 1993. **22**: 169-175.
236. Van Rompaey,E., Chen,Y., Müller,J.D., Gratton,E., Van Craenenbroeck,E., Engelborghs,Y., De Smedt,S., and Demeester,J., *Biol. Chem.* 2001. **382**: 379-386.
237. Hoff,A., André,T., Schäffer,T., Jung,G., Wiesmüller,K.H., and Brock,R., *Chembiochem* 2002. **3**: 1183-1191.
238. Gioannini,T.L., Zhang,D., Teghanemt,A., and Weiss,J.P., *J. Biol. Chem.* 2002. **277**: 47818-47825.
239. Lavalette,D., Tétreau,C., Tourbez,M., and Blouquit,Y., *Biophys. J.* 1999. **76**: 2744-2751.
240. Clamme,J.P., Azoulay,J., and Mély,Y., *Biophys. J.* 2003. **84**: 1960-1968.
241. Gutsmann,T., Müller,M., Carroll,S.F., McKenzie,R.C., Wiese,A., and Seydel,U., *Infect. Immun.* 2001. **69**: 6942-6950.
242. Schröder,N.W.J., Heine,H., Alexander,C., Manukyan,M., Eckert,J., Hamann,L., Göbel,U.B., and Schumann,R.R., *J. Immunol.* 2004. **173**: 2683-2691.
243. Metzger,J.W., Kempter,C., Wiesmüller,K.H., and Jung,G., *Anal. Biochem.* 1994. **219**: 261-277.
244. Reutter,F., Jung,G., Baier,W., Treyer,B., Bessler,W.G., and Wiesmüller,K.H., *J. Pept. Sci.* 2005. **65**: 375-383.
245. Braun,V. and Rehn,K., *Eur. J. Biochem.* 1969. **10**: 426-438.
246. Braun,V., *Biochim. Biophys. Acta* 1975. **415**: 335-377.
247. Mühlradt,P.F., Kiess,M., Meyer,H., Sussmuth,R., and Jung,G., *Infect. Immun.* 1998. **66**: 4804-4810.
248. Mühlradt,P.F., Kiess,M., Meyer,H., Süssmuth,R., and Jung,G., *J. Exp. Med.* 1997. **185**: 1951-1958.

249. Schild,H., Deres,K., Wiesmüller,K.H., Jung,G., and Rammensee,H.-G., *Eur. J. Immunol.* 1991. **21**: 2649-2654.

250. Wiesmüller,K.H., Fleckenstein,B., and Jung,G., *Biol. Chem.* 1991. **382**: 571-579.

251. Müller,S.D., Müller,M.R., Huber,M., vd Esche,U., Kirschning,C.J., Wagner,H., Bessler,W.G., and Mittenbühler,K., *Int Immunopharmacol.* 2004. **4**: 1287-1300.

252. Metzger,J., Jung,G., Bessler,W.G., Hoffmann,P., Strecker,M., Lieberknecht,A., and Schmidt,U., *J. Med. Chem.* 1991. **34**: 1969-1974.

253. Zuany-Amorim,C., Hastewell,J., and Walker,C., *Nat. Rev. Drug Discov.* 2002. **1**: 797-807.

254. Jung,G., *Angew. Chem. Int. Ed.* 1991. **30**: 1051-1068.

255. Kurimura,M., Takemoto,M., and Achiwa,K., *Chem. Pharm. Bull.* 1991. **39**: 2590-2596.

256. Triantafilou,M., Miyake,K., Golenbock,D.T., and Triantafilou,K., *J. Cell Sci.* 2002. **115**: 2603-2611.

257. Pfeiffer,A., Böttcher,A., Orso,E., Kapinsky,M., Nagy,P., Bodnar,A., Spreitzer,I., Liebisch,G., Drobnik,W., Gempel,K., Horn,M., Holmer,S., Hartung,T., Multhoff,G., Schutz,G., Schindler,H., Ulmer,A.J., Heine,H., Stelter,F., Schütt,C., Rothe,G., Szollosi,J., Damjanovich,S., and Schmitz,G., *Eur. J. Immonol.* 2001. **31**: 3153-3164.

258. Walton,K.A., Cole,A.L., Yeh,M., Subbanagounder,G., Krutzik,S.R., Modlin,R.L., Lucas,R.M., Nakai,J., Smart,E.J., Vora,D.K., and Berliner,J.A., *Arterioscler. Thromb. Vasc. Biol.* 2003. **23**: 1133-1136.

259. Stulnig,T.M., Huber,J., Leitinger,N., Imre,E.M., Angelisova,P., Nowotny,P., and Waldhausl,W., *J. Biol. Chem.* 2001. **276**: 37335-37340.

Meine akademischen Lehrer waren:

Prof. Albert, Prof. Bisswanger, Prof. Bock, Prof. Bohley, Prof. Breyer-Pfaff, Prof. Eckstein, Prof. Eisele, Prof. Fröhlich, Prof. Gauglitz, Prof. Hagenmaier, Prof. Hamprecht, Prof. Hanack, Dr. Hartmann, Prof. Jung, Dr. Günzl, Prof. Lindner, Dr. Kalbacher, Prof. Maier, Prof. Mayer, Prof. Mecke, Prof. Nakel, Prof. Oelkrug, Prof. Pfaff, Prof. Pfeiffer, PD Dr. Pommer, Prof. Probst, Prof. Rammensee, Prof. Reutter, Prof. Staudt, Prof. Stevanović, PD Dr. Stoeva, Prof. Strähle, Prof. Voelter, PD Dr. Voigt, Prof. Weber, Prof. Wegmann, Prof. Werringloer, Prof. Weser, Prof. Wiesmüller, Prof. Wohlleben.

LEBENSLAUF	Söhnke Voss
04. März 1971	geboren in Eutin
1977 – 1980	Grundschule Timmendorfer Strand
1980 – 1981	Grundschule Langenargen
1981 – 1987	Realschule Kressbronn
1987 – 1991	Wirtschaftsgymnasium Friedrichshafen
Juni 1991	Abitur
September 1992 – September 1994	Ausbildung als Medizinisch-Technischer Laborassistent an der Naturwissenschaftlich-Technischen Akademie Prof. Dr. Grübler in Isny
September 1994	Abschluss als staatlich geprüfter Medizinisch-Technischer Laborassistent
November 1994 – September 1995	Anstellung als Technischer Assistent an der Ludwig-Maximilians-Universität München bei Prof. Dr. Dr. Walter Neupert
Oktober 1995 – April 2001	Studium der Biochemie an der Eberhard-Karls-Universität Tübingen
April 1998	Mündliche Vordiplomprüfung
Juli 2000	Mündliche Diplomprüfung
August 2000 – April 2001	Anfertigung der Diplomarbeit „Nachweis der T-Zell Aktivierung durch peptidmodifizierte Oberflächen mit Fluoreszenzmikroskopie“ am Institut für Organische Chemie, Arbeitsgruppe Prof. Dr. Günther Jung, Eberhard-Karls-Universität Tübingen
April 2001	Diplom Biochemie
Juli 2001 – November 2005	Anfertigung der Doktorarbeit mit dem Titel „Molekulare Untersuchungen von Agonisten und Antagonisten der Toll-like Rezeptoren 2 und 4”, betreut von Prof. Dr. Günther Jung, Institut für Organische Chemie, Eberhard-Karls-Universität Tübingen, durchgeführt am Institut für Organische Chemie und am Interfakultären Institut für Zellbiologie, Arbeitsgruppe „Zelluläre Signaltransduktion“, Laborleiter PD. Dr. Roland Brock, Eberhard-Karls-Universität Tübingen